BRITISH COLUMBIA GEOLOGICAL SURVEY est. 1895

Organic-rich Upper Devonian shales of the Patry and Exshaw formations (Besa River Group) in the subsurface of Liard basin

Filippo Ferri
Margot McMechan
Barry Richards
Richard Friedman

BRITISH COLUMBIA
Ministry of Energy, Mines and Low Carbon Innovation

Paper 2021-02

Ministry of Energy, Mines and Low Carbon Innovation
Mines, Competitiveness, and Authorizations Division
British Columbia Geological Survey

Recommendation citation: Ferri, F., McMechan, M., Richards, M.B., and Friedman, R., 2021. Organic-rich Upper Devonian shales of the Patry and Exshaw formations (Besa River Group) in the subsurface of Liard basin. British Columbia Ministry of Energy, Mines and Low Carbon Innovation, British Columbia Geological Survey Paper 2021-01, 42p.

Front cover: Left side, core of the lower part of the Patry Formations with dark grey to black, calcareous mudstone and thin discontinuous, pale grey calcareous horizons. Nexen Energy Dunedin a-38-B well (4041.1 to 4041.2 m); from Nexen Energy Ltd. (2016). **Right side**, core of dark grey calcareous mudstone to shale in the upper part of the Patry Formation containing light grey detrital carbonate layers that locally form discontinuous lenses. The carbonate layers locally have sharp bases and appear to grade into dark grey shale or mudstone. The dark grey layer near the top of the core (arrow) may cap a flattened ripple. Chevron-Woodside Patry b-23-K well (3736.25 m).

Back cover. Photomicrograph of thin felsic tuff horizon at the base of the lower part of the Exshaw Formation at the 3710.4 m level of the Chevron-Woodside Patry b-23-K well (Apache Canada Ltd., 2012), with quartz, mica and lithic shards. The U-Pb zircon age of this tuff is 364.03 ± 0.31 Ma.

Ministry of
Energy, Mines and
Low Carbon Innovation

Organic-rich Upper Devonian shales of the Patry and Exshaw formations (Besa River Group) in the subsurface of Liard basin

Filippo Ferri
Margot McMechan
Barry Richards
Richard Friedman

Ministry of Energy, Mines and Low Carbon Innovation
British Columbia Geological Survey
Paper 2021-02

Organic-rich Upper Devonian shales of the Patry and Exshaw formations (Besa River Group) in the subsurface of Liard basin

Filippo Ferri[1a], Margot McMechan[2], Barry Richards[2], and Richard Friedman[3]

[1]British Columbia Geological Survey (retired); consultant, Victoria, British Columbia, V8W 9N3
[2]Geological Survey of Canada, Calgary, Alberta, T2L 2A7
[3]Pacific Centre for Isotopic and Geochemical Research, The University of British Columbia, Vancouver, British Columbia, V6T 1Z4
[a]corresponding author: Fil.Ferri@shaw.ca

Recommendation citation: Ferri, F., McMechan, M., Richards, M.B., and Friedman, R., 2021. Organic-rich Upper Devonian shales of the Patry and Exshaw formations (Besa River Group) in the subsurface of Liard basin. British Columbia Ministry of Energy, Mines and Low Carbon Innovation, British Columbia Geological Survey Paper 2021-01, 42p.

Abstract
Middle Devonian to middle Mississippian rocks of the Besa River Formation in the Rocky Mountains are distal, predominantly shale equivalents to more than 1000 m of more proximal carbonate rocks and interbedded shales in the subsurface to the east. Although relatively uniform in outcrop, petrophysical logs in the subsurface of Liard basin allow discrete formation-level units to be recognized, thus we propose that the unit be elevated to group status in the subsurface. The lower Besa River Group is subdivided into the Horn River, Fort Simpson and Exshaw formations together with a new unit, the Party Formation, that is currently only recognized in Liard Basin. The upper Besa River Group is undivided and contains shales that are time equivalent to the Banff, Prophet and Golata formations. Of particular economic interest are uppermost Devonian organic-rich strata, the Patry Formation (new status) and the Exshaw Formation. Patry shales are deep-water basin equivalents to upper ramp carbonate rocks and calcareous shales of the Kotcho Formation which, in turn, transition eastward into shelf carbonate rocks. Organic-rich Patry shales reflect establishment of anoxic bottom waters that spread across much of the Western Canada Sedimentary Basin as transgression peaked during deposition of the Exshaw Formation. Precise U-Pb zircon age determinations of tuffs recovered from cores at the base (364.354 ± 0.26 Ma), middle (364.03 ± 0.31 Ma) and top (363.07 ± 0.25 Ma) of the lower part of the Exshaw Formation and calculated rates of deposition suggest that the top of the Exshaw Formation in Liard basin is older than the Devonian-Carboniferous boundary (358.9 Ma). In north-central Liard Basin, organic-rich shales of the Patry Formation and lower part of the Exshaw Formation contain 6,196 x $10^9 m^3$ of marketable, dry gas in a north-northeast trending zone that is 200 m thick and 20-30 km wide. These shales are at depths of greater than 5 km, producing over-pressured reservoirs and resulting in prolific wells when stimulated through hydraulic fracturing.

Keywords: Besa River Formation, Besa River Group, Exshaw Formation, Patry Formation, shale gas, Liard Basin, Horn River Basin, British Columbia, shale, organic-rich, geochronology, tuff, geochemistry

1. Introduction

In central and western Liard basin (Fig. 1), Devonian to Mississippian organic-rich shales originally defined by Kidd (1963) as the Besa River Formation from outcrops in the Rocky Mountains of northeastern British Columbia, have been the focus of recent exploration and development (Adams, 2009). This deeply buried and highly overpressured sequence has proven to be prolific, and a recent assessment suggests a marketable natural gas resource of approximately 6,196 x $10^9 m^3$ (219 Tcf; National Energy Board, 2016). Although this gas is dry, initial average well production is impressive, and decline curves suggest ultimate per well natural gas recoveries of 922 x $10^6 m^3$ (33 Bcf; National Energy Board, 2016), making this unit an attractive development target.

The Besa River Formation outcrops along the eastern margin of the north-central Canadian Cordillera where it is up to 1600 m thick (Richards, 1989). It can be traced from near the Monkman Pass area of northeastern British Columbia (54^o 30’ N) northward into southern Yukon and the Northwest Territories (Stott et al., 1963; Stott and Taylor, 1968; Taylor and Stott, 1973, 1999; Bamber and Mamet, 1978; Douglas, 1976; Douglas and Norris, 1977a, b, c; Stott et al., 1983; Thompson, 1989; McMechan, 1994). These undifferentiated shales are equivalent to sequences in Liard basin that, in turn, are correlative to more proximal shale and shelf carbonate units several thousand metres thick exposed at the surface and found in the subsurface farther east (Fig. 2). Of particular economic interest are uppermost Devonian to lowermost Mississippian organic-rich strata, the Patry Formation (new status) and the Exshaw Formation.

In the first part of this paper, we review the tectonic context of Middle Devonian to Carboniferous sedimentation in the Cordillera. This summary is followed by a stratigraphic overview of the Liard basin and its eastern neighbour, the Horn

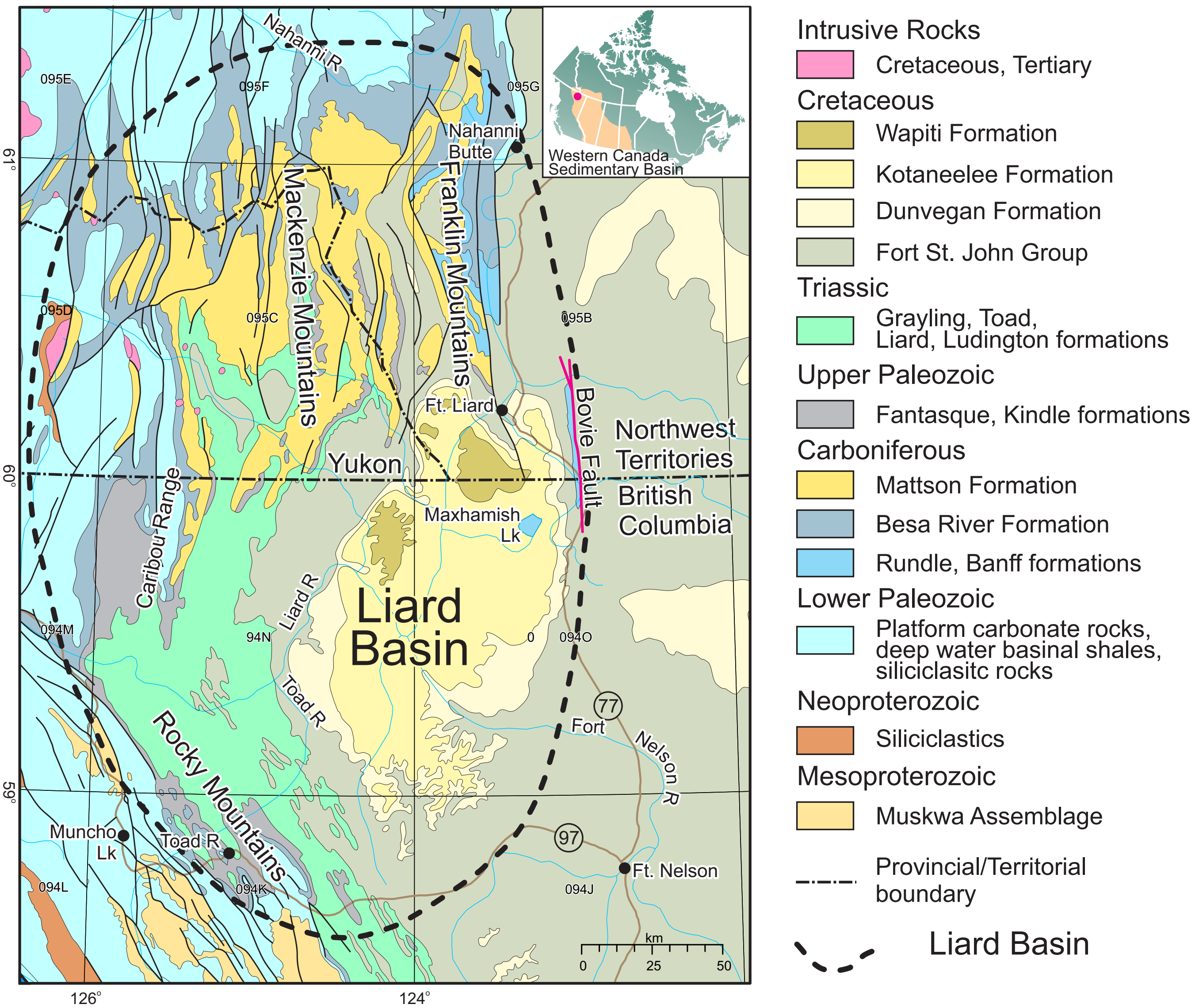

Fig. 1. Geology of northeastern British Columbia, after Wheeler and McFeely (1991), showing the general outline of the Liard basin at the eastern edge of the Canadian Cordillera. The basin is centred close to where the northwest trend of the Rocky Mountains in the south shifts to the more northerly trend of the Mackenzie and Franklin mountains in the north. Although Gabrielse (1967) originally defined the basin using the distribution of Carboniferous sandstones in the Mattson Formation, subsequent workers focused on the distribution of more extensive Cretaceous coarse siliciclastic rocks and used the limits of the Dunvegan and Kotaneelee formations to outline the basin (Leckie et al., 1991).

River basin (Fig. 1), and a review of correlations and regional variations in thickness and facies between exposed sections and subsurface sections across the Liard and Horn River basins and, farther eastward in the subsurface, to the plains of northeastern British Columbia and western Alberta. Although relatively uniform in outcrop, petrophysical logs allow the recognition of specific formations within the Besa River Formation and thus we propose that, in the subsurface, the unit be elevated to group status (Fig.2; see section 5). We then focus on the stratigraphy and reservoir characteristics of Patry and Exshaw formations, highlighting the features that make the interval an exceptional shale gas play. We present rock descriptions and data (see Appendix 1; BCGS_P2021-02.zip) including whole rock, trace and rare earth element geochemistry, mineralogical, Rock-Eval and thermal maturity, helium-derived porosity and gas saturation, organic carbon isotope, and U-Pb zircon analyses using core samples from four wells (Chevron-Woodside La Jolie b-3-K, Chevron-Woodside Patry b-23-K, Nexen Energy Patry a-68-D, Nexen Energy Dunedin a-38-B), and summarize exploration in Liard basin. We conclude with a model that envisages a transition from normal marine conditions in the early to late Famennian to anoxia at the beginning of Patry Formation sedimentation, to flooding of anoxic waters across much of the Western Canada Sedimentary Basin during a second-order transgression that reached its maximum during deposition of the lower part of the Exshaw Formation.

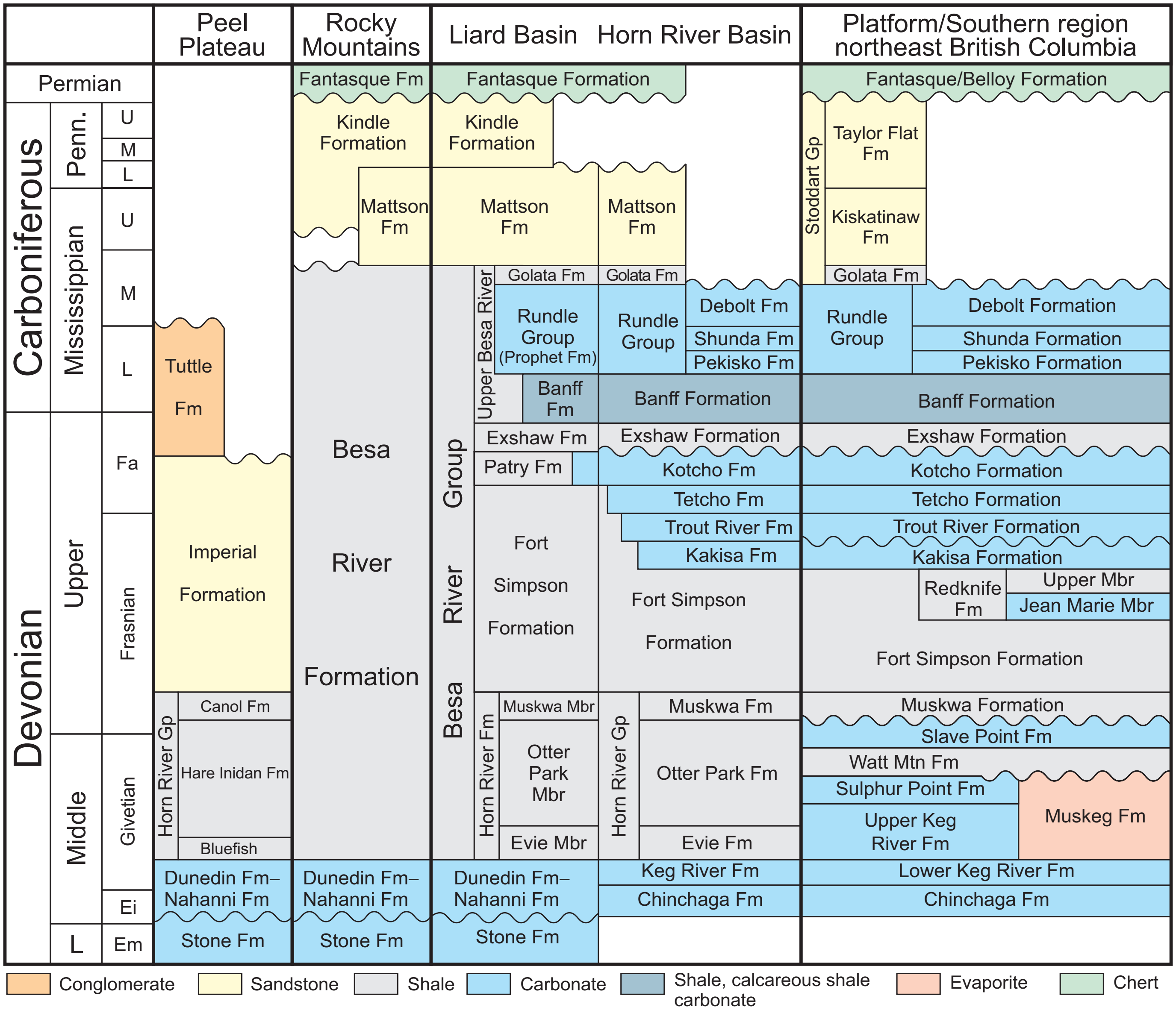

Fig. 2. Stratigraphic units in the Liard basin, the Horn River basin, and the platform succession to the east, illustrating correlations between exposures in the Rocky Mountains and Caribou Range of the Mackenzie Mountains (Ferri and Reyes, 2019a, b) to the subsurface of the Western Canada Sedimentary Basin. This diagram displays the westward shale-out of Middle Devonian to Middle Mississippian carbonate rocks into Besa River shales. Where exposed in the Rocky Mountains, Besa River rocks are extremely uniform and subunits are difficult to recognize, thus the formation-level term 'Besa River Formation' is used. However, discrete formation-level units can be recognized using petrophysical logs in the subsurface of Liard basin where we propose elevating Besa River unit rocks to the group level (see section 5), a usage that we apply in cross sections presented below. L – Lower; M – Middle; U – Upper; Em – Emsian; Ei – Eifelian; Fa – Famennian.

2. Tectonic context

In the Middle to Late Devonian, passive margin sedimentation along the northern and western flanks of Ancestral North America arising from the protracted breakup of the supercontinent Rodina (Neoproterozoic to Cambrian; Ross et al., 1991; Colpron et al., 2002) was interrupted by convergent plate processes. In the Arctic, this convergence is manifested by the Ellesmerian orogeny (Embry, 1988; Richards et al., 1997; Lane, 2007), with southerly directed shortening and coarse siliciclastic sedimentation (Fig. 3a). This shortening has been tied to the collision of a continental land mass called Pearya, which has been interpreted as part of, or associated with, the Siberian craton (Lane, 2007) or as a pericratonic land mass of the Franklin margin (Hadlari et al., 2013).

In the southwestern United States, this convergence is represented by the Antler orogeny (Burchfiel and Davis, 1972; Speed and Sleep, 1982), which is thought to have been caused by eastward subduction of oceanic lithosphere below the western margin of Ancestral North America (Richards, 1989; Richards et al., 1993, 2002; Nelson et al., 2006; Murphy et

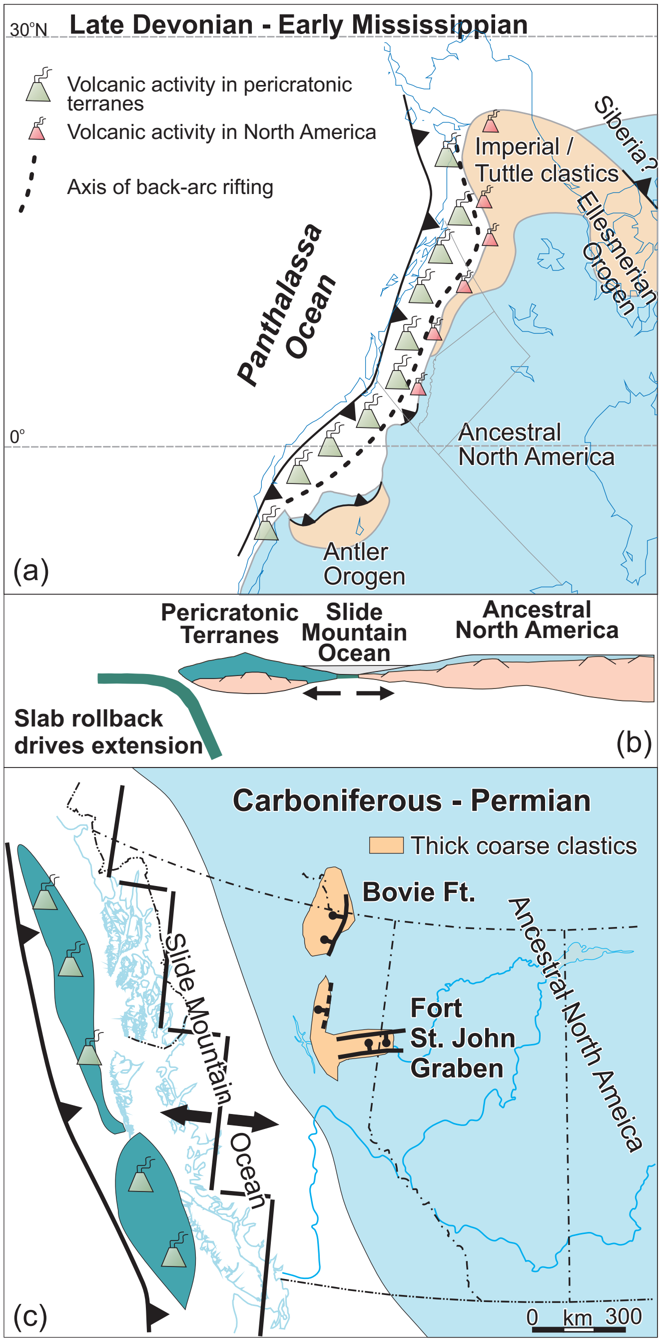

Fig. 3. a) Generalized reconstruction of western and northwestern Ancestral North America during the Late Devonian to Early Mississippian. The westward subduction of Panthalassa oceanic lithosphere created an arc system along the western edge of Ancestral North America. The dashed line shows the location of back-arc rifting which traces the western margin of current pericratonic sequences in the Cordillera. Contractional deformation is recorded by the Antler orogeny in the southern British Columbia and the United States. The impingement of a continental land mass (Siberia?) in the north led to the Ellesmerian orogeny. Modified from Colpron et al. (2007). **b)** Representation of subduction and incipient arc magmatism and back-arc extension along the western edge of Ancestral North America. **c)** Generalized reconstruction of western Ancestral North America during the Carboniferous to Permian. Continued eastward subduction and back-arc extension led to opening of the Slide Mountain ocean, the Fort Saint John graben system (part of the Peace River embayment), and normal movement along the Bovie structure, which created accommodation space for thick sequences of Carboniferous to Permian siliciclastic rocks in Liard basin.

al., 2006; Paradis et al., 2006) and is recorded by deposition of westerly derived siliciclastic rocks (Fig. 3). Contractional deformation of this age has also been documented or inferred in southern British Columbia (Smith et al., 1993; Savoy et al., 2000; Stevenson et al., 2000; Root, 2001; Richards et al., 2002).

Evidence throughout the rest of the Canadian Cordillera supports back-arc extensional processes related to eastward subduction (Richards 1989; Richards et al., 1993, 2002; Gordey and Anderson, 1993; Nelson et al., 2006). Slab roll-back of old, dense subducting oceanic lithosphere is the preferred model to explain earliest Tournaisian extensional dynamics in the overriding continental crust (Richards et al., 2002; Nelson et al., 2006). In this model, initial arc development along the western edge of Ancestral North America in the late Famennian to early Tournaisian was followed by or was concurrent with, back-arc extension that ultimately led to the Slide Mountain ocean (Fig. 3b; Richards, 1989; Richards et al. 1993; Nelson et al., 2006). Genetically related to this regional back-arc extension, Middle Devonian to Middle Mississippian units in northeastern British Columbia extend eastward from exposures in the Rocky Mountains (Ferri and Reyes, 2019a) and Caribou Range of the Mackenzie Mountains (Ferri and Reyes, 2019b) to the subsurface of the Western Canada Sedimentary Basin, including the Liard basin and the Horn River basin (Figs. 1, 2).

3. Stratigraphic overview: Liard basin and Horn River basin

The Liard basin is located along the west-central margin of the composite Western Canada Sedimentary Basin, straddling the borders between British Columbia, Yukon, and the Northwest Territories borders (Fig. 1). The basin was initially defined by thick sections of Carboniferous sandstones of the Mattson Formation (Gabrielse, 1967), whereas more recent work has used the distribution of Cretaceous rocks (Fig. 1; Leckie et al., 1991). Carboniferous sandstones are thickest in the northern part of the basin whereas Cretaceous rocks are more abundant to the south (Fig. 1). The accumulation and preservation of these deposits was accommodated by motion on the Bovie fault, a north-trending structure that is taken as the eastern margin of the Liard basin and the western margin of the Horn River basin (Figs. 4, 5). MacLean and Morrow, (2004) considered that the Bovie fault had a protracted history, with predominantly west-side-down displacement between the early Carboniferous and Early Cretaceous. However, many of the Late Devonian carbonate to shale transitions in Liard basin roughly follow the trend of the Bovie structure (Fig. 4). These relationships imply the Liard basin area was a depocenter as early as the Famennian and that the position of the hinge line fluctuated during the Late Devonian. Movement on older,

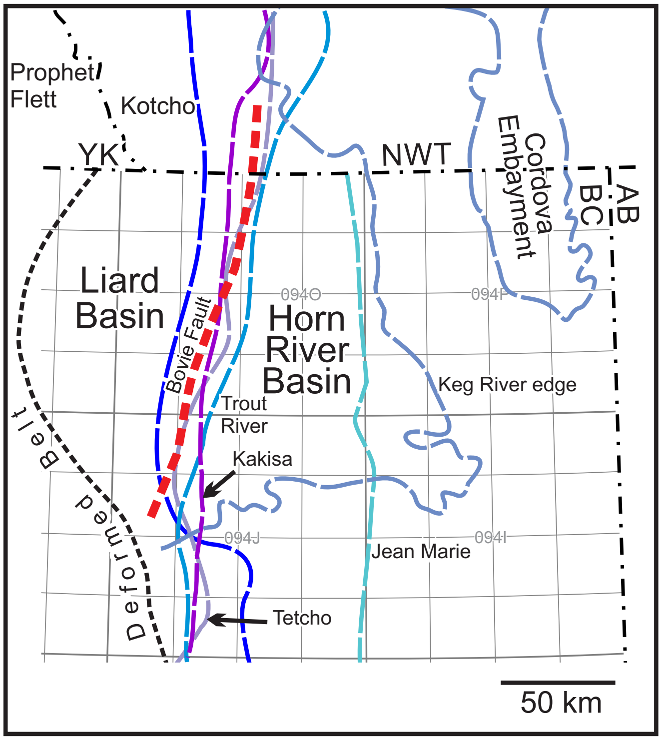

Fig. 4. Westward shale-out of Jean Marie to Kotcho formations near the Liard basin. The eastern boundary of the Liard basin is defined by the Bovie fault. The eastward deflection of the Kotcho Formation shale out line in its southern trace reflects its removal by the sub-Exshaw unconformity to the west of the line (see below). The Keg River edge defines the outlines of the Horn River basin and Cordova embayment during the Givetian.

smaller precursor faults or extensive deepening related to the Bovie structure may have broadly influenced carbonate and shale deposition (Ferri et al., 2015). Extensional displacement on the Bovie structure was followed by Late Cretaceous contractional motion related to the Laramide orogeny and development of the eastern Cordillera (MacLean and Morrow, 2004).

Middle Devonian to middle Mississippian shales of the Besa River Group represent deep-water basin equivalents to carbonate, sandstone, and shale successions deposited farther east (Fig. 2). During the late Middle Devonian, northwest and east - trending barrier reef complexes represented by the Presqu'ile (Upper Elk Point Group/Pine Point Formation, Sulphur Point Formation) and Slave Point formations developed east of the future Liard basin. These define the eastern boundary of Horn River basin, which contains shales of the lower and middle parts of the Horn River Group/Formation (Figs. 2, 5). In the early Late Devonian, deposition of transgressive organic-rich shales of the Muskwa Formation pushed carbonate deposition to the southeast, leading to accumulation of the Leduc reef complexes in the southern part of the Western Canada Sedimentary Basin. During the Late Devonian (Famennian), carbonate sedimentation (Kakisa to Kotcho formations) were re-established across much of the Western Canada Sedimentary Basin, but in broad shallow shelf environments that transitioned westward into slope, ramp, and deep-water basin settings. The carbonate to shale transitions of these units are the first manifestations of the eastern boundary of the Liard basin and roughly follow the future Bovie fault structure (Fig. 4).

Carbonate deposition was terminated by a major marine transgression in the late Famennian that was accompanied by deposition of organic-rich shales of the Exshaw Formation (Fig. 2). This unit and its equivalents covered much of the Western Canada Sedimentary Basin and other parts of North America. Widespread shelf and slope carbonate and shale deposition, represented by the Banff Formation and Rundle Group, was re-established at the beginning of the Early Mississippian and continued into the Middle Mississippian (Fig. 2). The transition from shelf carbonates into slope and ramp environments occurred in western Liard basin.

Marine shales of the Golata Formation were deposited above the Rundle Group and marked the onset of a late Viséan Mississippian to Early Pennsylvanian transgressive-regressive cycle that includes thick, southwardly prograding deltaic sequences of the Mattson Formation (Federowski et al., 2019). The Bovie structure was likely active at this time, providing the accommodation space for the accumulation of these thick deltaic siliciclastic deposits. These rocks are time equivalent to the Stoddart Group in the Peace River area, which were being deposited during formation of the Fort St. John graben complex

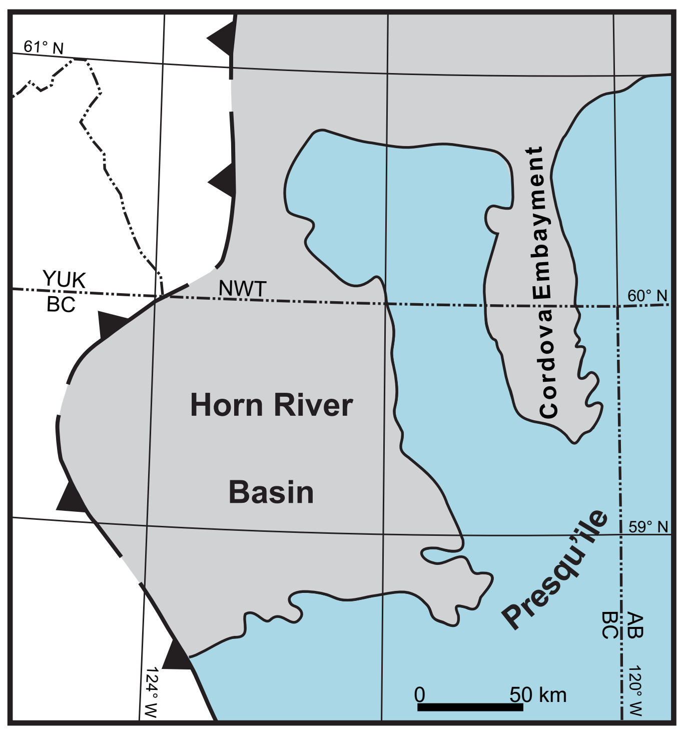

Fig. 5. Main depositional elements during the late Middle Devonian (Givetian) showing the outline of the Horn River basin and Cordova embayment during deposition of the Upper Keg River Formation. The westward thinning of Horn River units indicates that the Liard basin had not yet developed as a depositional element (see Fig. 6). Modified from Petrel Robertson (2003) and Morrow (2012).

in the Peace River embayment. It was during deposition of the thick Mattson sandstones, together with the concurrent development of the Bovie fault structure, that the Liard Basin was clearly defined as a major depocenter.

4. Stratigraphic analysis of units in Liard and Horn River basins and regional correlations with Western Canada Sedimentary Basin units to the east

Devonian and Carboniferous strata display systematic changes in thickness and facies between exposed sections in the Rocky and Mackenzie mountains, subsurface sections across the Liard and Horn River basins and, farther eastward in the subsurface, to the plains of northeastern British Columbia and western Alberta. Particularly significant are changes immediately beneath the Exshaw Formation, the sub-Exshaw unconformity, and the record of Antler orogeny-aged convergent tectonics as preserved in Late Devonian-Mississippian sedimentary sequences.

In the analysis below, we rely heavily on publicly available well data submitted to the British Columbia Oil and Gas Commission. The GeoSCOUT® software package, produced by GeoLOGIC Systems, was used to analyze these data and produce the maps, production data graphs, and log-based cross-sections. Surfer 8®, by Golden Software Inc., produced the contour maps. Formation tops were picked from well logs, cuttings and core descriptions by the senior author and were used to produce to the subsurface structure contour maps.

4.1. Sub-Exshaw Formation Frasnian and Famennian units

East-west transects along the central part of the Liard basin suggest that rocks in the upper part of the Kotcho Formation transition westward into calcareous organic-rich shales of the Patry Formation (Figs. 6, 7, 8). The Kotcho Formation represents deep-water equivalents to shelf carbonate rocks of the Wabamun Group and Palliser Formation (upper Famennian) in eastern British Columbia and Alberta (Figs. 9, 10; Andrichuk, 1960, Halbertsma, 1994; Moore, 1993; Peterhänsel, 2003). The Kotcho and Tetcho formations occupy mid-ramp to shale basin environments and consist mainly of crinoid, sponge, and brachiopod-bearing shaly limestone, calcareous shale, and limestone (Peterhänsel, 2003). Except for the more proximal parts of the ramp environments, deposition was likely below storm wave base (Peterhänsel, 2003). The Wabamun Group and Palliser Formation consist of limestone and dolostone that were deposited on a broad shelf that transitioned westward into a gently dipping ramp and shale basin, and eastward into evaporates (Fig. 10). Shelf and ramp environments were relatively limited in biodiversity, mainly crinoid meadows and calcite-producing algae (dasycladalean), with the latter disappearing in outer ramp environments (Moore, 1993; Halbertsma, 1994; Peterhänsel, 2003). In northeastern British Columbia, the lithofacies belts defined by the carbonate rocks in the Tetcho and Kotcho formations and the Wabamun Group follow a general northerly trend across the basin (Fig. 10). A similar trend is defined by the disappearance of Kotcho and Tetcho carbonate rocks into grey shales of the Fort Simpson Formation east of or within the Liard Basin (Fig. 4).

In central and southern Alberta, the upper part of the Wabamun Group contains green to grey, calcareous and pyritic shale to argillaceous limestones of the Big Valley Formation, which unconformably overlies carbonate rocks of the Stettler Formation (Fig. 9; Moore, 1993; Halbertsma, 1994; Caplan and Bustin, 1998; Colborne et al., 2015; Johnston et al., 2010). The Big Valley Formation, and its equivalent, the upper Costigan Member of the Palliser Formation, displays rocks and fossil assemblages that suggest sedimentation in water that was deeper than during deposition of underlying Stettler and Morro carbonate rocks (Moore, 1993; Halbertsma, 1994; Caplan and Bustin, 1998; Peterhänsel, 2003).

4.2. Sub-Exshaw Formation unconformity

Halbertsma (1994) and Richards et al. (1994b) suggested that Big Valley units are developed in northeastern British Columbia, particularly in Liard basin. Although Halbertsma (1994) indicated that the Big Valley Formation was largely removed by the sub-Exshaw unconformity east of Liard Basin, shaly sequences in the upper Kotcho Formation east and south of the Liard basin may be equivalent to this unit (Figs. 7, 11). The magnitude of the unconformity at the base of the Exshaw Formation varies across the Western Canada Sedimentary Basin. Generally, as Moore (1993) pointed out, regional sections containing the Exshaw and underlying Wabamun or Palliser horizons display parallelism suggesting a disconformity with little or no hiatus. In southern Alberta and adjacent Saskatchewan, biostratigraphy indicates that that the lower *trachytera* to *lowermost expansa* conodont zones are missing between the Exshaw and Big Valley formations (Fig. 12; Richards and Higgins, 1988; Meijer Drees and Johnson, 1994, 1996; Richards et al., 2002; Johnston et al., 2010). Meijer Drees and Johnston (1996) postulated that the lack of diagnostic fossils of this age is probably due to a combination of a condensed sequence and an environment not suitable for hosting these faunas. Although a disconformity likely exists at the base of the Exshaw Formation across most of northern British Columbia, evidence in the more distal parts, including Liard basin, suggests non-depositional disconformities or even conformable relationships (Fig. 12; Richards and Higgins, 1988; Meijer Drees and Johnston, 1994; Savoy et al., 1999; Richards et al., 2002; Kabanov et al., 2019).

Although a minor disconformity separates the Exshaw and Big Valley formations regionally, considerable pre-Exshaw uplift and erosion is indicated in the southern part of the Liard basin where rocks of the Exshaw Formation lie above units as deep in the section as the lower part of the Kakisa Formation (Fig. 13; see also Fig. 13.52 in Halbertsma, 1994 and Fig. 14.23 in Richards et al., 1994b). Interestingly, in northern British Columbian, this uplift has affected the western edges of the Western Canada Sedimentary Basin. Similar bevelling is seen in the Foothills of Alberta and British Columbia (Richards et al., 2002; Johnston et al., 2010) and in the Peace River arch

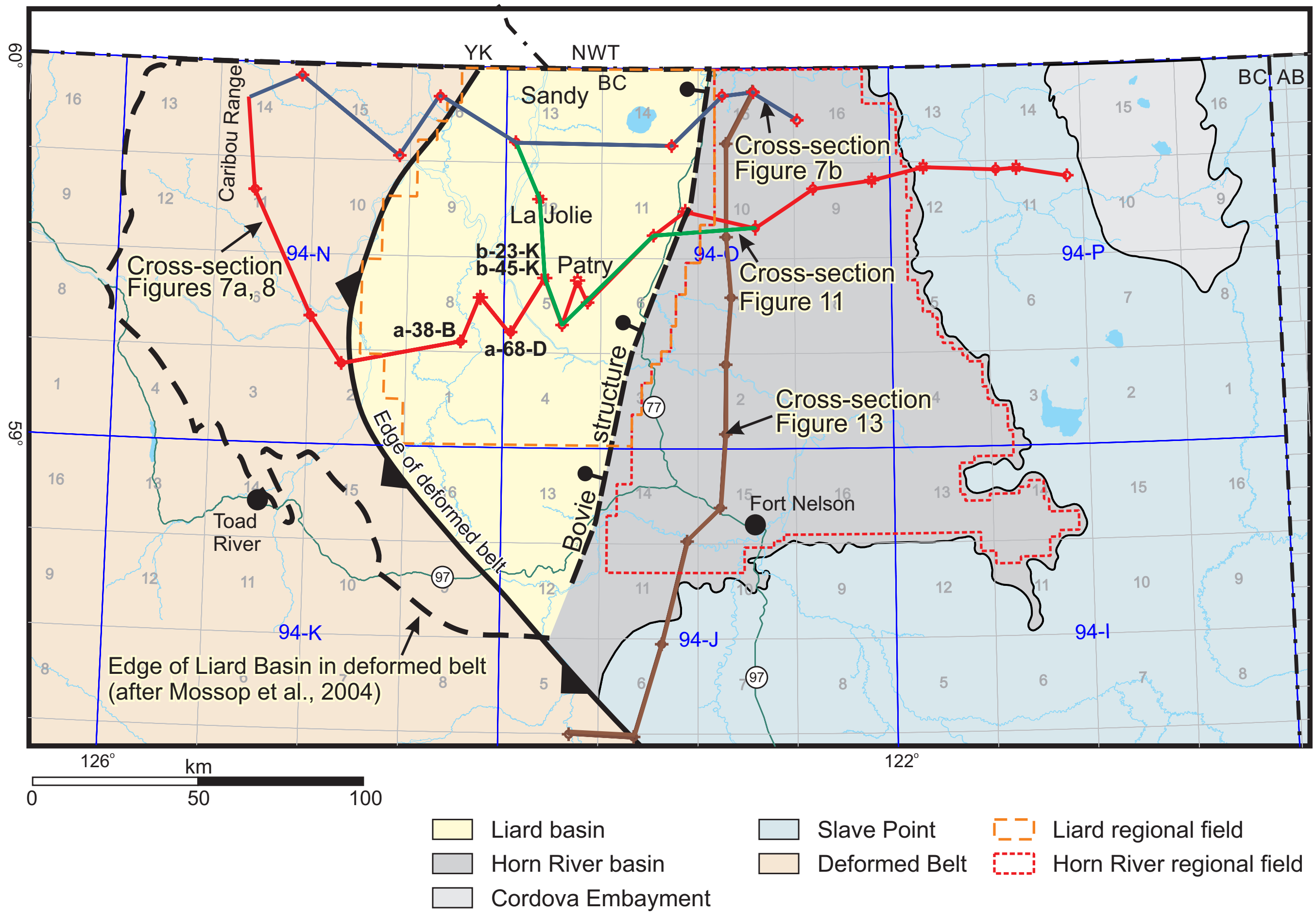

Fig. 6. Outlines of the Liard and Horn River basins with locations of subsurface cross-sections shown in Figs., 7a,7b, 8, 11 and 13. The locations of specific wells shown in Figs. 16, 17, 26, and 28 are also indicated. The names Sandy, Patry, and La Jolie refer to the development areas designated by the British Columbia Oil and Gas Commission that are used in naming well locations.

area of Alberta where an already thin Wabamun stratigraphy is locally absent (Halbertsma, 1994; Meijer Drees and Johnston, 1996). Johnston et al. (2010) have attributed excessive bevelling in southern Alberta to a peripheral bulge related to Antler orogeny-aged deformation farther west. The unconformity at the base of the Exshaw Formation in the Liard basin area may also be tied to Antler-aged deformation but related to back-arc basin extensional processes rather than a consequence of thrust loading.

4.3. Antler-aged orogenesis and Liard basin

As described above, Middle to Late Devonian convergent processes in the Arctic (Ellesmerian orogeny) resulted in southerly directed shortening and coarse siliciclastic sedimentation (Figs. 3a, 10; Imperial clastic wedge, Tuttle Formation molasse). In the middle part of the Besa River Group, the Fort Simpson Formation (Fig. 2) likely represents the southern distal extension of the Ellesmerian Imperial clastic wedge. In addition, the deposition of transgressive organic-rich shales of the Muskwa Formation and the southeastern shift of Leduc carbonate reef margins in the southern part of the Western Canada Sedimentary Basin at the beginning of the Frasnian is likely a reflection of the loading and clastic input related to this shortening.

Although Famennian to Tournaisian siliciclastic rocks of the southern Front and Main ranges of the Rocky Mountains are considered to have been derived, in part, from western sources (Richards et al. 1993; Savoy et al., 2000; Richards et al., 2002), the composition and limited extent of coarse-grained deposits of this age farther west are consistent with local sources, suggesting uplift and erosion of underlying stratigraphy in response to extensional block faulting (Gordey and Anderson, 1993). Furthermore, the feldspathic composition for some of the westerly sourced material recognized in the southern Front Ranges suggests it was likely shed from the incipient volcanic arc system developed along the western edge of Ancestral North America before opening of the Slide Mountain ocean.

Volcanic ash layers in the lower black shale member of the Exshaw Formation and the lower black shale unit of the overlying Banff Formation are more direct manifestations of Antler-aged orogenesis in the Western Canada Sedimentary Basin. These ash beds, with U-Pb zircon ages of ca. 360 Ma (Richards et al., 2002; Ferri et al., 2015; see details below) that are near the frequency peak of mid to late Paleozoic magmatism

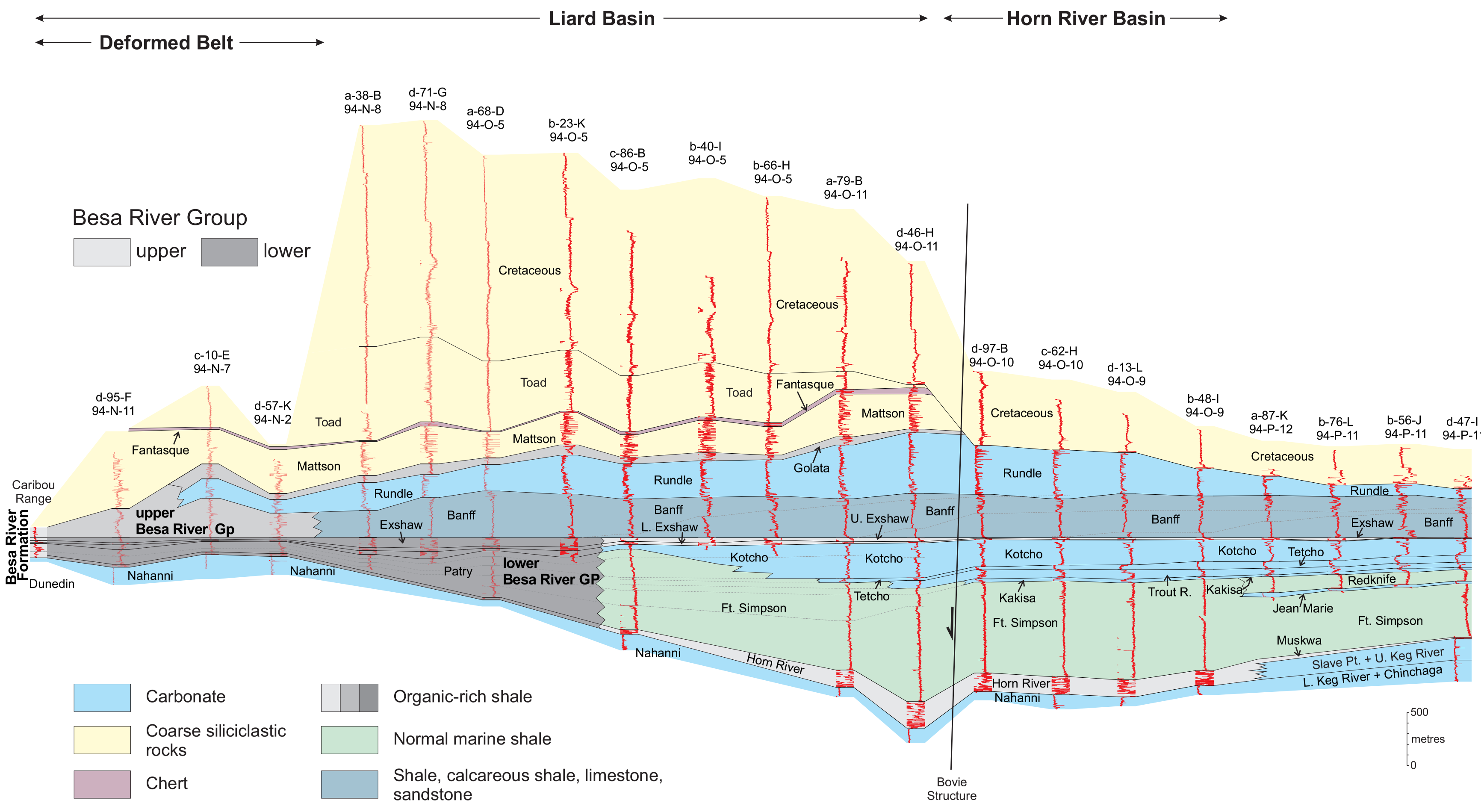

Fig. 7. a) East-west cross-section extending from the western edge of the Cordova embayment across the Horn River and Liard basins into the Caribou Range in the Mackenzie Mountains based on well data. The top of the Exshaw Formation is used as the datum; the gamma-ray trace for each well is shown in red line. This section displays the westward disappearance of Middle Devonian to Middle Mississippian carbonate rocks into shales of the Besa River Group. The Besa River Group begins west of the shale-out of the Kotcho Formation. **b)** East-west cross-section from east of the Bovie fault west to the Caribou Range using the top of the Nahanni Formation as a datum. This section illustrates in detail the disappearance of the Kotcho Formation and the correlation of subsurface marker units that are lacking in the condensed Besa River section exposed in the Caribou Range. See Fig. 6 for section locations.

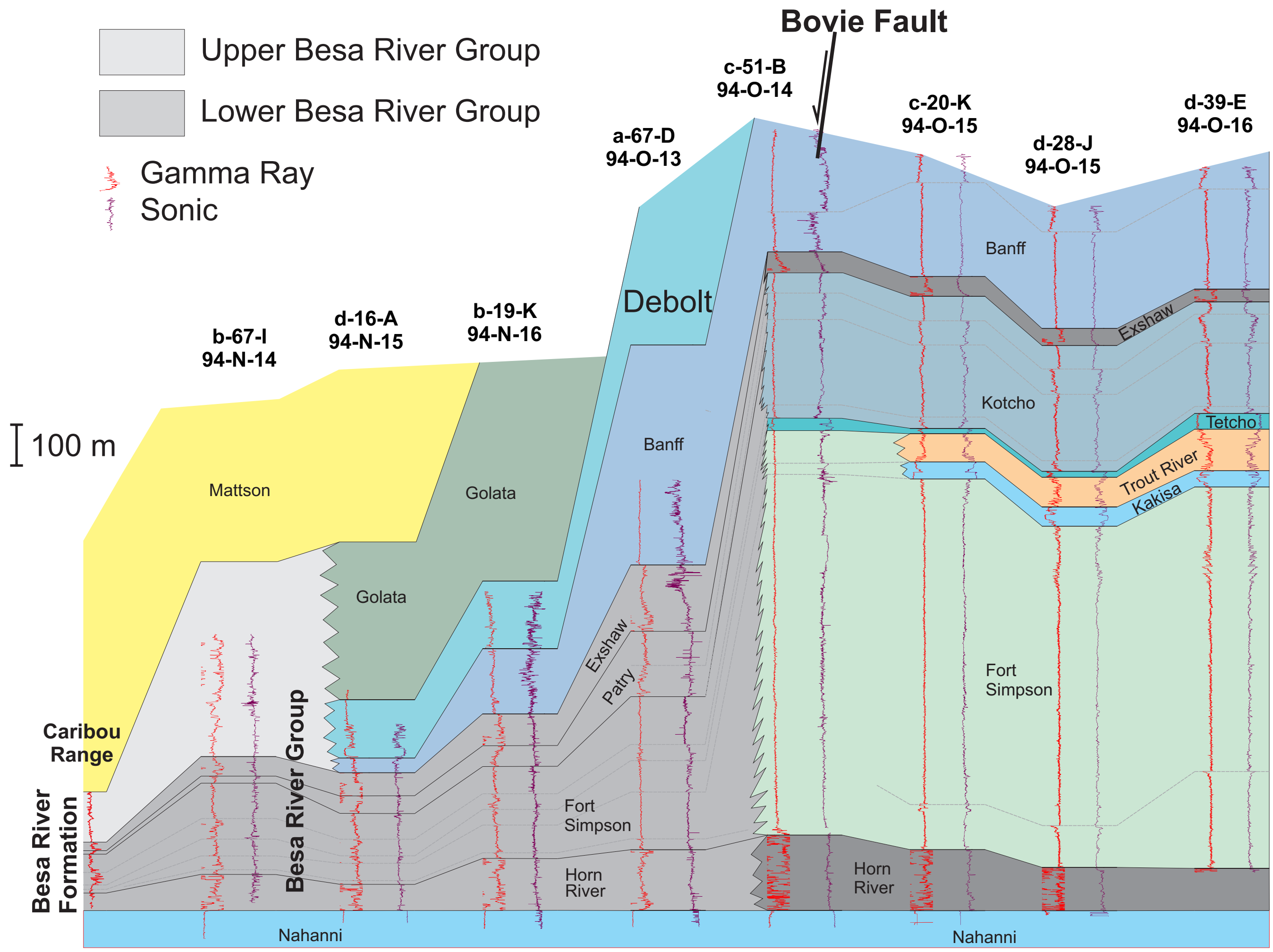

Fig. 7. continued.

documented in Ancestral North American rocks (Nelson et al., 2006), were likely derived from volcanic centres along the western edge of Ancestral North America.

In the Carboniferous, it is likely that back-arc extensional tectonics tied to the opening of the Slide Mountain ocean (Fig. 3b) led to the deposition of Stoddart Group siliciclastic rocks of the Fort St. John graben (Fig. 3c; Douglas et al., 1970; Barclay et al., 1990; Nelson et al., 2006). It is also probable that the accommodation space for similarly aged siliciclastic rocks of the Mattson Formation in Liard basin was produced by motion on the Bovie structure (Richards et al., 1993). Regional isopach maps of Exshaw and Carboniferous siliciclastic rocks in the Western Canada Sedimentary Basin outline orthogonal depocentres in the Peace River area that likely link with the Liard basin (Fig. 14). Barclay et al. (1990) and Richards et al. (1994b, their Figures 14.14, 14.19, 14.24) have shown that thickness variations in the Banff Formation record extension in the Peace River embayment and along its west margin began as early as the Tournaisian, and isopach maps of the Exshaw Formation also show thickening within the outline of the Peace River embayment and Liard basin (Fig. 14; Fig. 13.26 in Halbertsma 1994), which would indicate that sub-basin generation initiated even earlier, in the latest Famennian. This is supported by irregular uplift (block faulting) and erosion of Kakisa to Kotcho formations in the Liard basin before deposition of the Exshaw Formation (Fig. 13). Finally, the general north-south trending facies patterns within the Wabamun Group and equivalent units (Figs. 4, 10), that run parallel to the Bovie structure, and the orientation of subsequent Carboniferous siliciclastic depocentres suggest that back-arc extension in the west was controlling deposition of more proximal successions.

5. Elevation of Besa River Formation in the subsurface to group status

The name Besa River Formation was first used by Kidd (1963) in the Rocky Mountains of northeastern British Columbia. The name was later extended into the subsurface of Liard basin (Pan American Petroleum Ltd., 1967), although its application has been inconsistent (Apache Canada Ltd., 2012; Nexen Energy, 2014a, b). Generally, 'Besa River Formation' is

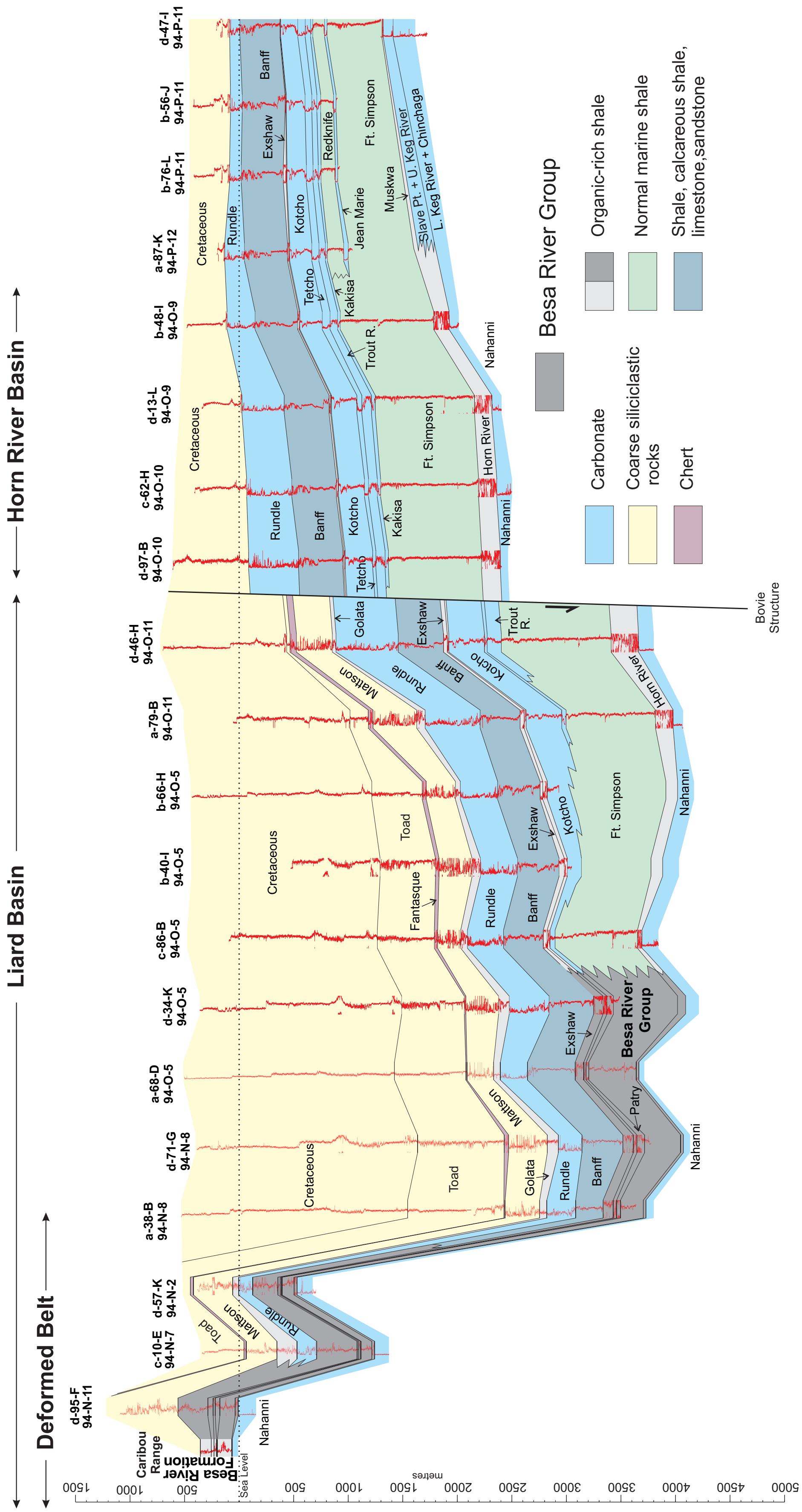

Fig. 8. The same line of section as in Fig. 7a, but using the surface elevation of each well as a datum to illustrate the displacement on the Bovie fault and highlight the depths at which the Patry and Exshaw formations are encountered (4-5 km).

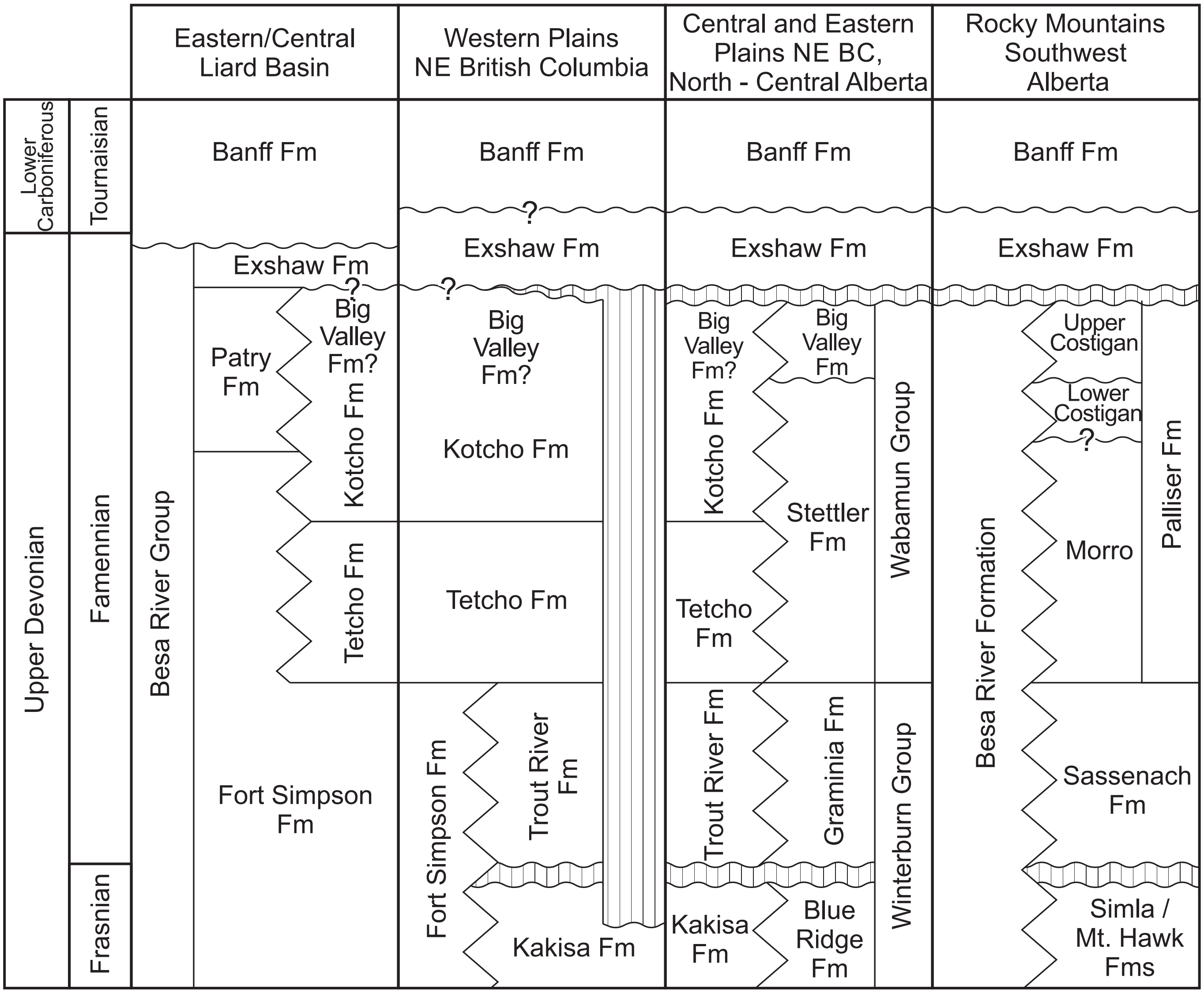

Fig. 9. Generalized correlation of Late Frasnian to Early Tournaisian strata along the British Columbia-Alberta portion of the Western Canada Sedimentary Basin. Unconformities are displayed by wavy lines, with a vertical hatch pattern representing periods of significant erosion. Modified from Moore (1993), Halbertsma (1994), and Peterhänsel (2003).

applied to shales below the Banff Formation, where the upper part of the Kotcho Formation is replaced westward by a thick, organic-rich radioactive zone (Figs. 2, 6-8; Patry member of Ferri et al., 2015, Patry Formation herein, see below). This organic-rich horizon is immediately below a thickened basal Exshaw Formation which, together with the Patry Formation, has been commonly termed the "first black shale" (Pan American Petroleum Ltd., 1960; Apache Canada Ltd., 2012; Poco Petroleum Ltd., 2000; British Columbia Ministry of Energy and Mines, 2005). Ross and Bustin (2008) subdivided the Besa River Formation in central Liard Basin into the 'upper black shale, the middle shale and the lower black mudstone members, with the upper member equivalent to the Exshaw Formation and the lower member being equivalent to the Horn River Formation (Fig. 15).

Although relatively uniform in outcrop (e.g., Ferri and Reyes 2019 a, b), and superficially uniform in core and cuttings, petrophysical subsurface logs allow discrete formations units with distinctive radioactive markers to be recognized in what has traditionally been referred to as the Besa River Formation (e.g., the Horn River and Exshaw formations; Ferri et al., 2015; Ross and Bustin, 2008, Fig. 7) and thus we propose the unit be elevated to group status in the subsurface of Liard basin. We recommend that the term Besa River Group be used, west of where the Kotcho Formation disappears, for rocks between the top of the Nahanni/Dunedin Formation and the base of the Banff Formation (Figs. 2,7). Farther west, as carbonate rocks in the upper part of the Banff Formation and Rundle Group disappear, the upper contact of the Besa River Group is at the base of the Mattson Formation, in part including shales equivalent to the Golata Formation. The top of the Exshaw Formation would thus mark the boundary between the upper and lower parts of

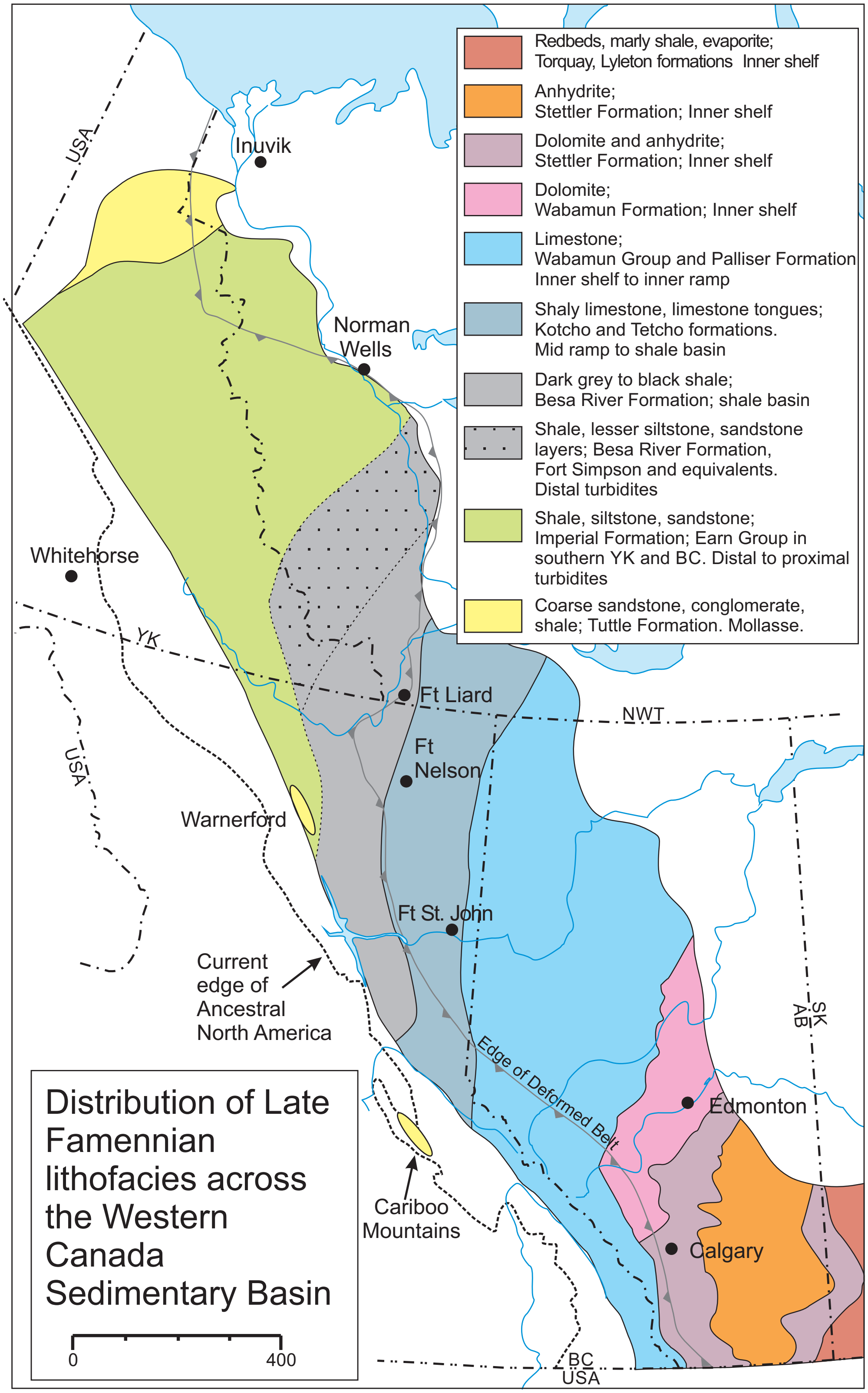

Fig. 10. Distribution of late Famennian lithofacies across the Western Canada Sedimentary Basin. Carbonate shelf facies transition northwestward into ramp and deep-water basin facies. Modified from Moore (1993); Halbertsma (1994); and Peterhänsel (2003) Farther northwest, deep-water shales record influx of turbidites sourced from uplifted terranes in the northern Yukon and Northwest Territories. Coarse siliciclastic rocks are also recorded in the Warneford area of the Kechika trough (MacIntyre, 1998) and in the Cariboo Mountains of southern British Columbia (Struik, 1988).

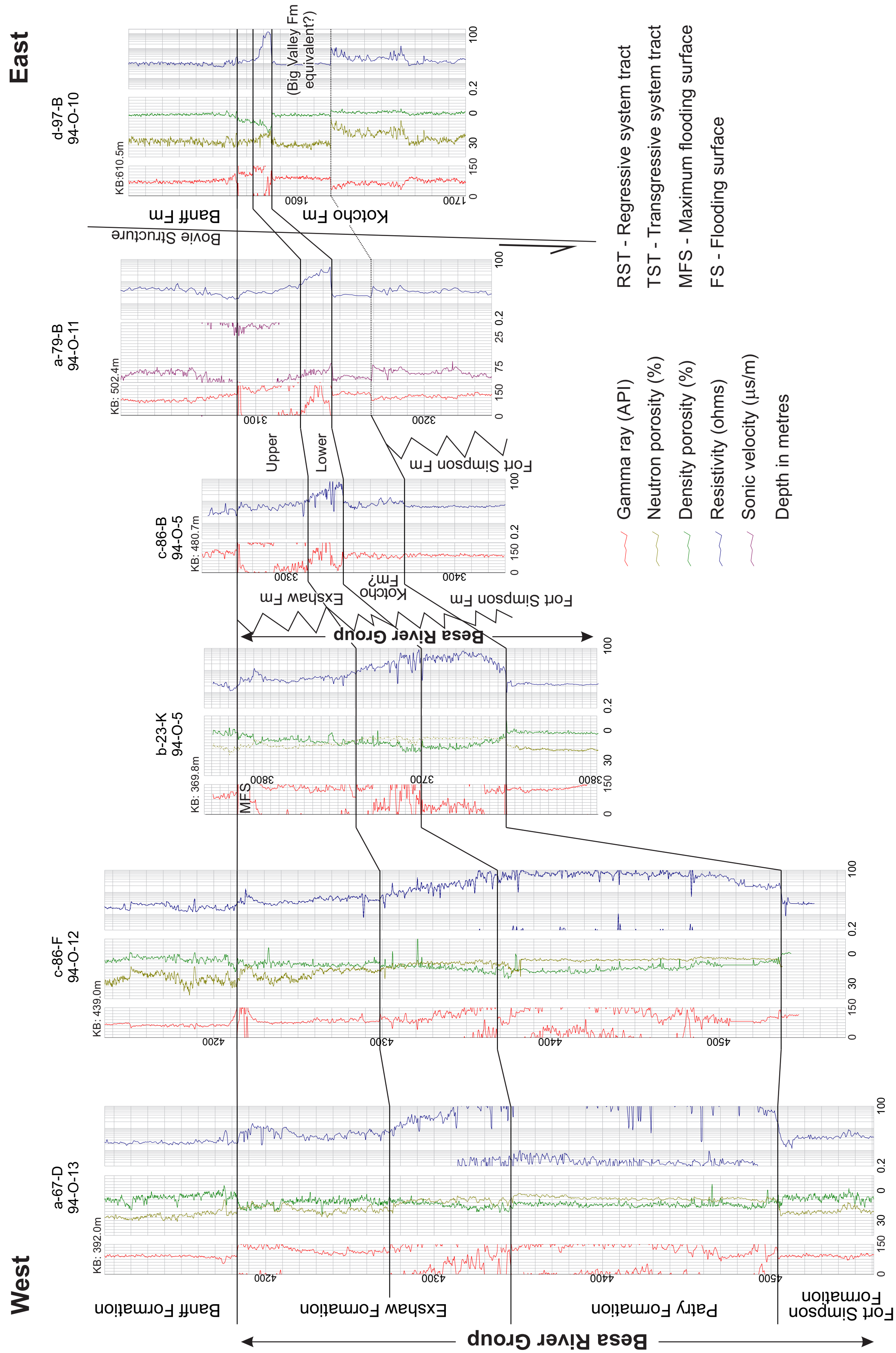

Fig. 11. Stratigraphic correlation of the Exshaw Formation and its equivalents from Horn River basin, across the Bovie structure, and into Liard basin. The Exshaw and Patry formations thicken markedly across the Bovie structure, and the Kotcho Formation disappears westward at the expense of the Patry Formation. The datum is the top of the Exshaw Formation; see Fig. 6 for location.

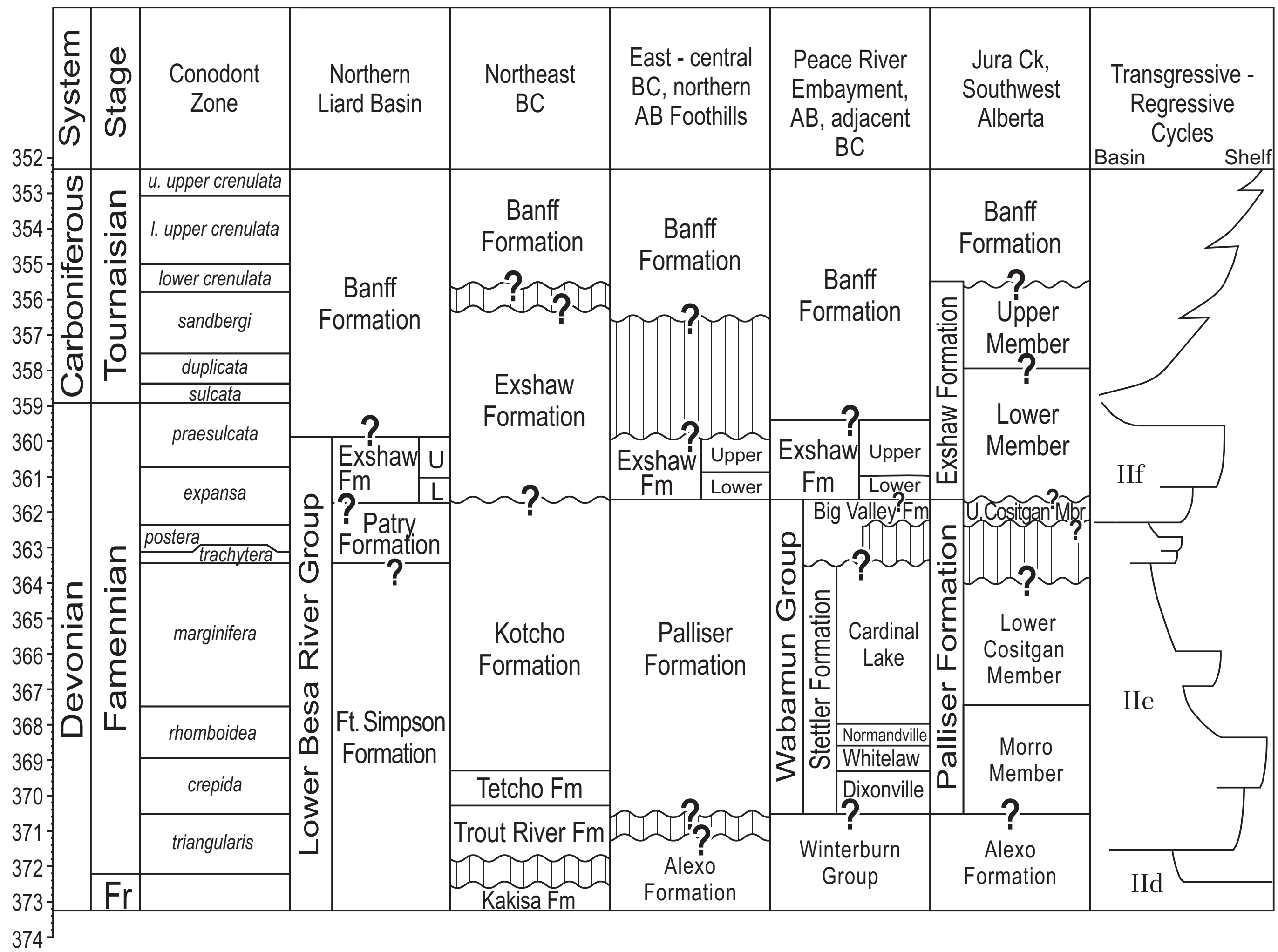

Fig. 12. Lithostratigraphic correlation relative to conodont zonation, modified after Richards et al. (2002). Conodont zonation for the Famennian is from Kaufmann (2006) and for the Tournaisian from the International Commission on Stratigraphy (2017). The absolute time scale is from (Cohen et al., 2013). Vertical lines between unconformities indicates non-deposition; question marks indicate that the position of boundaries relative to conodont zonation is uncertain. Devonian transgressive-regressive cycles are modified from Morrow and Sandberg (2008); the Carboniferous curve is interpreted from Ross and Ross (1985, 1988). Stratigraphic data are from Johnston and Chatterton (1991), Geldsetzer et al. (1993), Johnston and Meijer Drees (1993), and Richards et al. (2002). Jura Creek in southwestern Alberta is the type section for the Exshaw Formation. The uncertainty in ages on this diagram are with respect to conodont zonation. Fr-Frasnian.

the Besa River Group (Figs. 2, 7).

Correlation of subsurface Besa River Group sections into surface exposures in the Caribou Range based on gamma ray traces is shown at the western end of Figs. 7a and b. This interpretation suggests that exposed Horn River equivalent strata are likely very thin and that the first (from the base) radioactive zone in the Besa River Formation originally correlated with the Muskwa horizon by Ferri et al. (2011) is a radioactive zone in stratigraphy that is equivalent to the middle part of the Fort Simpson Formation (Fig. 7). This radioactive horizon becomes more pronounced towards the west. In the western Rocky Mountains and Mackenzie Mountains of northernmost British Columbia, the Besa River Formation rests on Middle Devonian carbonate rocks of the Dunedin Formation, equivalent to the lower part of the Keg River Formation of Horn River Basin (Taylor and Stott, 1999; McMechan et al., 2012; Fig. 7). Farther west, in Ketchika trough and Selwyn basin, the Besa River Formation is represented by the Earn Group. Here, the underlying Dunedin Formation and carbonate rocks of the Stone to Nonda formations transition into shales and siltstones of the Road River Group.

6. Analysis of uppermost Devonian to lowermost Mississippian organic-rich strata in Liard basin: the Patry Formation (new status) and the Exshaw Formation

In central Liard Basin, shales in the upper part of the Kotcho Formation grade westward into black, organic-rich shales that we define formally below as the Patry Formation (Fig. 2; originally informally designated as the 'Patry member' by Ferri et al., 2015). Together with the lower part of the overlying

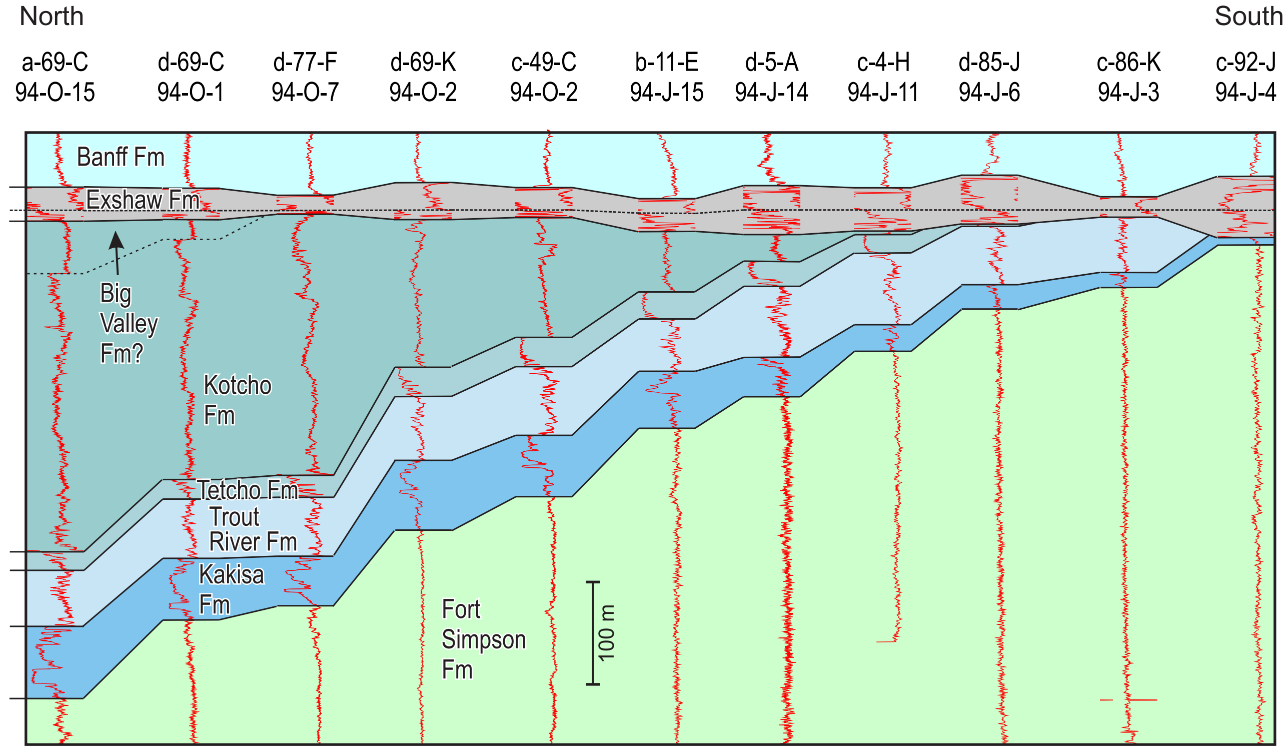

Fig. 13. North-south cross-section, western Horn River basin illustrating the southward erosion of units below the Exshaw Formation. Datum is at the base of the Exshaw Formation, gamma ray log in red. See Fig. 6 for location.

Exshaw Formation, these units comprise the horizon currently being developed for shale gas resources. In the following we detail both units based on examination and analyses of cores from four wells: Chevron-Woodside Patry b-23-K; Chevron-Woodside La Jolie b-3-K; Nexen Energy Patry a-68-D; and Nexen Energy a-38-B Dunedin (see Fig. 6 for locations).

6.1. Patry Formation (new status)

Previously referred to as the informal ‘Patry member’ by Ferri et al. (2015), herein we formally introduce the name ‘Patry Formation’ for organic-rich, calcareous shale and shale in the Besa River Group above the Fort Simpson and beneath the Exshaw Formation. The name is taken from Patry Creek, near the type section penetrated by the Chevron-Woodside Patry b-23-K well. Based on petrophysical logs and using measured drill depths, the top of the unit in the well is at 3723.7 m and the bottom is at 3774.1 m (Fig. 16). In core, as recorded by the driller, the bottom contact is at 3777.4; the upper contact was not recovered in core (Fig. 16). Complete cores of the unit were also obtained from the Nexen Energy Patry a-68-D, Nexen Energy Dunedin a-38-B (Fig. 17), and Chevron-Woodside La Jolie b-3-K wells, which can serve as reference sections.

6.1.1. Contact relationships

On gamma ray curves, the Patry Formation has values that are intermediate between those of the Fort Simpson and Exshaw formations (Figs. 16, 17). The upper contact of the Patry Formation is taken as the base of the highly radioactive zone defining the Exshaw Formation. The lower contact corresponds to the appearance of lower gamma ray counts typical of Fort Simpson shales, which commonly coincides with a sharp gamma ray spike and a pronounced decrease in resistivity (Figs. 16, 17). The high organic content and gas saturation of the unit also deflects the combined density and neutron curves into close proximity or to cross-over and it has a higher resistivity than underlying Fort Simpson shales (Figs. 16, 17). Lithologically, the upper contact is gradational, with carbonate laminations that characterize the Patry Formation developed in the lower few m of the Exshaw Formation, and thus the regional sub-Exshaw unconformity (see above) appears to be lacking. This transition is well expressed in the Chevron-Woodside La Jolie b-3-K core (Kabanov et al., 2019). The lower contact with the Fort Simpson Formation is gradational across several cm, with the organic content and dark colour decreasing down section. In the Chevron Woodside Patry b-23-K core, the base of the unit is a 20 cm-thick zone of bedded or disseminated pyrite, which corresponds to the gamma ray spike shown in Fig. 16.

6.1.2. Lithology

Although the Patry Formation is defined primarily on its petrophysical log signature, it also contains distinct lithologic characteristics. Relative to the Exshaw Formation, the Patry Formation is more calcareous and, in its upper half, contains abundant calcareous turbidite-like layers (Figs. 18, 19). Calcareous laminations up to a few mm thick are locally graded and commonly display lenses that resemble starved ripples

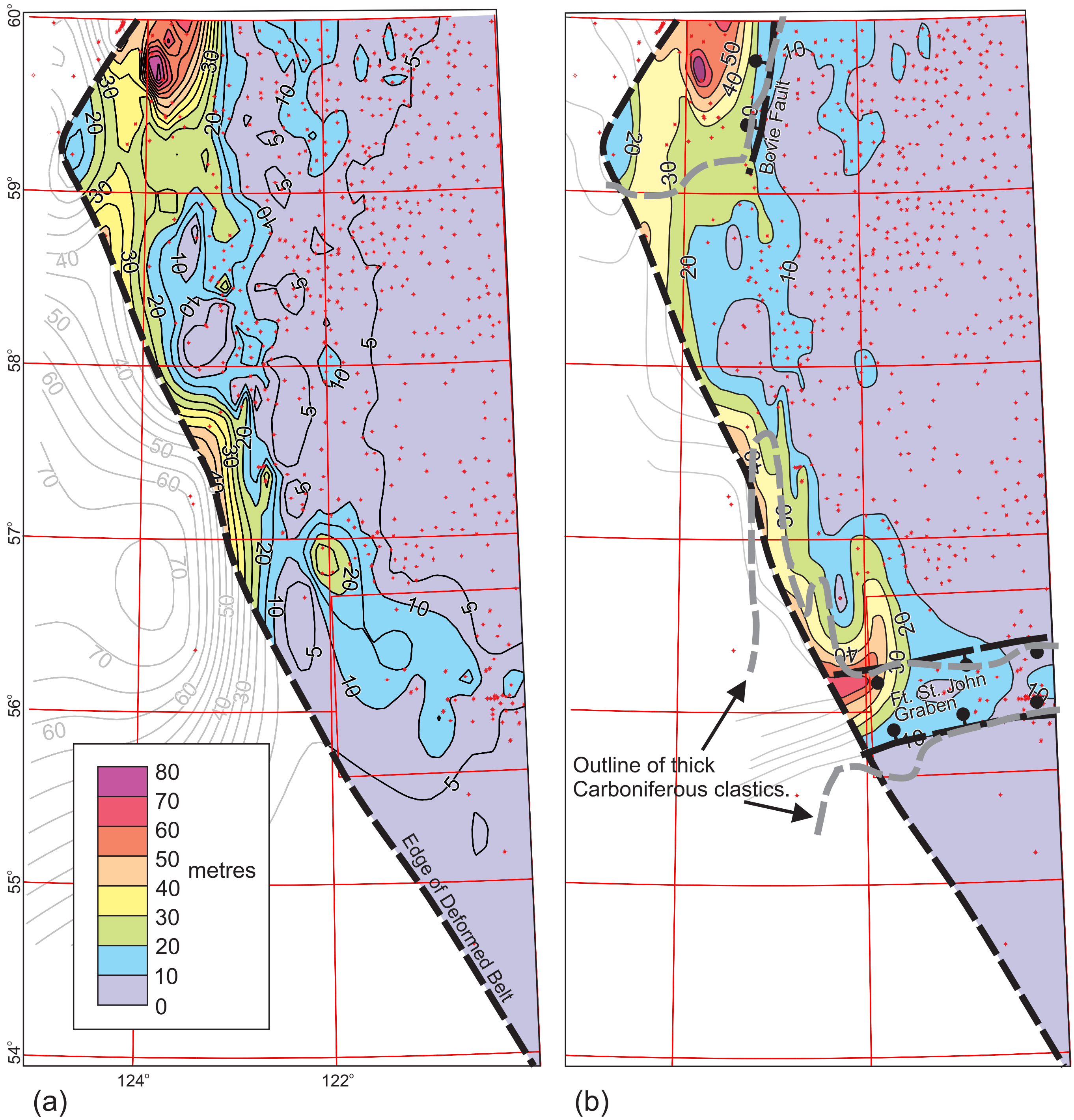

Fig. 14. Contoured isopach maps of the lower Exshaw Formation using about 500 data points. Data were gathered within the GeoSCOUT® software platform. **a)** Data contoured using the Golden Software Surfer 8® program, applying a minimum curvature algorithm. **b)** Hand contouring of the same data with interpretation highlighting the area of the Dawson Creek Graben complex. A north-south structural grain displayed by the data follows the trend of the Bovie structure and is roughly orthogonal to the Dawson Creek graben. Grey dashed lines delineate thick Carboniferous siliciclastic rocks that form depocenters roughly coinciding with the Fort St. John graben and the area west of the Bovie fault zone (i.e. Liard Basin). The distribution of thick Carboniferous sections also suggests a north-south trending sub-basin on the north side of the Fort St. John graben that is likely bounded on the east by a fault roughly parallel to and on strike with the Bovie structure.

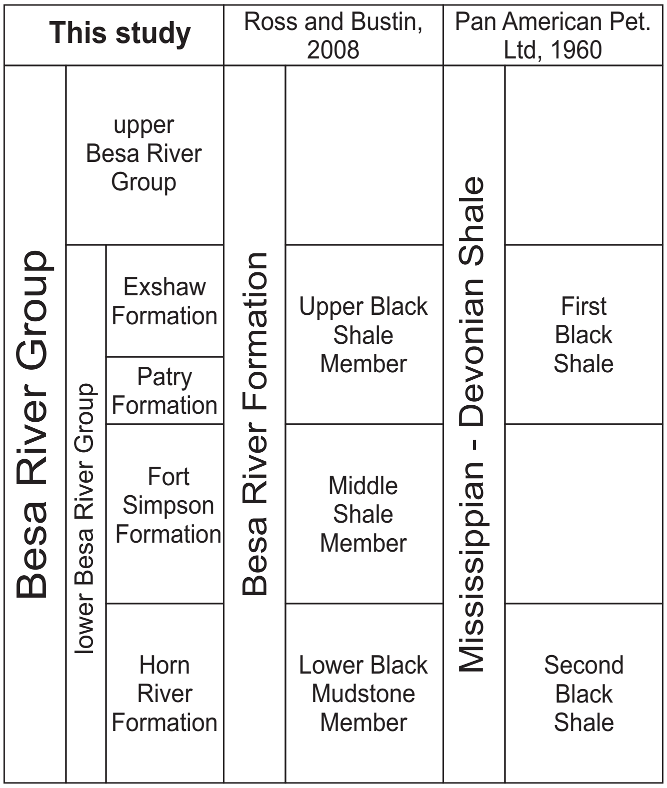

Fig. 15. Comparison of terminology used to describe Besa River shales in the subsurface of Liard Basin.

(Fig. 19). These calcareous laminations locally display sharp bases and grade upward into darker, organic-rich layers likely formed by passive settling of suspended material between mass flow pulses. Some horizons contain crinoid ossicles, other shell fragments, and radiolarian tests (Figs. 18, 20). Lenses or thin layers of finely crystalline pyrite are also common (about 6 % nodules or crystal masses, Fig. 19).

The abundance of calcareous laminations decreases towards the base of the Patry Formation, as does the overall carbonate content, but disseminated to nodular pyrite is common. Basal layers grade to slightly calcareous grey to dark grey shale to siltstone that is less carbonaceous than those in the Patry and Exshaw formations and outwardly resembles the Fort Simpson Formation.

6.1.3. Age, correlation, and distribution

Direct geochronologic data are lacking from the Patry Formation, but U-Pb zircon ages from tuffs at the base of the Exshaw Formation of ca. 364 Ma (see below) indicate that it is late Famennian. The Patry Formation correlates with the upper part of the Kotcho Formation in the subsurface to the east (Fig. 12). The unit is currently only recognized in the central and western parts of Liard Basin and extends into the outcrop belt of the Rocky Mountains, although Ferri et al. (2011, 2012) and Ferri and Reyes (2019a, b) did not recognize the unit in measured sections within western-most parts of Liard basin. Subsurface mapping indicates it thickens to the north, with as much as 200 m of section at the British Columbia-Yukon border (see below).

6.2. Exshaw Formation

In central and eastern Liard basin, dark organic-rich shales of the Exshaw Formation lie between calcareous shales of the Banff Formation and those of either the Patry or Kotcho formations (Figs. 11, 16, 17). These shales correlate with the lower part of the Exshaw Formation as defined at its type section in southern Alberta (Warren, 1937; Macqueen and Sandberg, 1970; Richards et al., 1994a; Richards et al., 2002). The silty limestones and dolostones in the upper part of the type section are not developed in Liard basin. Calcareous siltstone that may correspond to this upper unit was only observed east of the Foothills in the southern part of the Fort Nelson map area. This area experienced significant pre-Exshaw uplift and erosion and may have remained high during Exshaw deposition, which resulted in shallower water calcareous sedimentation. The subsurface definition of the Exshaw Formation in Liard basin is similar to that presented by Richards et al. (1994b) and by industry workers. In southern Alberta and parts of British Columbia, the lowermost Banff Formation contains radioactive dark shale above the upper part of the Exshaw Formation (Richards et al., 1994a; Caplan and Bustin, 1998; Richards et al., 2002). Caplan and Bustin (1998) have shown that, as the calcareous siltstone in this subunit disappears, the lowermost shales of the Banff Formation merge with radioactive shales in the lower part of the Exshaw Formation and are difficult to separate on logs. As described above, the sub-Exshaw unconformity is not developed in Liard basin, and the transition from the Patry Formation to the Exshaw Formation appears gradational.

6.2.1. Lithology

The upper part of the Exshaw Formation in the Liard basin consists of dark grey to black carbonaceous and siliceous mudstone to shale displaying poor partings and thin laminations up to 2 mm thick (Figs. 18, 19). Light grey silty horizons locally have sharp bases and intervening darker horizons have higher organic carbon contents. The lower part of the Exshaw Formation is slightly paler, contains better developed laminates, and can be slightly calcareous or contain sporadic, thin graded calcareous layers similar to those in the Patry Formation. Radiolarian remains are common, either dispersed or concentrated in horizons several cm thick (Fig. 20). Felsic tuffs are in the upper part of the Exshaw Formation in the Nexen Energy Dunedin a-38-B well and in the lowermost part, just above the contact with the Patry Formation, in cores from Nexen Energy Dunedin a-38-B (Fig. 17) and Chevron -Woodside Patry b-23-K (Fig. 20).

6.2.2. U-Pb geochronology

Three samples of felsic tuff were collected for U-Pb zircon geochronology. CA-TIMS analyses were carried out at the Pacific Centre for Isotopic and Geochemical Research, at

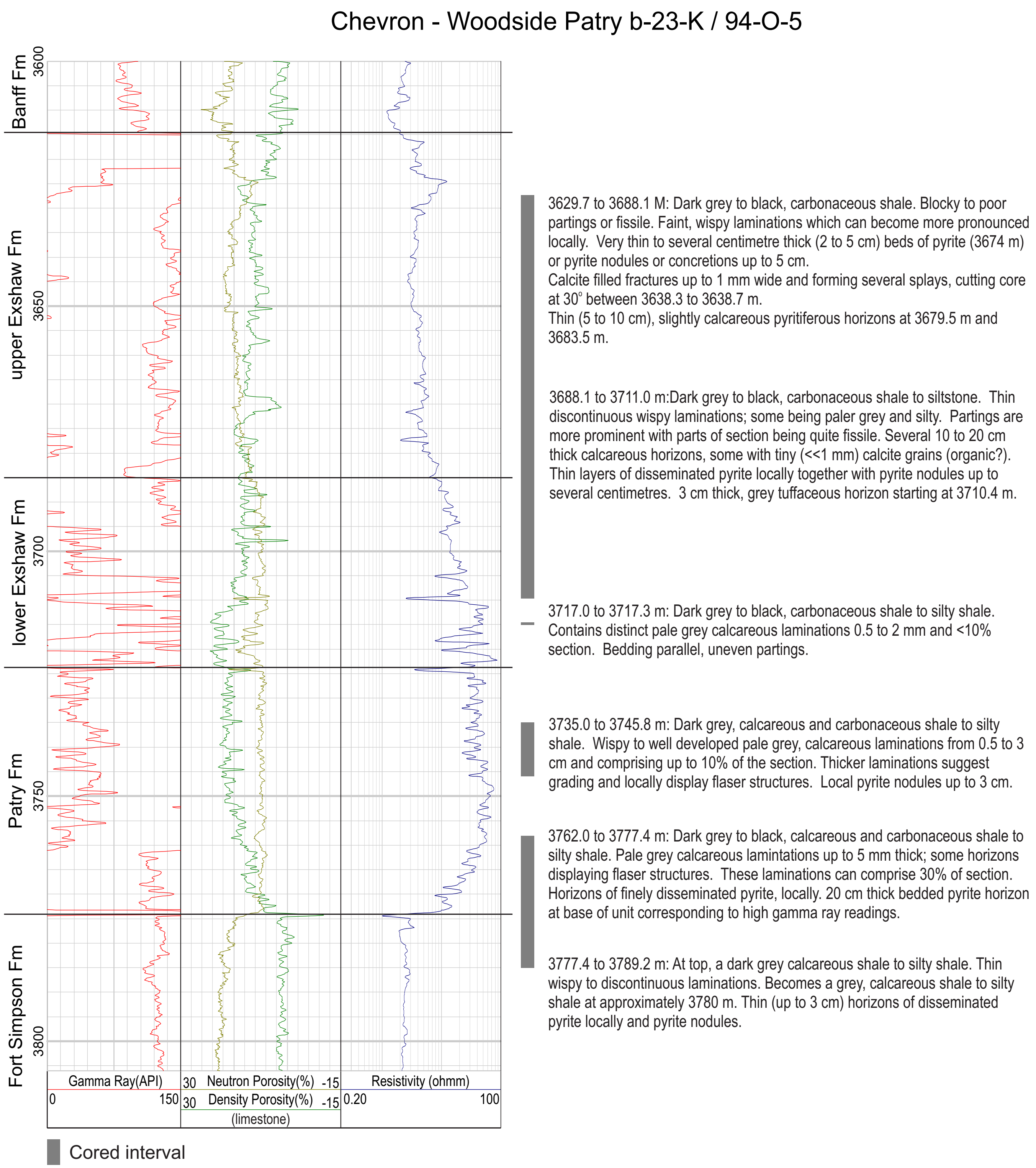

Fig. 16. Patry Formation-Exshaw Formation section in the Chevron-Woodside Patry b-23-K well, the type section of the Patry Formation. Elevation is measured below KB (kelly bushing, which is 369.8 m above sea level). The gamma ray scan of the core was used to adjust the position of the core so as to match the true vertical depth profile of the well.

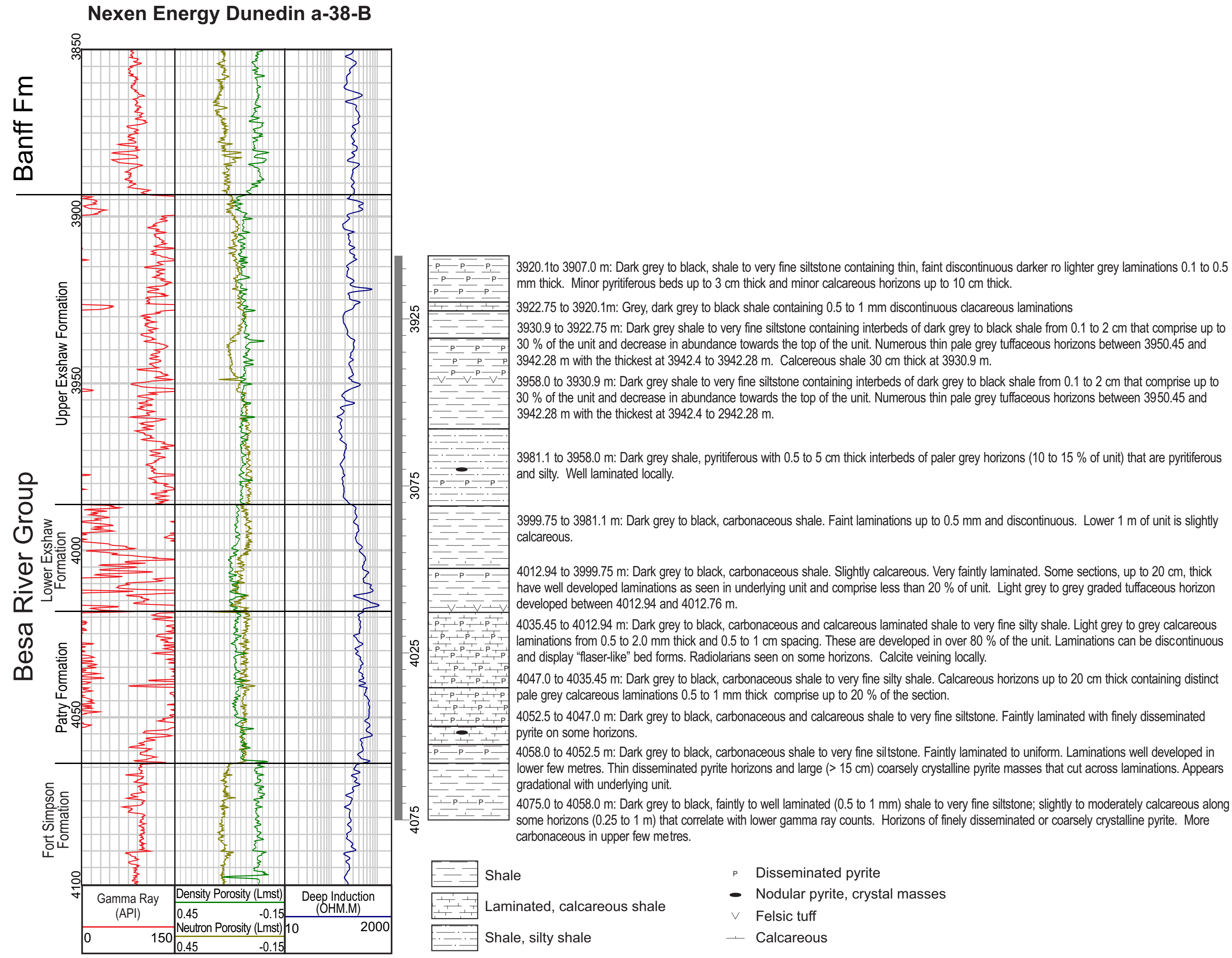

Fig. 17. Patry Formation-Exshaw Formation section in the Nexen Energy Dunedin a-38-B well, a reference section for the Patry Formation. Elevation is measured below KB (kelly bushing, which is 546 m above sea level). The gamma ray scan of the core was used to adjust the position of the core so as to match the true vertical depth profile of the well.

the University of British Columbia (See Appendix 2.1.1.for method details and Appendix 1 for full analytical results). Tuff in all samples is grey to pale grey and consists of fine to coarse fragments of quartz, feldspar, muscovite and grey aphanitic rock fragments (Fig. 20). Tuff at the very base of the Exshaw Formation in the Nexen Energy Dunedin a-38-B well yielded an age of 364.35 ± 0.26 Ma (Fig. 21c, Appendix 1). Tuff in middle of the lower part of the Exshaw Formation in the Chevron -Woodside Patry b-23-K well yielded an age of 364.03 ± 0.31 Ma (Fig. 21b; Appendix 1) and tuff in the middle of the upper part of the Exshaw Formation from the Nexen Energy Dunedin a-38-B well contained zircons that returned an age of 363.07 ± 0.25 Ma (Fig. 21a, Appendix 1).

6.2.3. Sedimentation rates, age, and correlation of the Exshaw Formation

The high precision of the new U-Pb zircon ages and the accurate position of the samples enables us to calculate a sedimentation rate of 18.2 ± 7.0 Ka/m (5.5 cm/Ka) for lower to middle Exshaw Formation deposits in the Nexen Dunedin a-38-B well. Assuming that the same sedimentation rate applies for the entire Exshaw Formation, we calculate that the age of rocks at the top of the unit is about 362.2 Ma, which implies that the Devonian-Mississippian boundary (ca. 358.9 Ma, Cohen et al., 2013) is 10s of m higher in the section, and occurs within the Banff Formation. In contrast, biostratigraphic data from southern Alberta indicate that this boundary is in the

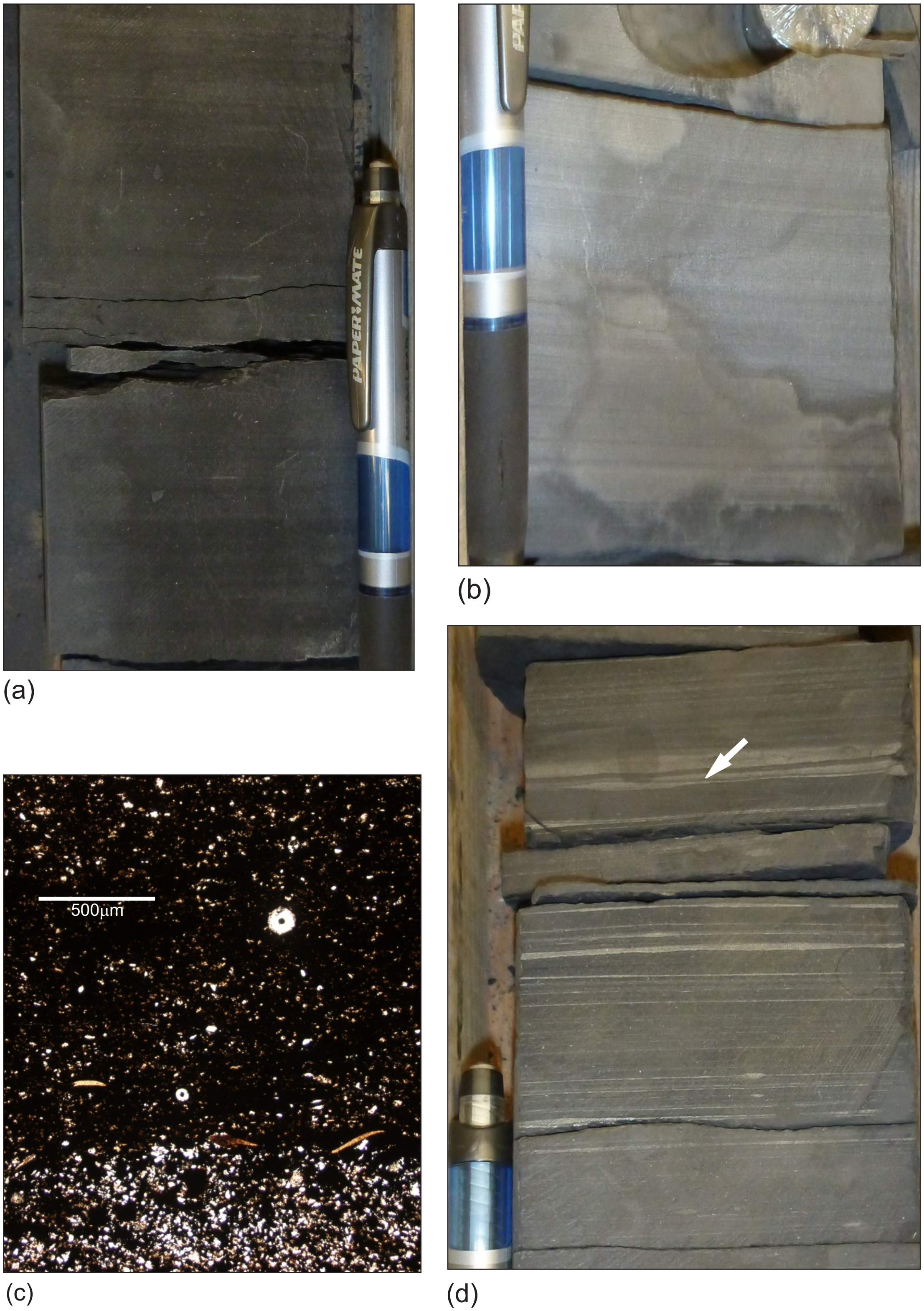

Fig. 18. Photographs of core from the Exshaw and Patry formations of the Chevron-Woodside Patry b-23-K well. **a)** Rhythmically laminated dark grey mudstone to shale in the upper part of the Exshaw Formation at the 3657.75 m level. The lighter grey horizons commonly show sharp bases and grade into overlying darker grey and more organic-rich horizons. **b)** Laminated and slightly paler grey shale to mudstone, lower part of the Exshaw Formation, 3699.5 m level. **c)** Photomicrograph of dark grey laminated and calcareous shale in the lower part of the Patry Formation, 3775.2 m level. Note crinoid ossicles and shell fragments. **d)** Dark grey calcareous mudstone to shale in the upper part of the Patry Formation containing light grey detrital carbonate layers that locally form discontinuous lenses, 3736.25 m level. The carbonate layers locally have sharp bases and appear to grade into dark grey shale or mudstone. The dark grey layer near the top of the core (arrow) may cap a flattened ripple.

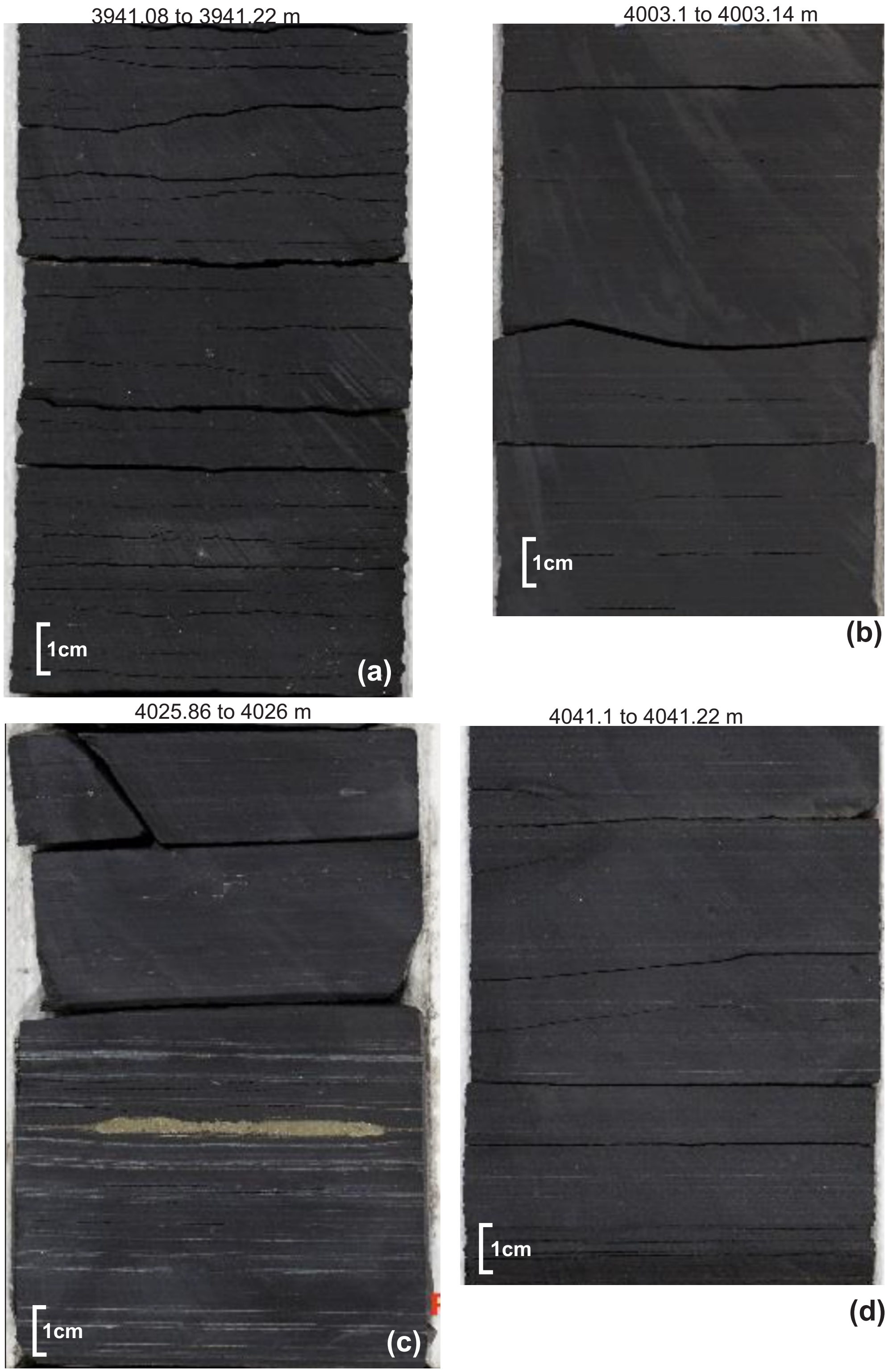

Fig. 19. Photographs of core from the Exshaw and Patry formations of the Nexen Energy Dunedin a-38-B well, from Nexen Energy Ltd. (2016). **a)** Dark grey to black, faintly laminated shale to mudstone in the upper part of the Exshaw Formation; 3941.08 and 3941.22 m. **b)** Laminated, dark grey to black, slightly calcareous mudstone from the lower part of the Exshaw Formation; 4003.01 to 4003.14 m. **c)** Dark grey to black, calcareous mudstone from the upper part of the Patry Formation displaying the distinctive discontinuous pale grey, calcareous horizons. These are not as well developed as in the Chevron-Woodside Patry b-23-K well and may be a reflection of being located farther west of the sediment source; 4025.85 to 4026 m. Pale yellow pyrite forms a thin lens in the centre of the section. **d)** Dark grey to black, calcareous mudstone from the lower part of the Patry Formation; 4041.1 to 4041.2 m. The discontinuous, pale grey calcareous horizons are thinner and not as well developed as in the upper part.

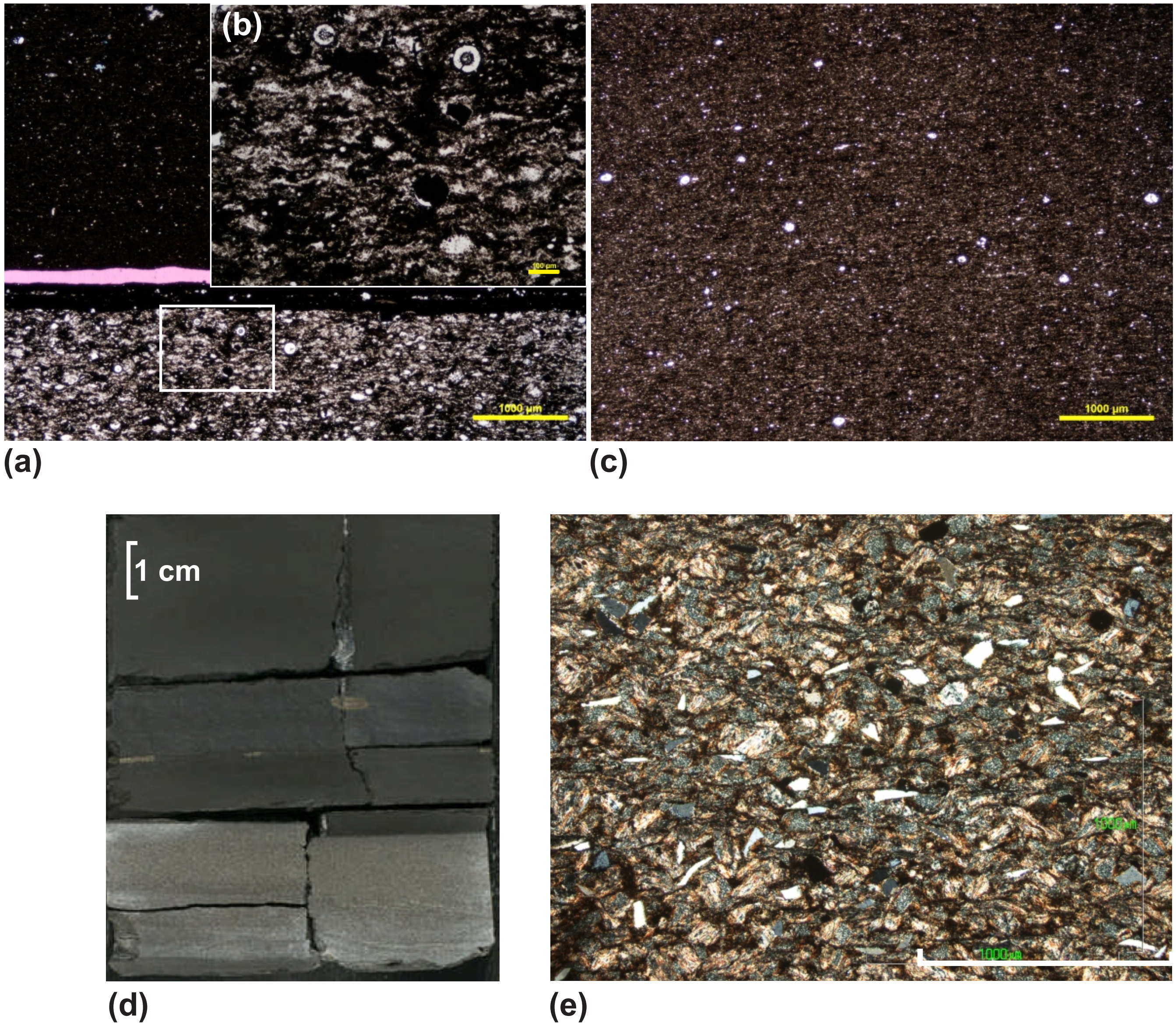

Fig. 20. a) to c) core photomicrographs of the Exshaw Formation from the Nexen Energy Dunedin a-38-B well, from Nexen Energy Ltd. (2016). **a)** Photomicrograph of mudstone in the upper part of the Exshaw Formation (3976.11 m) with a black mudstone layer overlying a layer with abundant radiolarian remains. **b)** Close up of the area outlined by the white box in a). **c)** Photomicrograph of mudstone in the upper part of the Exshaw Formation (3962.99 m) with dispersed circular features that are likely recrystallized radiolarians tests. **d)** Thin felsic tuff horizon at the base of the lower part of the Exshaw Formation at the 3710.4 m level of the Chevron-Woodside Patry b-23-K well (Apache Canada Ltd., 2012). **e)** Photomicrograph of felsic tuff shown in d), with quartz, mica and lithic shards.

upper part of the Exshaw Formation (see Richards et al., 2002). Tuff of similar age to that in Liard Basin has been defined in the lower part of Exshaw Formation in southern Alberta (Richards et al., 2002), although biostratigraphic control indicates that the upper contact of the lower part is Upper Devonian (Richards et al., 2002) and Josh et al. (2013) reported younger tuffs in the upper part of the lower Exshaw (Jura Creek and Mount Rundle areas; 360.0 ± 0.1 Ma, 360.2 ± 0.1 Ma and 358.9 ± 0.1 Ma). This would suggest that the upper part of the Exshaw Formation might be entirely early Carboniferous at some localities in southern Alberta.

Although highly radioactive organic-rich shales in the lower part of the Exshaw Formation in Liard Basin are similar to rocks in southern Alberta, they are considerably thicker in Liard Basin and do not appear to sit unconformably on underlying units. Furthermore, in contrast to calcareous siltstones in the upper part of the Exshaw Formation in southern Alberta, shale and mudstone are predominant, likely reflecting a more distal, deeper water setting.

6.3. Depths and isopachs

The lower Exshaw-Patry section is at depths of greater than 5,000 m in the northern part of the Liard Basin (Fig. 22), likely because of motion along the Bovie structure. Isopachs of the

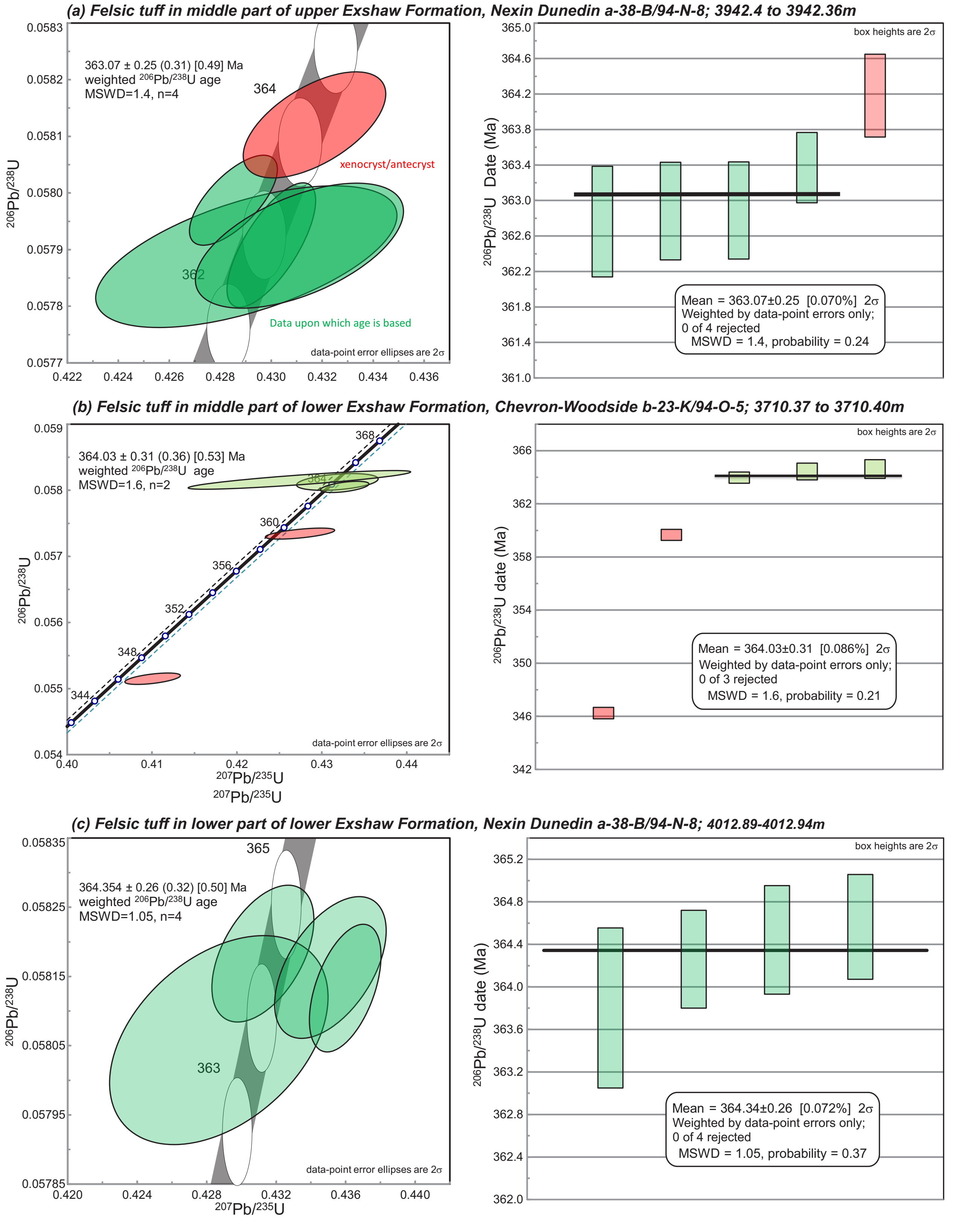

Fig. 21. Concordia plots and mean dates of pooled concordant zircons recovered from Exshaw Formation tuffs. See Appendix 1 for procedures and Appendix 2 for full analytical results. **a)** Felsic tuff in middle of the upper part of the Exshaw Formation, Nexin Dunedin Patry a-38-B/94-N-8; 3942.4 to 3942.36m. **b)** Felsic tuff in middle of the lower part of the Exshaw Formation, Chevron-Woodside Patry b-23-K/94-O-5; 3710.37 to 3710.40m. **c)** Felsic tuff in middle of the lower part of the Exshaw Formation, Nexin Dunedin Patry a-38-B/94-N-8; 4012.89-4012.94m.

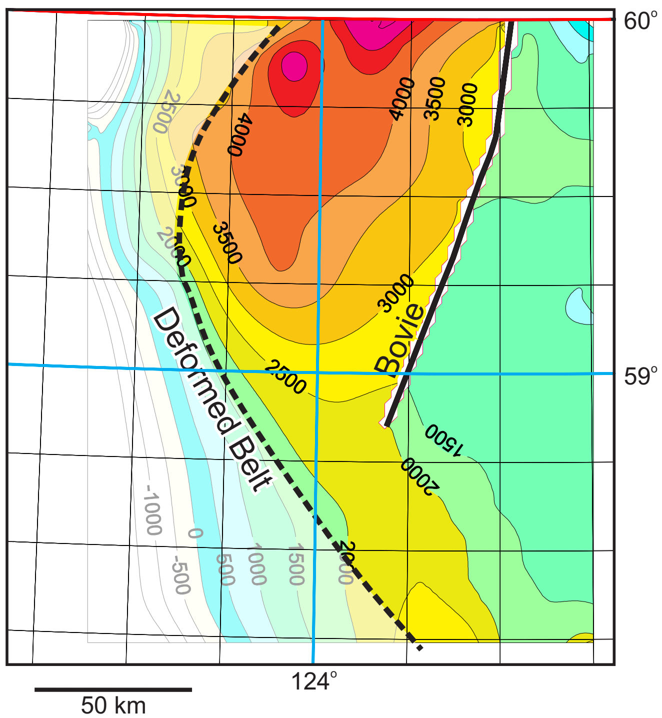

Fig. 22. Depth to the top of the lower part of the Exshaw Formation. Elevation in metres below surface. The depths reached by the lower part of the Exshaw Formation and the Patry Formation, particularly in the northern part of the Liard Basin, account for the high reservoir pressures and enhanced productivity of these units.

Patry Formation define a northerly trending zone, about 50 km wide, where the unit thickens to nearly 200 m (Fig. 23). Data for the lower Exshaw Formation, which together with the Patry Formation comprise the pay zone in the Besa River Group, outline a similar region (Fig. 23). Unlike the Patry Formation, isopachs of the Exshaw Formation delineate a relatively thin unit east of the Bovie structure that abruptly thickens west of and along a trend that roughly parallels the fault (Fig. 23). The combined thickness of the Patry Formation and the lower part of the Exshaw formations is nearly 300 m near the British Columbia-NWT border (Fig. 23). Interpretation of 2D seismic data across this thickened zone delineates a series of clinoforms that thin appreciably to the west (Leslie-Panek et al., 2020).

6.4. Reservoir characterization

The ultimate potential of a shale gas reservoir is determined not only by its organic carbon content, porosity, and permeability, but by its bulk geochemistry and mineralogy, the latter of which determine the ability of a reservoir to efficiently fracture when the confining pressure is exceeded (i.e. 'fracability'). The following discussion of these characteristics relies heavily on public domain data obtained from cores in several wells in Liard basin, particularly the Chevron-Woodside Patry b-23-K and the Nexen Energy Ltd. Dunedin a-38-B, both of which have extensive core across the sequence and have datasets that were obtained through systematic sampling. The summaries presented below and in Figs. 24-30 are based on data found in the Appendices and within well files at the British Columbia Oil and Gas Commission (Apache Canada Ltd., 2012; Nexen Energy ULC., 2014a, b; 2016).

6.4.1. Methods

Detailed analytical methods are presented in Appendix 2. Organic geochemistry data of core samples from the Chevron-Woodside b-23-K well were obtained by programmed pyrolysis using a Source Rock Analyzer (SRA) at Weatherford Laboratories in Calgary, AB, Canada (Apache Canada Ltd., 2012). Bulk mineralogy of core samples through X-ray diffraction, together with helium-derived porosity and gas saturation, were also obtained at Weatherford Laboratories. Whole rock, trace and rare earth element data were determined by ICP-ES and ICP-MS through Origin Analytical Laboratories Inc., Houston, Texas (Apache Canada Ltd., 2012).

Organic geochemistry data from core samples of the Nexen Energy a-38-B Dunedin well were generated from a Rock-Eval VI programmed pyrolysis apparatus at the Geological Survey of Canada laboratories, Calgary. Whole rock, trace and rare earth element geochemistry of core samples were determined by ICP-MS after a four-acid digestion at the laboratories of Bureau Veritas Commodities Ltd., Vancouver. Semi-quantitative bulk mineralogy was determined by X-ray diffraction at Schlumberger Reservoir Laboratories, Calgary (Nexen Energy, 2016). Helium porosimetry together with hydrocarbon and water saturations were also acquired at Schlumberger Reservoir Laboratories, AB, Canada (Nexen Energy, 2016).

Organic geochemistry on core from the Nexen Energy Patry a-68-D well was obtained by using a HAWK Resource Workstation programmed pyrolysis apparatus at the Trican Geological Solutions laboratories, Calgary (Nexen Energy, 2014b). Helium porosimetry, gas saturation and semi-quantitative mineral abundances through X-ray diffraction were performed on core samples at Schlumberger Reservoir Laboratories, Calgary, AB (Nexen Energy, 2014b). Organic carbon isotope analyses were performed at the Isotope Science Laboratory of the University of Calgary.

6.4.2. Rock-Eval pyrolysis data and thermal maturity

Rock-Eval pyrolysis is a technique that evaluates oil and gas shows, oil and gas generation potential, and thermal maturity, and identifies organic matter type (Tissot and Welte, 1978, pp. 443-447; Espitalie et al. 1985a, b, 1986; Peters, 1986). Due to the high thermal maturity (2.11 to 3.16 % Ro) of Patry and Exshaw rocks (Apache Canada Ltd., 2012; Nexen Energy Ltd., 2014a, b; 2015, 2016), total organic carbon (TOC) is the only significant Rock-Eval parameter. Depth profiles across the Besa River Group show an abrupt increase in TOC contents at the base of the Patry Formation, with the highest values in the lower part of the Exshaw Formation. TOC contents are generally greater than 2 wt. % and are more than 10 wt. % in the lower part of the Exshaw Formation (Figs. 24-28).

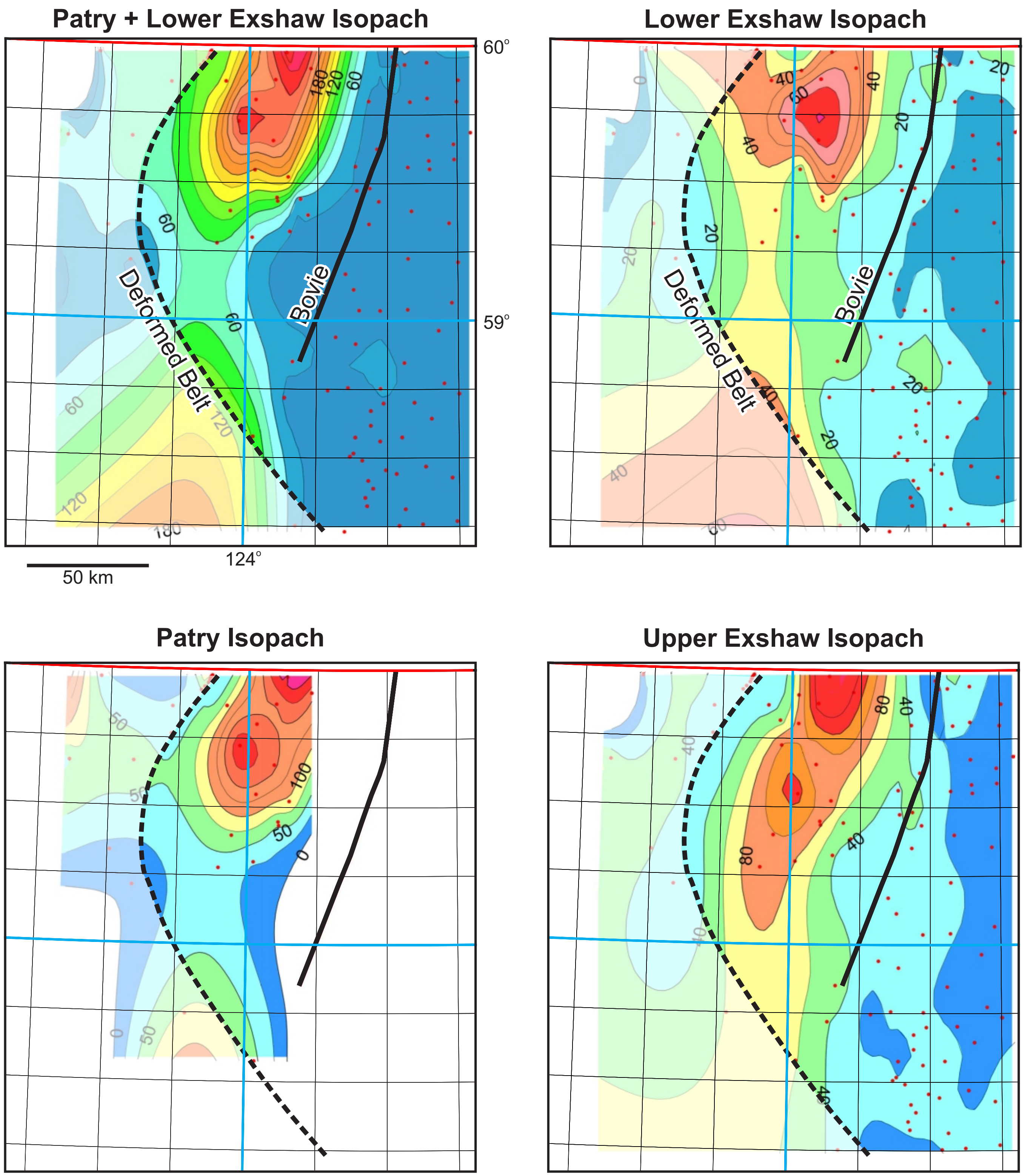

Fig. 23. Isopach maps for the Exshaw and Patry formations. Contour intervals in metres.

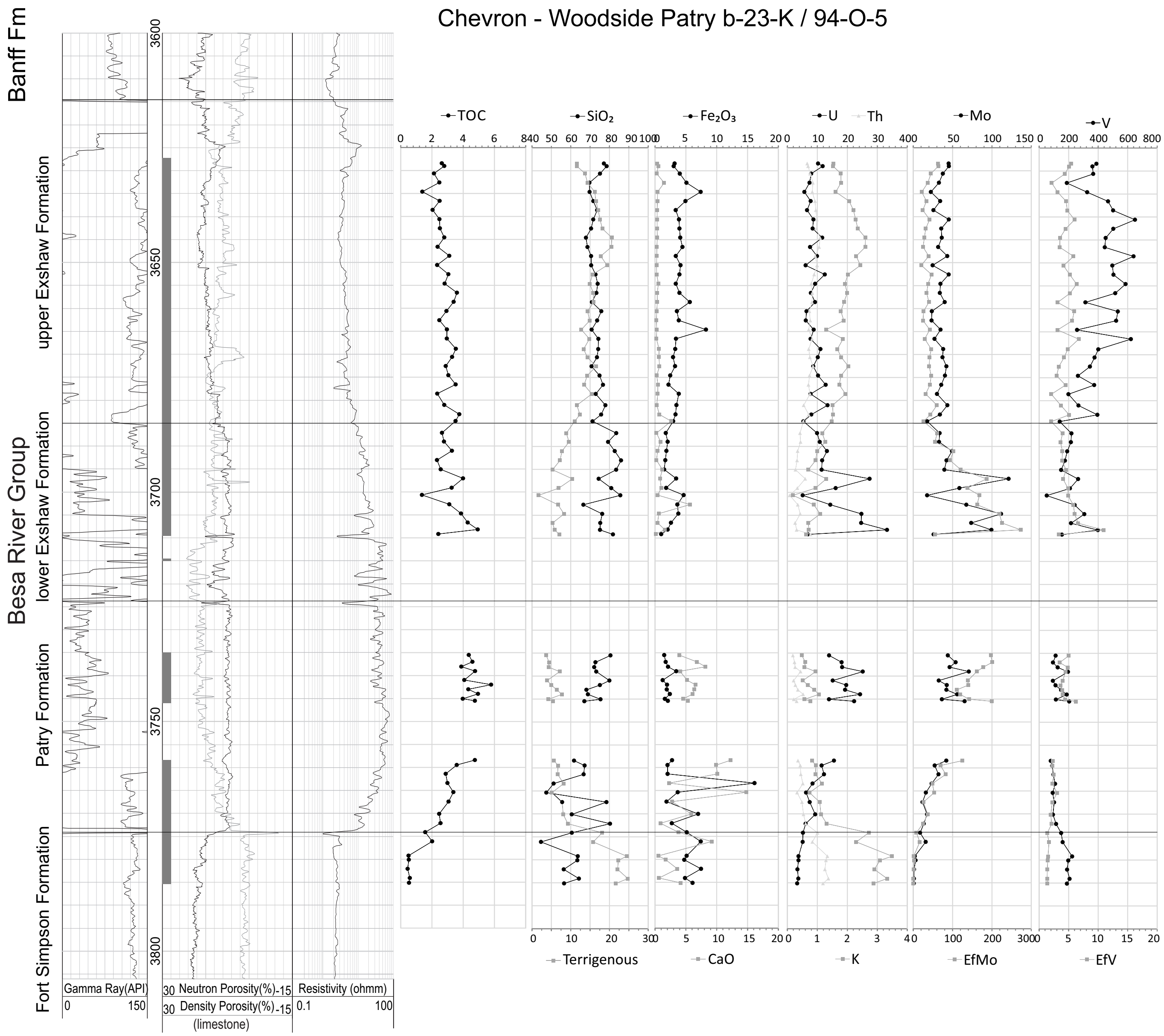

Fig. 24. Chevron-Woodside Patry b-23-K well with depth profiles across the Exshaw and Patry formations of total organic carbon, elemental data, total gamma ray counts, density-neutron and resistivity. Data are from Apache Canada Ltd. (2012). EfMo and EfV refers to the enrichment factor of the element relative to its composition in an average shale. Average shale compositions used for EfMo and EfV calculations are from Wedepohl (1971, 1991).

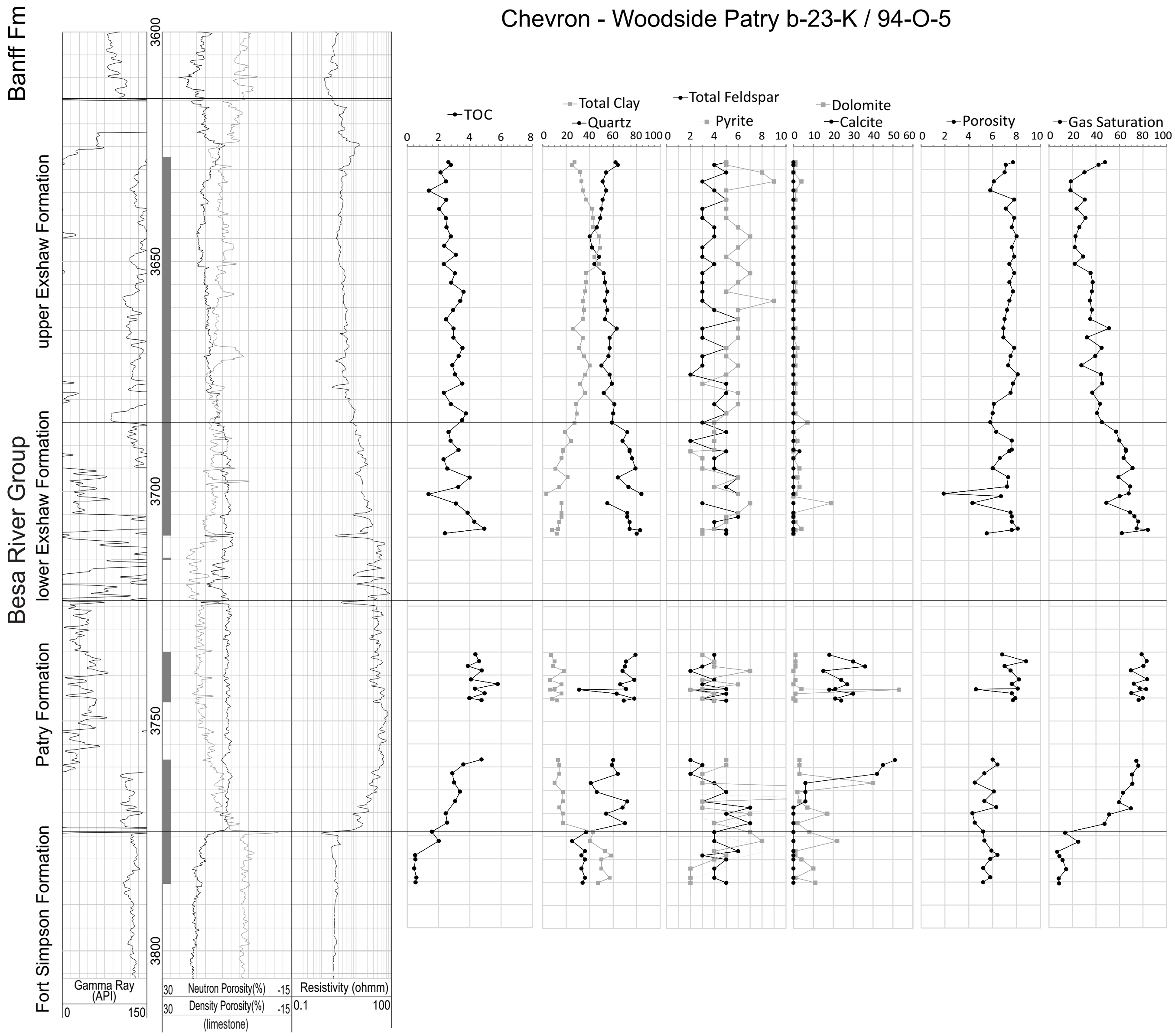

Fig. 25: Chevron-Woodside Patry b-23-K well with depth profiles across the Exshaw and Patry formations of total organic carbon, porosity, gas saturation, XRD data total gamma ray counts, density-neutron, and resistivity. Data are from Apache Canada Ltd. (2012).

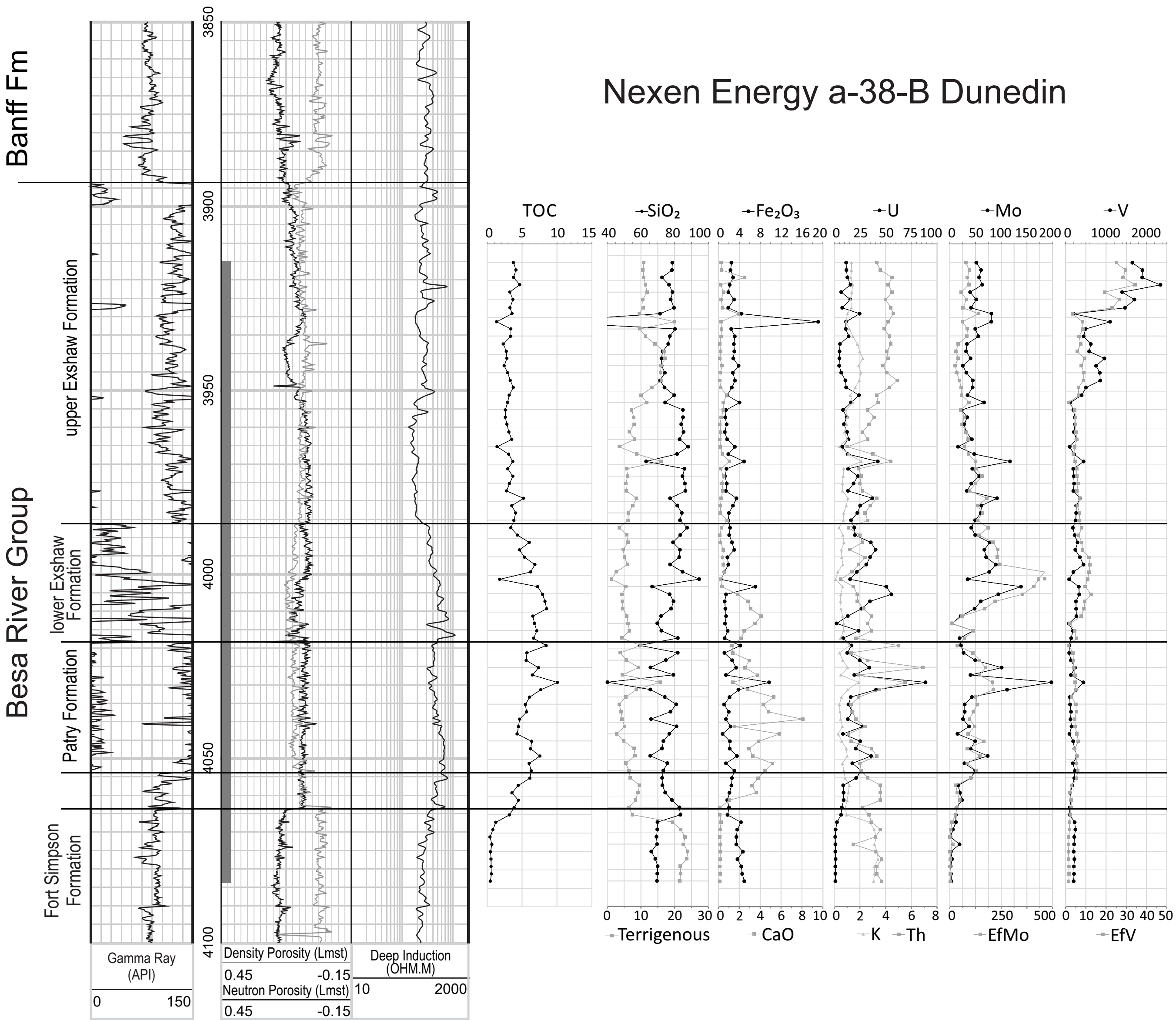

Fig. 26. Nexen Energy a-38-B Dunedin well with depth profiles across the Exshaw and Patry formations of total organic carbon content, elemental data, total gamma ray counts, density-neutron, and resistivity. Rock-eval and elemental data are from this report (Appendix 2). EfMo and EfV refers to the enrichment factor of the element relative to its composition in an average shale. Average shale compositions used for EfMo and EfV calculations are from Wedepohl (1971, 1991).

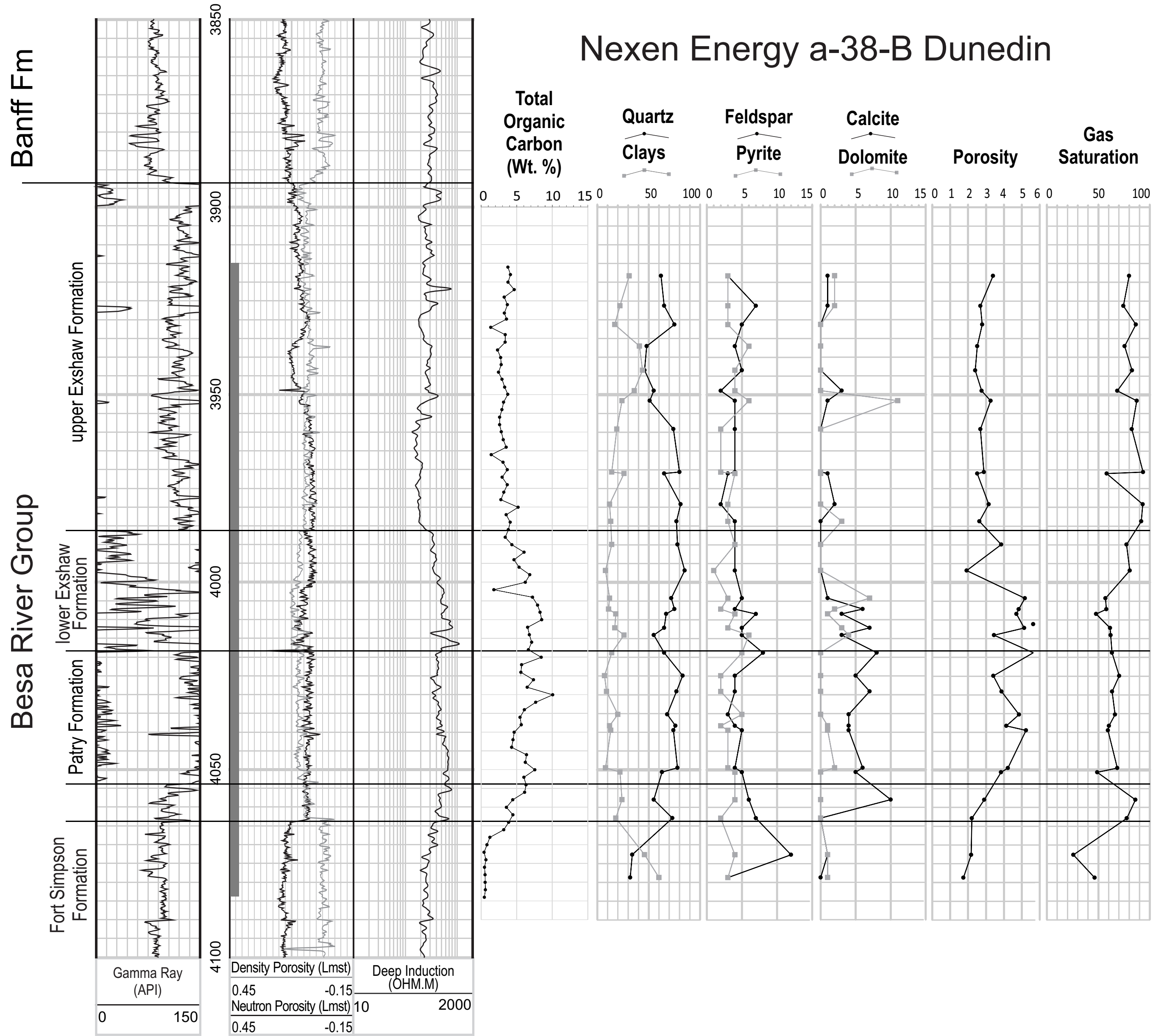

Fig. 27. Nexen Energy a-38-B Dunedin well with depth profiles across the Exshaw and Patry formations of total organic carbon content porosity, gas saturation, XRD data, total gamma ray counts, density-neutron, and resistivity. Rock-eval data from this report (Appendix 2); XRD data are from Nexen Energy Ltd. (2016).

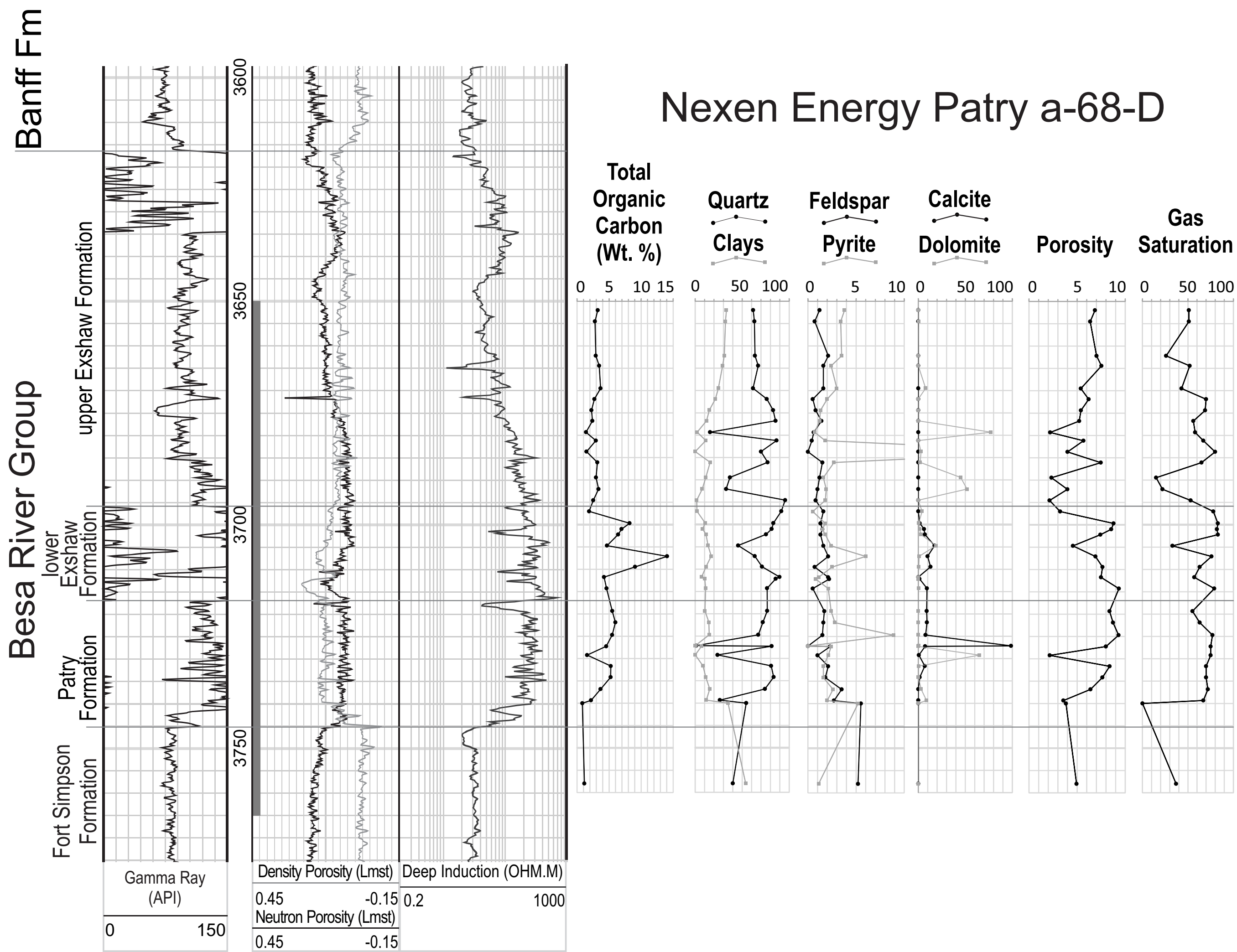

Fig. 28. Nexen Energy Patry a-68-D well with depth profiles across the Exshaw and Patry formations of total organic carbon porosity, gas saturation, XRD data, total gamma ray counts, density-neutron, and resistivity profiles. Data are from Nexen Energy Ltd. (2014b).

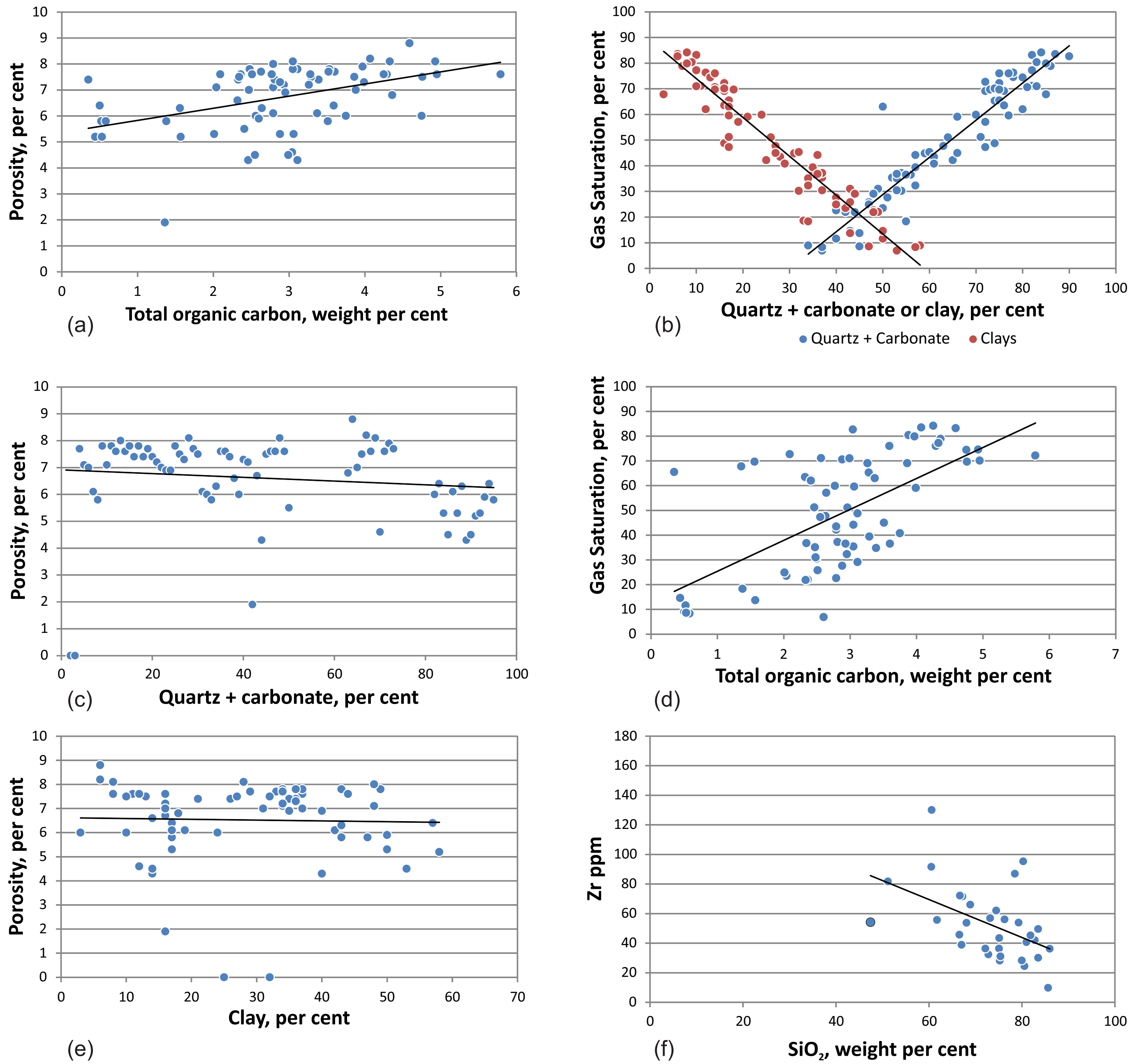

Fig. 29. Co-variation diagrams based on XRD and lithogeochemical data from cores of the Exshaw and Patry formations, the Chevron-Woodside Patry b-23-K well. **a)** Porosity versus total organic carbon. **b)** Gas saturation versus total quartz and carbonate or clay. **c)** Porosity versus total quartz and carbonate minerals. **d)** Gas saturation versus total organic carbon. **e)** Porosity versus clay content. **f)** Zr versus SiO_2. The negative slope of the Zr versus SiO_2 plot supports a predominantly organic source for quartz in the sequence. Data are from Apache Canada Ltd. (2012).

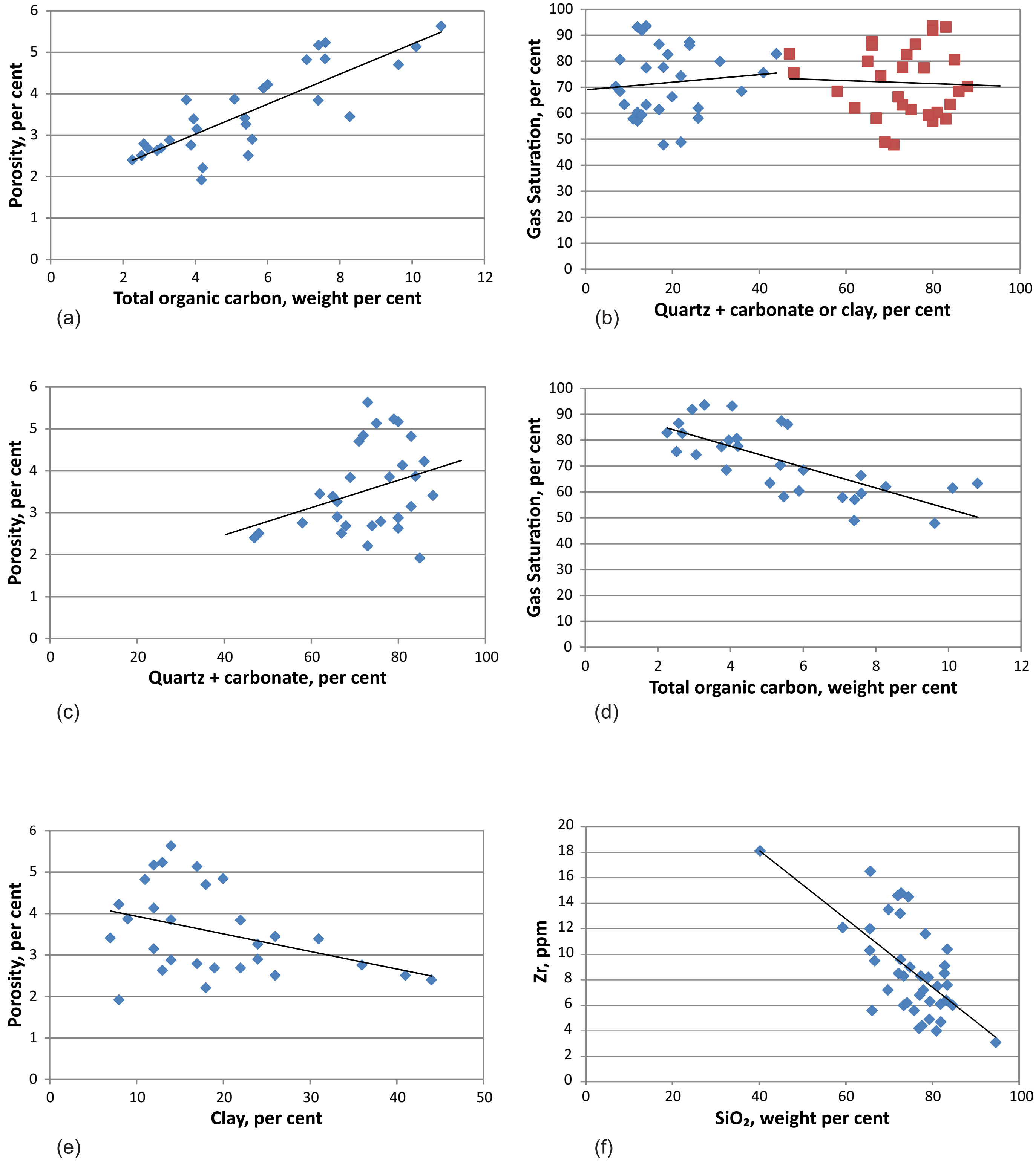

Fig. 30: Co-variation diagrams based on XRD and lithogeochemical data from cores of the Exshaw and Patry formations, Nexen Energy Dunedin a-68-D well. **a)** Porosity versus total organic carbon. **b)** Gas saturation versus total quartz and carbonate or clay. **c)** Porosity versus total quart and carbonate. **d)** Gas saturation versus total organic carbon. **e)** Porosity versus clay content. **f)** Zr versus SiO_2. The negative slope of the Zr versus SiO_2 plot supports a predominantly organic source for quartz in the sequence. Due to partial digestion, the absolute abundances of Zr are lower. Lithogeochemical and Rock-Eval data from this report (Appendix 2). Lithogeochemical data were calculated from elemental abundances and Rock-Eval data in Appendix 2. X-ray, gas saturation, and porosity data are from Nexen Energy Ltd. (2014b).

6.4.3. Lithogeochemistry and mineralogy

Lithogeochemical data show silica contents greater than 50% across the Patry-lower Exshaw zone, with sections averaging 60 to 90 % (Figs. 24-28). X-ray diffraction data indicate that most of this material is quartz, likely originating from radiolarian tests (Fig. 20). The organic origin of the silica is also supported by the negative correlation of Zr (or Ti) versus SiO_2 (Figs. 29f, 30f; Sano et al., 2013). Terrigenous content, as measured by total Al_2O_3+K_2O+TiO_2, together with clay and feldspar concentrations, are lowest across the Patry-lower Exshaw zone and increase into the upper part of the Exshaw Formation, being highest in the Fort Simpson Formation (Figs. 25, 27, 28). The highest TOC contents also correlate with the lowest terrigenous concentrations.

6.4.4. Porosity and permeability

Core-based porosity measurements from across the Patry and Exshaw formations range from 2 to 10 % (Figs. 25, 27, 28). Furthermore, cross-plots of porosity versus total organic carbon content generally show a positive correlation (Figs. 29, 30). Porosity in these overmature, organic-rich shale sequences is typically concentrated in the organic matter (Slatt and O'Brien, 2011; Chalmers et al., 2012; Mastalerz, et al., 2013; Tian et al., 2015; Dong et al., 2015; Lohr et al., 2015). Gas saturation generally increases with organic matter and, although this is not the case in the Nexen Energy Dunedin a-38-B well, where the percentage of gas-saturated porosity increases with the amount of organic matter (Fig. 27). Although average TOC levels across the Patry-Exshaw interval in Nexen Energy Dunedin a-38-B are higher than in the other wells, average porosities are lower, likely reflecting the lower thermal maturity (Fig. 27). Observations in other shale successions have shown that the porosity and pore sizes in organic matter increases with a rise in thermal maturity (Mastalerz et al., 2013; Chalmers and Bustin, 2015).

Permeability in the Patry-Exshaw horizon is in the 10 to 100s of nano Darcy range and are comparable to other shale sequences currently being developed (Jarvie, 2012; Table 1). The impressive initial flow rates observed from these wells reflect the over pressured nature of the reservoir together with efficient stimulation of these silica-rich horizons via hydraulic fracturing.

6.4.5. Organic carbon isotopes

The ratio of $^{13}C/^{12}C$ in the Earth's crust has varied throughout time due to the partitioning of these isotopes between organic and inorganic reservoirs, the latter being primarily marine carbonate rocks (Saltzman and Thomas, 2012). Because carbon isotope ratios of inorganically or biologically precipitated carbonate are similar to those of dissolved carbon in the oceans, the change in these ratios in the crust, as defined by $\delta^{13}C$, is a function of the flux in the amount of carbon removed from the oceans in the form of organic matter (Saltzman and Thomas, 2012). Because organisms preferentially fractionate ^{12}C, organic matter is strongly depleted in ^{13}C relative to atmospheric and ocean carbon reservoirs. Thus, when there is a global increase in organic matter deposition and preservation, the $\delta^{13}C$ of the ocean increases, whereas $\delta^{13}C$ decreases when organic matter is oxidized (Kump and Arthur, 1999). This variation of $\delta^{13}C$ through time provides a possible method for correlating and dating the host sequences.

Most studies involving carbon isotopes have focused on marine carbonate rocks produced inorganically or by biological precipitation (i.e., cements and fossils; Kump and Arthur, 1999). These data yield characteristic signatures when plotted through time based on the negative and positive excursions of $\delta^{13}C$ values from carbonates ($\delta^{13}C_{carb}$; Saltzman and Thomas, 2012; Buggisch and Joachimski, 2006). Although $\delta^{13}C$ from organic matter ($\delta^{13}C_{org}$) is much more negative, the magnitude, duration and timing of these excursions should be similar to

Table 1. Selected characteristics of major Devonian and Mississippian shale gas plays in North America.

Unit	Besa River Gp[1, 2]	Horn River Gp[3, 4]	Barnett Fm[4]	Marcellus Fm[4]	Woodford Fm[4]
Basin	Liard	Horn River	Fort Worth	Appalachian	Arkoma
Age	Late Devonian to Early Mississippian	Middle to Late Devonian	Middle to Late Mississippian	Middle Devonian	Late Devonian
Depth (m)	3,700 – 5,500	1,900 – 3,100	2,000 – 2,500	1,200 – 2,500	1,800 – 4,000
Thickness (m)	80 – 300	140 - 280	60 – 300	60	30 – 275
TOC (wt. %)	1 – 15 (5)	1 – 5	3 – 12 (4)	2 – 13 (4)	3 – 12 (5)
Silica (wt. %)	25 – 90 (68)	60	45	37	55
Maturity (%Ro)	2.11 – 3.16 (2.63)	1.4-2.2 (2.0)	0.85 – 2.1 (1.6)	0.9 – 5.0 (1.5)	0.7 – 4.0 (1.5)
Porosity (%)	2 – 9 (6)	3 – 6	4 – 6 (5)	4 – 12 (6)	3 – 9 (5)
Permeability (nD)	3 – 2080 (216)	0 – 200 (20)	0–100 (50)	0 – 70 (20)	0 – 700 (25)
Pressure (MPa)	79	20 – 53	22 – 28	17 – 36	22 – 47

[1]Apache Canada (2012), Nexen Energy (2014b, 2016); [2]British Columbia Oil and Gas Commission (2016); [3]British Columbia Oil and Gas Commission (2014); [4]Jarvie (2012)

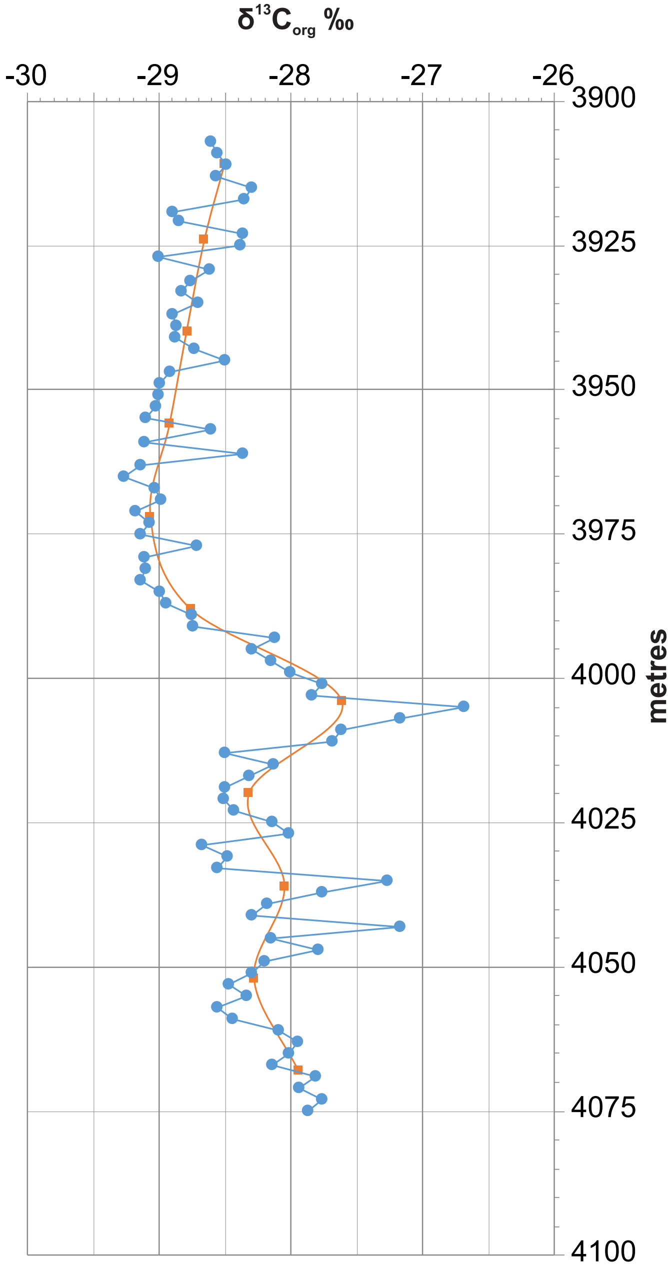

Fig. 31: Stable carbon isotope profile on analyses of organic material ($\delta^{13}C_{org}$) from core of the Nexen Energy Dunedin a-38-B well. The blue data points and line represent analyses at approximately 1m intervals. The orange points and line define an average model based on values averaged at 8m intervals.

$\delta^{13}C_{carb}$. Abundant data on long-term $\delta^{13}C_{org}$ trends are lacking and some studies have shown differences in magnitude and/or timing between $\delta^{13}C_{carb}$ and $\delta^{13}C_{org}$ excursions during specific time periods (Jenkyns, 2010; Saltzman et al., 2011; Saltzman and Thomas, 2012), although the reasons for these differences is poorly understood and may be related, in part, to carbonate diagenesis. Recent data from lower Paleozoic strata in the Yukon have shown good correlation between $\delta^{13}C_{carb}$ and $\delta^{13}C_{org}$ excursions, although of different magnitudes (Strauss et al., 2020). Even with these uncertainties, the following discussion will assume covariation between $\delta^{13}C_{carb}$ and $\delta^{13}C_{org}$ curves during the Devonian.

A total of 85 samples were collected at approximately 2 m intervals from the Nexen Energy Dunedin a-38-B core and analyzed to determine $\delta^{13}C_{org}$ at the Isotope Science Laboratory of the University of Calgary (see Appendix 2 for detailed analytical techniques). Values range from -29.27 to -26.69‰ with intra sample values varying from 0.1 to 0.5‰ (Fig. 31; Appendix 1). Below 3990 m, $\delta^{13}C_{org}$ averages approximately -28 to -28.5‰ with excursions to -26.69, 27.27 and -27.17‰ at 4005, 4035 and 4043m, respectively. Above the 3990 m level, $\delta 13C_{org}$ becomes more negative, averaging -29.1‰ and slowly increases to an average of -28.5‰ at the top of the core. The most significant feature of the data is the negative excursion of some 2‰ between 4005 and 3980 m (Fig. 31).

Compiled $\delta^{13}C_{org}$ and $\delta^{13}C_{carb}$ data for the Famennian define large positive excursions at its boundaries that correspond to major extinction events (Kellwasser and Hangenberg, respectively; Buggisch and Joachimski, 2006). Between these events, $\delta^{13}C$ values are relatively uniform and do not define prominent excursions (Buggisch and Joachimski, 2006; Saltzman, 2005; Kaiser et al., 2008). A negative excursion, similar in magnitude to that defined in the Nexen Energy Dunedin a-38-B core, is also recorded in some European sections within the middle to upper *expansa* Zone to lower *praesulcata* zone (Buggisch and Joachimski, 2006; Kaiser et al., 2008). Geochronology of tuff in the Nexen Energy Dunedin a-38-B core, together with published radiometric and biostratigraphic age constraints on Devonian stage and zonation boundaries (Becker et al., 2012), suggests this cored section encompasses these conodont zones and that these negative excursions may be correlative.

7. History of exploration in Liard basin and the Besa River Group resource play

The first well drilled into Liard Basin was spudded in 1952 (Central Leduc Oils Ltd., 1952; c-10-E/94-N-7), testing Middle Devonian carbonate rocks along the eastern edge of the deformed belt. By the end of the 1950s, only a handful of wells targeting Middle Devonian carbonate rocks and Mississippian siliciclastic and carbonate rocks were drilled. In 1958, a well was spudded by Pan American Petroleum Ltd. (1960, d-64-K/94-N-16) in a large anticline trending along the Beaver River and the British Columbia-Yukon boundary. This well terminated in dolomite of the Nahanni Formation and produced 101,430 m^3 (3,600,000 ft^3) gas per day on a drill stem test. Further drilling along the structure in the 1960s by Pan American Petroleum Ltd. and Amoco Canada Ltd. delineated 7.8 x 10^9 m^3 (258 Bcf; British Columbia Oil and Gas Commission, 2014) of gas-in-place in the Beaver River gas field. This gas field first saw production in 1971 and was connected to a gas plant in Fort Nelson by a 24-inch pipeline. Similar structurally controlled reservoirs were subsequently delineated along strike in the Yukon (Kotaneelee Field) and Northwest Territories (Pointed Mountain Field), which were

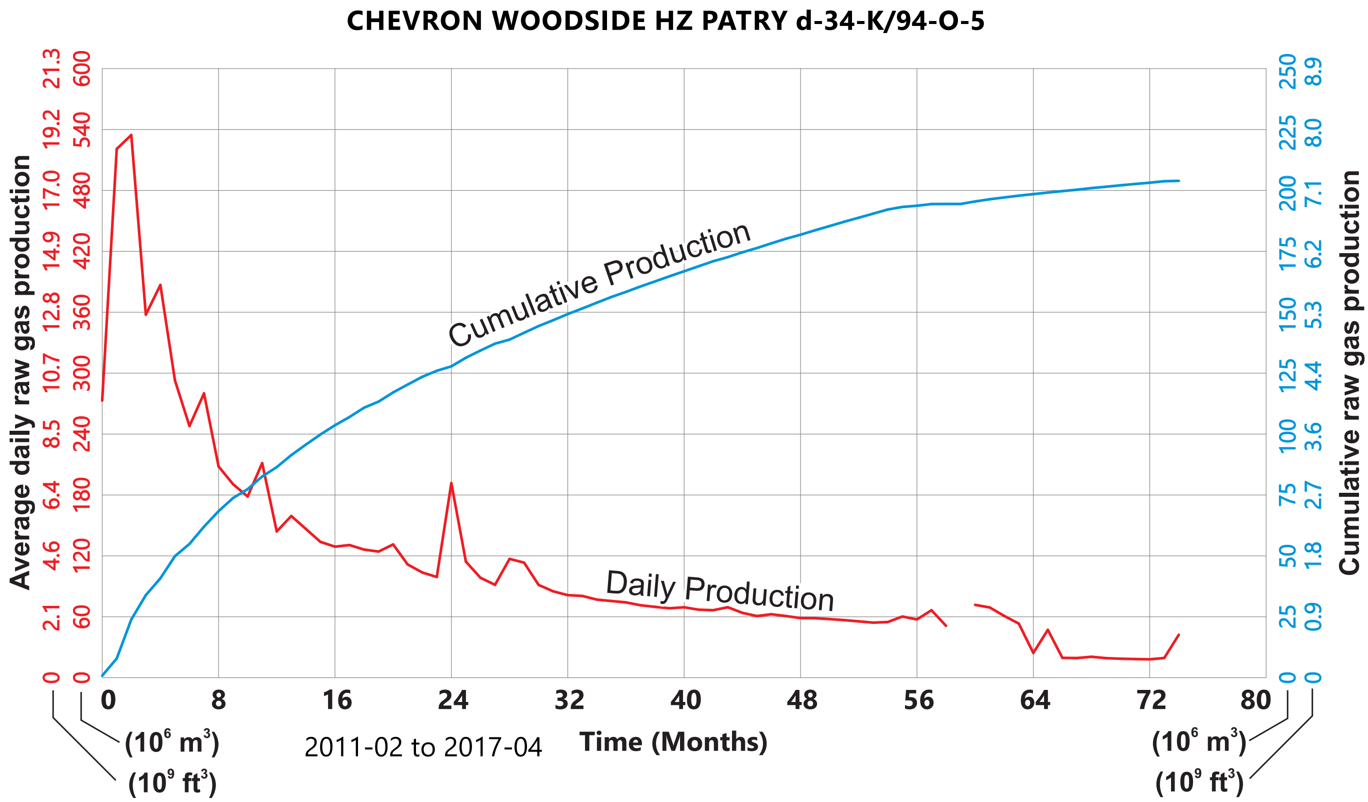

Fig. 32. Daily and cumulative raw gas production data for the Chevron Woodside Horizontal d-34-K / 94-O-5 well. The initial production of this well reflects the very high pressures at these depths (approximately 3700 m; 75 to 85 MPa; 10,900 to 12,000 psi). The horizontal leg of this well is approximately 850 m long and was hydraulically fractured in six zones. The ultimate potential of this well is 450 x 106 m^3 of raw gas (15.8 billion cubic feet (Bcf); National Energy Board, 2016). Doubling the horizontal length and increasing the density of the hydraulically fractured zones would likely push the ultimate recovery per well to 921 x 106 m^3 (32.3 Bcf; National Energy Board, 2016). Gas production data are from the data download web page of the British Columbia Oil and Gas Commission < http://www.bcogc.ca/online-services >.

connected to the pipeline at Beaver River in 1972. By the end of the 1980s, fewer than 50 wells were drilled into Liard basin.

The discovery of underpressured gas in the late 1990s in the Cretaceous Chinkeh Formation led to the drilling of about 100 wells and the delineation of the Maxhamish gas field along the west side of the Bovie structure (10.7 x $10^9 m^3$; 377 Bcf gas in place British Columbia Oil and Gas Commission, 2014). Completion of about 145 wells into the Chinkeh Formation continued until the end of 2005 with little or no activity elsewhere in Liard basin. Gas was also found in the Mattson Formation in the northern part of the Maxhamish area. An oil lag (?) along the western margin of the Maxhamish gas pool was delineated in the Chinkeh Formation, containing 888 x $10^3 m^3$ (5.6 M barrels) of original oil in place (British Columbia Oil and Gas Commission, 2014).

Between 2006 and 2010 only 12 new wells were drilled into the Maxhamish gas and oil pools. At this time, the industry exploration development model underwent a significant change, shifting from conventional to unconventional targets. Late in the decade, Apache Canada Ltd. spudded the first of four wells into the lower part of the Besa River Group and proved the prolific nature of the Patry Formation and lower Exshaw Formation horizons. Further delineation wells were drilled by Nexen Energy, Apache Canada Ltd/Chevron Canada Ltd., and Paramount Resources Ltd. in the years up to 2016 that suggest a marketable resource of some 6,196 x $10^9 m^3$ (219 Tcf) of dry gas in the Besa River Group (National Energy Board, 2016). The potential of gas-bearing, organic-rich shales in Patry Formation lower Exshaw Formation zone is best exemplified by data from the Chevron Woodside Patry d-34-K horizontal well, which has about seven years of production data (Fig. 32). Approximately 203.5 x $10^6 m^3$ of gas has been produced from this well and it may have an ultimate potential of about 450 x $10^6 m^3$ (~16 Bcf; National Energy Board, 2016).

8. Discussion: Besa Group depositional model

The preservation of delicate laminae in the Patry and Exshaw formations in Liard basin indicates deposition below storm wave base and the lack of bioturbation and the abundance of diagenetic pyrite indicates anoxic bottom waters. Anoxia during deposition of the Patry and Exshaw formations is reflected by enrichment of elements such as Mo, U, and V relative to concentrations in normal marine shales (Algeo and Maynard, 2008; Sano et al., 2013; Figs. 24, 26). These conditions would

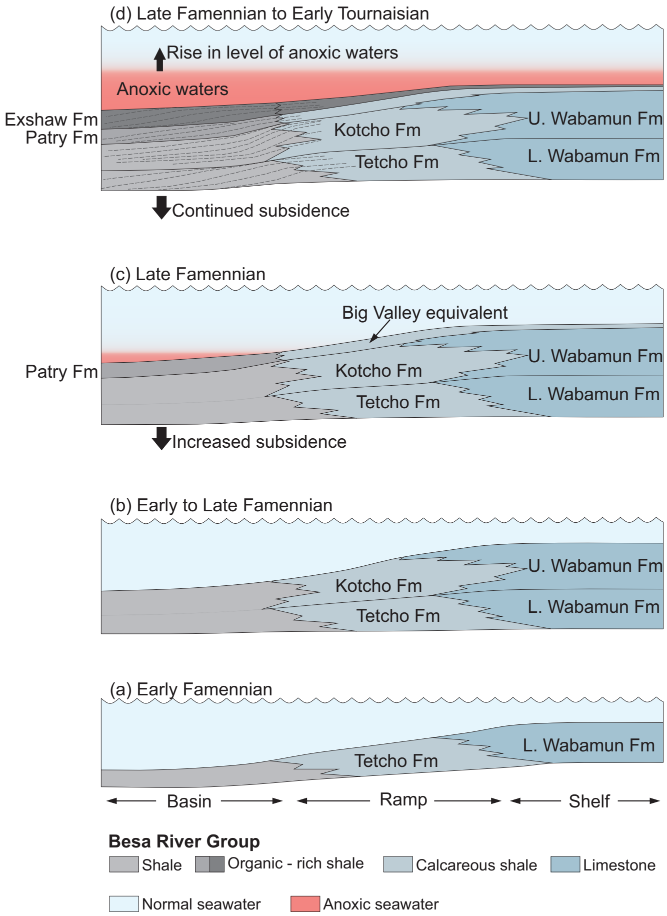

Fig. 33. Schematic representation of shelf to deep-water basin sedimentation in central and northern Liard Basin during the Famennian to early Tournaisian, showing the transition from carbonate rocks of the Wabamun Formation into calcareous shales of the Tetcho and Kotcho formations and then into deeper water basin shales of the Besa River Group. **a) and b).** Normal marine conditions during the Early to Late Famennian. **c).** Anoxic bottom waters at the beginning of Patry deposition in the Liard Basin during the late Famennian. Liard Basin likely underwent increased subsidence beginning in the Late Famennian in response to back-arc extension farther west. **d).** The beginning of a second-order transgression that reaches maximum during deposition of the lower part of the Exshaw Formation (clinoforms are schematic). It is as this time that anoxic waters flood across much of the Western Canada Sedimentary Basin.

also have enhanced preservation of organic matter. The sharp basal contact of many of the laminae as the lower part of Bouma-like fining upward sequences (with graded bedding, clastic carbonate lenses resembling starved ripples, and bioclastic detritus) capped by organic-rich interflow laminae is consistent with deposition as distal turbidites, likely sourced from shallower shelf environments to the east. Although arc-magmatism and uplift along western and northwestern margins of Ancestral North American shed some siliciclastic material into the Western Canada Sedimentary Basin (Fig. 10), seismic and well data indicate that the terrigenous material in Liard basin came from the east and northeast (Leslie-Panek et al., 2020). Chemical abundances and mineralogical data indicate that sediment supply decreased during deposition of the Patry Formation and the lower part of the Exshaw Formation (Figs. 24-29). With this decrease, dilution of organic matter also decreased, which improved the overall richness of the zone. The lower clay content also increased reservoir quality and likely improved the efficiency of the zone for hydraulic fracturing.

The Exshaw Formation appears highly diachronous across the Western Canada Sedimentary Basin. The age data and stratigraphic relationships suggest the anoxic environment represented by the lower part of the Exshaw Formation occurred earlier and deeper within Liard Basin, transgressing eastward and sweeping across much of the Western Canada Sedimentary Basin towards the close of the Devonian (Fig. 33). Rocks in the Tetcho and Kotcho formations are distal representatives of a broad carbonate shelf defined by the Wabamun Group and Palliser Formation (Fig. 33; Moore, 1993; Halbertsma, 1994; Peterhänsel, 2003). The Tetcho and Kotcho formations record mid- to outer-ramp settings and transition into shale facies within Liard basin. During deposition of the Tetcho Formation and much the Kotcho Formation, carbonate and shaly carbonate rocks transitioned westward into grey shales typical of the Fort Simpson Formation. Uppermost shaly carbonate rocks of the Kotcho Formation appear to pass westward into organic-rich calcareous shales of the Patry Formation. Although Kotcho deposition represents a general transgressive cycle across the Western Canada Sedimentary Basin, it contains a regressive carbonate succession in its middle part (Figs. 7, 9, 12). Shales in the upper Kotcho Formation record a transgressive event and are likely equivalent to the Big Valley Formation and Upper Costigan Member of the Wabamun Group and Palliser Formation, respectively (Figs. 7, 9, 12). More proximal shelf localities in southern Alberta record the presence of a pre-Big Valley unconformity, although the distal setting of the Liard Basin likely registers continuous sedimentation. In parts of southeastern Alberta and Saskatchewan, Big Valley lithologies and facies are very similar to the overlying Exshaw and Bakken formations (Halbertsma, 1994). These have been interpreted as either deposition related to restricted, shelf conditions within a regressive system (Halbertsma, 1994) or as part of a transgressive sequence (Richards et al., 2002).

The likely stratigraphic equivalence of the Big Valley Formation and rocks in the upper part Kotcho Formation to the Patry Formation supports these two units being lateral facies of an overall transgressive sequence (Figs. 7, 33). Deposition continued uninterrupted in central Liard basin while uplift and erosion generated the sub-Exshaw Formation unconformity along parts of the basin margin (Fig. 13) and other parts of the Western Canada Sedimentary Basin. The top of the Exshaw Formation in Liard basin is likely late Famennian whereas in more proximal settings of southern Alberta it is earliest Mississippian. Seismic data outline a series of westward-prograding clinoforms in these units (Leslie-Panek et al., 2020), which is broadly reflected in stratigraphic sections (Fig.7b) and isopachs (Fig 24).

Deposition of gas-saturated, organic-rich shales in the uppermost part of the lower Besa River Group in central Liard Basin occurred as part of two world-wide anoxic events at the close of the Devonian (Dasberg and Hangenberg events) and follows a similar event at the Frasnian-Famennian boundary (Kellwasser event; Caplan and Bustin, 1999; Buggisch and Joachimski, 2006; Kaiser et al., 2011; Bond et al., 2013; Formolo et al, 2014). During this time, the Western Canada Sedimentary Basin was affected by tectonism related to subduction and back-arc extension along the western margin of Ancestral North America. Although an unequivocal manifestation of back-arc extension in northeastern British Columbia did not appear until deposition of early Carboniferous coarse siliciclastic rocks of the Stoddart Group in the Peace River embayment and Liard basin, isopach patterns of the Exshaw Formation strongly suggest this subsidence began in the late Famennian (Fig.15; Halbertsma, 1994; Richards et al., 1994b), and ca. 364 Ma felsic tuffs at the base of the Exshaw Formation imply that back-arc magmatism was underway by the late Famennian. Furthermore, differential erosion of pre-Exshaw units suggests faulting may have been active even earlier (Fig. 13). The greater thickness of Patry Formation rocks in Liard basin relative to time equivalent shales in the upper part of the Kotcho Formation (Fig. 7) would support earlier extension, although these relationships could simply reflect normal basinward thickening related to clinoform deposition (Leslie-Panek et al., 2020; Fig. 7b).

The Liard basin, together with the Fort St. John graben in the Peace River embayment, likely experienced greater subsidence during the late Famennian. Thicker sections of the Exshaw Formation outlined by isopach maps display a marked northerly trend that are similar in orientation to the Bovie fault (and orthogonal to the orientation of the Fort St. John graben) and correspond to thick sections of Stoddart Formation siliciclastic rocks (Fig. 14). This sub-Stoddart subsidence may have influenced depositional trends of units (i.e. shale out of Wabamun Group units; Figs. 4, 10, 33) and localized the position, orientation, and thickness of clinoforms in Liard basin.

9. Conclusions

Sections of Middle Devonian to middle Mississippian shale assigned to the Besa River Formation in northeastern British Columbia extend eastward from exposures in the Rocky Mountains and Caribou Range of the Mackenzie Mountains to the subsurface of the Western Canada Sedimentary Basin, including Liard basin. These Devonian and Carboniferous strata display systematic changes in thickness and facies between exposed sections, subsurface sections across the Liard and Horn River basins and, farther eastward in the subsurface, to the plains of northeastern British Columbia and western Alberta. Some 300 m of Besa River shale can be traced eastward into more than1000 m of coeval, predominantly calcareous rock types. Where exposed, rocks of the Besa River Formation are so uniform that further subdivision is not required. However, in the subsurface of Liard basin, petrophysical logs allow discrete formations to be recognized and thus we elevate the unit to group status. Accordingly, we recommend that the term 'Besa River Group' be used in the subsurface of Liard basin for rocks between base of the Banff Formation and the top of the Nahanni/Dunedin Formation west of the Kotcho Formation shale-out. The top of the Besa River Group becomes younger to the west as carbonate rocks in the Banff and Prophet formations disappear westward into shale such that the upper contact of the Besa River Group is at the base of the Mattson Formation. In addition, we propose the term 'Patry Formation' (previously informal Patry 'member') for organic-rich shales conformably above the Fort Simpson Formation and beneath the Exshaw Formation in the subsurface of Liard basin, west of where laterally equivalent ramp carbonate rocks of the Kotcho Formation disappear. We specify the type locality of the Patry Formation as the in the Chevron-Woodside Patry b-23-K/94-O-5 well in central Liard Basin where the unit is about 50 m thick. Complete cores of the unit were also obtained from the Nexen Energy Patry a-68-D, Nexen Energy Dunedin a-38-B (Fig. 17), and Chevron-Woodside La Jolie b-3-K wells, which can serve as reference sections.

Calculated rates of sedimentation based on new U-Pb zircon age determinations of tuffs recovered from cores at the base (364.354 ± 0.26 Ma), middle (364.03 ± 0.31 Ma) and top (363.07 ± 0.25 Ma) of the lower part of the Exshaw Formation suggest that the top of the Exshaw Formation in Liard basin is late Famennian, that is, older than the Devonian-Carboniferous boundary (358.9 Ma). When compared to data farther south for the Exshaw Formation, this calculation and the new ages indicate that the unit is diachronous across the Western Canada Sedimentary Basin.

Deposition of gas-saturated, organic-rich shales in the uppermost part of the lower Besa River Group occurred as part of two world-wide anoxic events at the close of the Devonian (Dasberg and Hangenberg events) and follows a similar event at the Frasnian-Famennian boundary. The preservation of delicate laminae in the Patry and Exshaw formations indicates deposition below storm wave base, and the lack of bioturbation and the abundance of diagenetic pyrite indicates anoxic bottom waters. Anoxia during deposition of the Patry and Exshaw formations is reflected by enrichment of elements such as Mo, U, and V relative to concentrations in normal marine shales. These conditions would also have enhanced preservation of organic matter. The sharp basal contact of many of the laminae as the lower part of Bouma-like fining upward sequences (with graded bedding, clastic carbonate lenses resembling starved ripples, and bioclastic detritus) capped by organic-rich interflow laminae is consistent with deposition as distal turbidites, likely sourced from shallower shelf environments to the east. The age data and stratigraphic relationships indicate that the Patry Formation represents the Late Famennian transition from normal marine to anoxic conditions that ultimately transgressed eastward to sweep across much of the Western Canada Sedimentary Basin towards the close of the Devonian. Deposition continued uninterrupted in central Liard basin while uplift and erosion generated the sub-Exshaw Formation unconformity along parts of the basin margin and other parts of the Western Canada Sedimentary Basin. This uplift was the result of back-arc extension linked to eastward subduction along the western margin of Ancestral North America. Isopachs and many of the Late Devonian carbonate to shale transitions in Liard basin roughly follow the trend of the Bovie fault, a north-trending structure that is taken as the eastern margin of the Liard basin and the western margin of Horn River basin, suggesting that stresses that ultimately led to the formation of this structure were driving subsidence.

Deeply buried (5 km), highly overpressured, and gas charged, both the Patry Formation and overlying organic-rich shales as the base of the Exshaw Formation have been the focus of recent exploration and development. The gas-charged Patry Formation-lower part of the Exshaw Formation section can be over 200 m thick, with organic carbon contents between 2 and 10 wt. per cent and porosities in the 6 to 8 per cent range. In addition, the location of these shales at greater than 5 km depth has produced highly overpressured reservoirs and resulted in prolific well production when hydraulically fractured, suggesting ultimate recoveries of 922 x $10^6 m^3$ (33 Bcf; National Energy Board, 2016). These characteristics point to a potential recoverable resource of some 6,196 x $10^9 m^3$ (219 Tcf) of marketable gas (National Energy Board, 2016).

Acknowledgements

The data presented in this paper were collected between 2010 and 2018. The senior author thanks the many assistants he worked with over the years including Lauren Wilson, Lisa Fodor, Gabrielse Altebaumer, Lindsay Kung, Arend Stamhuis and Matt Griffiths. The senior author also thanks Adrian Hickin and Dave Huntley for assistance, and Mark Hayes and Jeff Johnson (British Columbia Oil and Gas Commission) for their help and insights on the subsurface geology of the Liard Basin. This effort would not have been possible without the financial and laboratory support provided by the Geological Survey of Canada, particularly through the Program of Energy Research and Development (PERD). Many insights were also gained during collaboration in the Canada-Korea Shale Gas Study of the Western Canada Sedimentary Basin, a joint effort between the Geological Survey of Canada and the Korean Institute of Geoscience and Mineral Resources. This paper also builds on collaboration between the British Columbia Ministry of Energy, Mines and Petroleum Resources, the Yukon Geological Survey, and the Northwest Territories Geological Survey. Part of the material in this paper was compiled as part of a resource assessment of the Liard Basin, which was initiated by the National Energy Board of Canada and coordinated with input from the British Columbia Ministry of Energy, Mines and Petroleum Resources, the British Columbia Oil and Gas Commission, the Yukon Geological Survey and the Northwest Territories Geological Survey.

References cited

Adams, C., 2009. Summary of shale gas activity in northeast British Columbia 2008. Ministry of Energy, Mines and Petroleum Resources, Oil and Gas Report, 2009-1,18 p.

Algeo, T.J. and Maynard, J.B., 2008. Trace-metal covariation as a guide to water-mass conditions in ancient anoxic marine environments. Geosphere, 4, 872-887.

Andrichuk, J.M., 1960. Facies analysis of Upper Devonian Wabamun Group in west-central Alberta, Canada. American Association of Petroleum Geologists Bulletin, 44, 1651-1681.

Apache Canada Ltd., 2012. Well history report, Apache Patry b-023-K/094-O-05. British Columbia Oil and Gas Commission, Well Report 26990.

Bamber, E.W. and Mamet, B.L., 1978. Carboniferous biostratigraphy and correlation, northeastern British Columbia and southwestern District of Mackenzie. Geological Survey of Canada, Bulletin 266, 65 p.

Barclay, J. E., Krause, F. F., Campbell, R. I., and Utting, J.,1990. Dynamic casting and growth faulting: Dawson Creek Graben Complex, Carboniferous - Permian Peace River Embayment, western Canada. Bulletin of Canadian Petroleum Geology, 38A, 115-145.

Becker, R.T., 1993. Anoxia, eustatic changes, and Upper Devonian to lowermost Carboniferous global ammonoid diversity. In: House, M.R., (Ed.), The Ammonoidea: Environment, Ecology, and Evolutionary Change. Systematics Association Special Volume 47, pp. 115-163.

Becker, R.T., Gradstein, F.M., and Hammer, O., 2012. The Devonian Period. In: Gradstein, F.M., Ogg, J.G., Schmitz, M., and Ogg, G., (Eds.), The Geologic Time Scale 2012, Vol. 2. Elsevier, Amsterdam, the Netherlands, pp. 559–601.

Behar, F., Beaumont, V., and De B. Penteako, H.L., 2001. Rock-Eval 6 technology: Performances and developments. Revue de L'institut Francais du Petrole, 56, 111-134.

Bond, D.P.G., Zatoń, M., Wignall, P.B., and Marynowski, L., 2013. Evidence for shallow-water "Upper Kellwasser" anoxia in the Frasnian–Famennian reefs of Alberta, Canada. Lethaia 46, 355-368.

British Columbia Ministry of Energy and Mines, 2005. Gas shale potential of Devonian strata, northeastern British Columbia. British Columbia Ministry of Energy and Mines, Oil and Gas Reports, 2005-1, 229 p.

British Columbia Oil and Gas Commission, 2014. Hydrocarbon and by-product reserves in British Columbia. <https://www.bcogc.ca> last accessed June 20, 2021.

British Columbia Oil and Gas Commission, 2016. Pool reserves report, 2016. <https://www.bcogc.ca> last accessed June 20, 2021.

British Columbia Oil and Gas Commission, 2014. Horn River Basin Unconventional Shale Gas Play Atlas. <https://www.bcogc.ca> last accessed June 20, 2021.

Buggisch, W. and Joachimski, M.M., 2006. Carbon isotope stratigraphy of the Devonian of Central and Southern Europe; Palaeogeography, Palaeoclimatology, Palaeoecology, 240, 68-88.

Bustin, R.M., Cameron, A.R., Grieve, D.A., and Kalkreuth, W.D. 1983. Coal petrology, its principles, methods and applications. Geological Association of Canada short course notes, Geological Association of Canada, Volume 3, 273 p.

Burchfiel, B.C. and Davis, G.A., 1972. Structural framework and evolution of the southern part of the Cordilleran orogen, western United States. American Journal of Science, 272, 97-118.

Caplan M.L. and Bustin, R.M., 1998. Sedimentology and sequence stratigraphy of Devonian-Carboniferous, strata southern Alberta. Bulletin of Canadian Petroleum Geology, 46, 187-514.

Caplan, M.L. and Bustin, R.M., 1999. Devonian–Carboniferous Hangenberg mass extinction event, widespread organic-rich mudrock and anoxia: causes and consequences. Palaeogeography, Palaeoclimatology, Palaeoecology, 148, 187-207.

Central Leduc Oils Limited., 1952. Well history report; Central Leduc Oils Limited, Toad River Joint Venture No. 1. British Columbia Oil and Gas Commission, Well Report 38.

Chalmers, G.R., Ross, D.J.K., and Bustin, R.M., 2012. Geological controls on matrix permeability of Devonian gas shales in the Horn River and Liard basins, northeastern British Columbia, Canada. International Journal of Coal Geology, 103, 120-131.

Chalmers, G.R.L. and Bustin, R.M., 2015. Porosity and pore size distribution of deeply-buried fine-grained rocks: Influence of diagenetic and metamorphic processes on shale reservoir quality and exploration. Journal of Unconventional Oil and Gas Resources, 12, 134-142.

Cohen, K.M., Finney, S.C., Gibbard, P.L. and Fan, J.-X. 2013. The ICS International Chronostratigraphic Chart. Episodes 36: 199-204. <https://stratigraphy.org/ICSchart/ChronostratChart2020-03.pdf> last accessed June 20, 2021.

Colborne, J., Reinson, G. and Bustin, R.M. 2015. Stratigraphic framework and depositional controls on reservoir occurrence, Big Valley Formation, southern Alberta. Bulletin of Canadian Petroleum Geology, 63, 192-223.

Colpron, M., Nelson, J.L., and Murphy, D.C., 2007. Northern Cordilleran terranes and their interactions through time. GSA Today, 17, 4-10.

Colpron, M., Logan, J. M., and Mortensen, J. K., 2002. U-Pb zircon age constraint for late Neoproterozoic rifting and initiation of the lower Paleozoic passive margin of western Laurentia. Canadian Journal of Earth Sciences, 39, 133-143.

Crowley, J.L., Schoene, B., and Bowring, S.A., 2007. U-Pb dating of zircon in the Bishop Tuff at the millennial scale. Geology, 35, 1123-1126.

Dong, T., Harris, N.B., Ayranci, K., Twemlow, C.E., and Nassichuk, B.R., 2015. Porosity characteristics of the Devonian Horn River shale, Canada. insights from lithofacies classification and shale composition. International Journal of Coal Geology, 141-142, 74-90.

Douglas, R.J.W., 1976. Geology, La Biche River, District of Mackenzie. Geological Survey of Canada Map 1380A, 1:250,000 scale.

Douglas, R., J. W. and Norris, D. K., 1977a. Geology, Virginia Falls, District of Mackenzie. Geological Survey of Canada Map 1378A, 1:250,000 scale.

Douglas, R., J. W. and Norris, D. K., 1977b. Geology, Sibbeston Lake, District of Mackenzie. Geological Survey of Canada, Map 1377A, 1:250,000 scale.

Douglas, R., J. W. and Norris, D. K. 1977c. Geology, Camsell Bend, District of Mackenzie. Geological Survey of Canada Map 1375A, 1:250,000 scale.

Douglas, R.J.W., Gabrielse, H., Wheeler, J.O., Stott, D.F., and Belyea, H.R., 1970. Geology of Western Canada. In: Douglas, R.J.W., (Ed.), Geology and Economic Minerals of Canada. Geological Survey of Canada, Economic Geology Report 1, pp. 366-488.

Embry, A.E., 1988. Middle-Upper Devonian sedimentation in the Canadian Arctic Islands and the Ellesmerian Orogeny. In: in McMillan, N.J., Embry, A.F., and Glass, D.J., (Eds.), Devonian of the World, V. II. Canadian Society of Petroleum Geologists Memoir 14, pp. 15-28.

Erdmer, P., Heaman, L., Creaser, R.A., Thompson, R.I., and Danghtry, K.L., 2001. Eocambrian granite clasts in southern British Columbia shed light on Cordilleran hinterland crust. Canadian Journal of Earth Sciences, 38, 1007-1016.

Espitalié, J., Deroo, G., and Marquis, F. 1985a. Rock-Eval pyrolysis and its applications (Part Two). Institut Français du Pétrole, Oil & Gas Science and Technology-Review, 40, 755-784.

Espitalié, J., Deroo, G., and Marquis, F. 1985b. Rock-Eval pyrolysis and its applications (Part One). Institut Français du Pétrole, Oil & Gas Science and Technology- Review, 40, 563-579.

Espitalié, J., Deroo, G., and Marquis, F. 1986. Rock-Eval pyrolysis and its applications (Part Three). Institut Français du Pétrole, Oil & Gas Science and Technology- Review, 41, 73-89.

Fedorowski, J., Bamber, E.W., and Richards B.C., 2019. Bashkirian rugose corals from the Carboniferous Mattson Formation in the Liard Basin, northwest Canada – stratigraphic and paleobiogeographic implications. Acta Palaeontologica Polonica, 64, 851-870.

Ferri, F., and Reyes, J., 2019a. Rock-Eval, lithogeochemistry, gamma ray spectrometry, vitrine reflectance, and X-ray diffraction analysis of the Besa River Formation in the Rocky Mountains of northeastern British Columbia. British Columbia Ministry of Energy, Mines and Petroleum Resources, British Columbia Geological Survey GeoFile 2019-10, 3p.

Ferri, F. and Reyes, J., 2019b. Rock-Eval, lithogeochemistry, gamma ray spectrometry, thermal maturity, X-ray diffraction analysis, and organic carbon isotope geochemistry of the Besa River Formation, west-central Liard Basin, British Columbia (94N/14). British Columbia Ministry of Energy, Mines and Petroleum Resources, British Columbia Geological Survey GeoFile 2019-11, 5p.

Ferri, F., Hickin, A. S., and Huntley, D. H., 2011. Besa River Formation, western Liard Basin, British Columbia (NTS 094N): geochemistry and regional correlations. In: Geoscience Reports 2011, British Columbia Ministry of Energy and Mines, pp. 1-18.

Ferri, F., Hickin, A.S., and Reyes, J. 2012. Horn River basin–equivalent strata in Besa River Formation shale, northeastern British Columbia (NTS 094K/15). In: Geoscience Reports 2012, British Columbia Ministry of Energy and Mines, pp. 1-15.

Ferri, F., McMechan, M., Fraser, T., Fiess, K., Pyle, L., and Cordey, F. 2013. Summary of field activities in the western Liard Basin, British Columbia. In: Geoscience Reports 2013, British Columbia Ministry of Natural Gas Development, pp. 13-31.

Ferri, F., McMechan, M., and Creaser, R., 2015. The Besa River Formation in Liard Basin, British Columbia. In: Oil and Gas Geoscience Reports 2015, British Columbia Ministry of Natural Gas Development, pp. 1-27.

Ferri, F., McMechan, M., and Creaser, R., 2016. Depositional model for shale gas deposits of the Besa River Formation in Liard Basin, British Columbia. American Association of Petroleum Geologists, Annual Convention and Exhibition. Search and Discovery Article #10858. <https://www.searchanddiscovery.com/pdfz/documents/2016/10858ferri/ndx_ferri.pdf.html> last accessed June 20, 2021.

Fromolo, M.J., Riedinger, N., and Gill, B.C., 2014. Geochemical evidence for euxinia during the Late Devonian extinction events in the Michigan Basin (U.S.A.). Palaeogeography,

Palaeoclimatology, Palaeoecology, 414, 146-154.
Gabrielse, H. 1967. Tectonic evolution of the northern Canadian Cordillera. Canadian Journal of Earth Sciences, 4, 271-298.
Gehman, H. M. Jr., 1962. Organic matter in limestones. Geochimica et Cosmochimica Acta, 26, 885-897.
Geldsetzer, H.H.J., Goodfellow, W.D., and McLaren, D.J. 1993. The Frasnian–Famennian extinction event in a stable cratonic shelf setting: Trout River, Northwest Territories, Canada. Palaeogeography, Palaeoclimatology, Palaeoecology, 104, 81-95.
Gerstenberger, H., and Haase, G. 1997. A highly effective emitter substance for mass spectrometric Pb isotopic ratio determinations. Chemical Geology 136, 309-312.
Gordey, S. P., Abbott, J. G., Tempelman - Kluit, D. J., and Gabrielse, H. 1987. 'Antler' clastics in the Canadian Cordillera. Geology, 15, 103–107.
Gordey, S. P. and Anderson, R. G., 1993. Evolution of the northern Cordilleran miogeocline, Nahanni map area (105I), Yukon and Northwest Territories. Geological Survey of Canada, Memoir 428, 214 p.
Hadlari, T., Davis, W. J., and Dewing, K. 2013. A pericratonic model for the Pearya terrane as an extension of the Franklinian margin of Laurentia, Canadian Arctic. Geological Society of America Bulletin, 126, 182-200.
Halbertsma, H.L. 1994. Devonian Wabamun Group of the Western Canada Sedimentary Basin. In: Mossop, G.D. and Shetsen, I. (compilers), Geological Atlas of the Western Canada Sedimentary Basin. Canadian Society of Petroleum Geologists and Alberta Research Council, pp. 203-220. <https://static.ags.aer.ca/files/document/Atlas/chapter_13.pdf> last accessed June 20, 2021.
International Commission on Stratigraphy, 2017. The Carboniferous time scale, sub-commission on Carboniferous stratigraphy, < http://www.carboniferous.stratigraphy.org/per/per.asp>, last accessed June 20, 2021.
Jacob, H., 1989. Classification, structure, genesis, and practical importance of natural solid bitumen ("migrabitumen"). International Journal of Coal Geology, 11, 65-79.
Jaffey, A.H., Flynn, K.F., Glendenin, L.E., Bentley, W.C., Essling, A.M. 1971. Precision measurement of half-lives and specific activities of ^{235}U and ^{238}U. Physical. Review C4, 1889–1906.
Jarvie, D. M., 2012. Shale resource systems for oil and gas: Part 1-Shale-gas resource systems. In: Breyer, J.A. (Ed.), Shale Reservoirs Giant Resources for the 21st century. American Association of Petroleum Geologists Memoir 97, pp. 69-87.
Johnston, D.I., and Chatterton, B.D.E., 1991. Famennian conodont biostratigraphy of the Palliser Formation, Rocky Mountains, Alberta and British Columbia. Canada. Geological Survey of Canada, Bulletin 417, pp. 163-183.
Johnston, D.I. and Meijer Drees, N.C., 1993. Upper Devonian conodonts in west central Alberta and adjacent British Columbia. Bulletin of Canadian Petroleum Geology, 41, 139-149.
Johnston, D.I., Henderson, C.M., and Schmidt, M.J. 2010. Upper Devonian to Lower Mississippian conodont biostratigraphy of uppermost Wabamun Group and Palliser Formation to lowermost Banff and Lodgepole formations, southern Alberta and southeastern British Columbia, Canada: Implications for correlations and sequence stratigraphy. Bulletin of Canadian Petroleum Geology, 58, 295-341.
Kabanov, P., Richards, B.C., Hyun Suk Lee, Thapa, P., King, H.M., and Mort, A., 2019. Reference surface and subsurface sections of the Besa River Formation, Liard Basin, British Columbia. Part 1. Geological Survey of Canada Open File 8468, 58p.
Kaiser, S.I., Becker, R.T., Steuber, T., and Aboussalam, S.Z.,2011. Climate-controlled mass extinctions, facies, and sea-level changes around the Devonian–Carboniferous boundary in the eastern Anti-Atlas (SE Morocco). Palaeogeography, Palaeoclimatology, Palaeoecology, 310, 340-364.
Kaiser, S.I., Steuber, T. and Becker, R.T. 2008. Environmental change during the Late Famennian and Early Tournaisian (Late Devonian-Early Carboniferous): implications from stable isotopes and conodont biofacies in southern Europe. Geological Journal, 43, 241-260.
Kane, J.S., Arbogast, B.F., and Leventhal, J.S., 1990. Characterization of Devonian Ohio Shale SDO-1 as a USGS geochemical reference sample. Geostandards Newsletter, 14, 169-196.
Kaufmann, B. 2006. Calibrating the Devonian Time Scale: A synthesis of U-Pb ID-TIMS ages and conodont stratigraphy; Earth Science Reviews, 76, 175-190.
Kidd, F.A. 1963. The Besa River Formation. Bulletin of Canadian Petroleum Geology, 11, 369-372.
Lafargue, E., Marquis, F., and Pillot, D., 1998. Rock-Eval 6 applications in hydrocarbon exploration, production, and soil contamination studies. Revue de L'institut Francais du Petrole, 53, 421-437.
Lane, L.S., 2007. Devonian-Carboniferous paleogeography and orogenesis, northern Yukon and adjacent Arctic Alaska. Canadian Journal of Earth Sciences, 44, 679-694.
Leckie, D.A., Potocki, D.J., and Visser, K. 1991. The Lower Cretaceous Chinkeh Formation: A frontier-type play in the Liard Basin of Western Canada. American Association of Petroleum Geologists Bulletin, 75, 1324-1352.
Leslie-Panek, J., McMechan, M., and Ferri, F. 2020. Northeast British Columbia Liard Basin: A seismic stratigraphy study. Interpretation 8, T579–T588.
Lohr, S.C., Baruch, E.T., Hall, P.A., and Kennedy, M.J., 2015. Is organic pore development in gas shales influenced by the primary porosity and structure of thermally immature organic matter? Organic Geochemistry, 87, 119-132.
Ludwig, K. R., 2003. Isoplot 3.00, A Geochronological Toolkit for Microsoft Excel. University of California at Berkeley.
Mastalerz, M., Schimmerlmann, A., Drobniak, A. and Chen, Y., 2013. Porosity of Devonian and Mississippian New Albany Shale across a maturation gradient; insights from organic petrology, gas adsorption, and mercury intrusion. American Association of Petroleum Geologists Bulletin, 97, 1621-1643.
MacIntyre, D.G., 1998. Geology, geochemistry and mineral deposits of the Akie River area, northeast British Columbia. British Columbia Ministry of Energy, Mines and Petroleum Resources, Bulletin 103, 91 p.
MacLean, B. C. and Morrow, D.W., 2004. Bovie Structure: its evolution and regional context; Bulletin of Canadian Petroleum Geology, 52, 302-324.
Mackowsky, M. -Th., 1982. Methods and tools of examination. In: Stach, E., Mackowsky, M.-Th., Teichmüller, M., Taylor, G.H., Chandra, D., and Teichmüller, R., (Eds.), Stach's Textbook of Coal Petrology, third edition. Gerbruder Borntaeger, Berlin, pp. 295-299.
McMechan, M.E., 1994. Geology, Dawson Creek, west of the sixth meridian, British Columbia. Geological Survey of Canada, Map 1858A, 1:250,000 scale.
McMechan, M. E., Ferri, F. and MacDonald, L., 2012. Geology of

the Toad River area (NTS 94N), northeast British Columbia. In: British Columbia Ministry of Energy, Mines and Petroleum Resources, Geoscience Reports 2012, pp. 17-40.

Macqueen, R.W. and Sandberg, C.A., 1970. Stratigraphy, age and inter-regional correlation of the Exshaw Formation, Alberta Rocky Mountains. Bulletin of Canadian Petroleum Geology, 18, 32-66.

Mattinson, J.M. 2005., Zircon U-Pb chemical abrasion ("CA-TIMS") method: Combined annealing and multi-step partial dissolution analysis for improved precision and accuracy of zircon ages. Chemical Geology, 220, 47-66.

Meijer Drees, N.C., and Johnston, D.I., 1994. Type section and conodont biostratigraphy of the Upper Devonian Palliser Formation, southwestern Alberta. Bulletin of Canadian Petroleum Geology, 42, 55-62.

Meijer Drees, N.C., and Johnston, D.I., 1996, Famennian and Tournaisian biostratigraphy of the Big Valley, Exshaw and Bakken formations, southeastern Alberta and southwestern Saskatchewan. Bulletin of Canadian Petroleum Geology, 44, 683-694.

Moore, P.F., 1993. Devonian. In: Stott, D.F., and Aitken, J.D. (Eds.), Sedimentary Cover of the Craton in Canada. Geological Survey of Canada, Geology of Canada, no. 5, pp. 150-201.

Morrow, D.W., 2012. Devonian of the northern Canadian mainland sedimentary Basin (a contribution to the Geological Atlas of the northern Canadian Mainland Sedimentary Basin). Geological Survey of Canada, Open File 6997, 88p.

Morrow, J.R. and Sandberg, C.A., 2008. Evolution of Devonian carbonate-shelf margin, Nevada. Geosphere, 4, 445-458.

Mundil, R., Ludwig, K. R., Metcalfe, I., and Renne, P. R., 2004. Age and timing of the Permian mass extinctions: U/Pb Dating of closed-system zircons. Science, 305, 1760-1763.

Murphy, D.C., Mortensen, J.K., Piercey, S.J., Orchard, M.J., and Gehrels, G.E., 2006. Mid-Paleozoic to early Mesozoic tectonostratigraphic evolution of Yukon-Tanana and Slide Mountain terranes and affiliated overlap assemblages, Finlayson Lake massive sulphide district, southeastern Yukon. In: Colpron, M. and Nelson, J.L., (Eds.), Paleozoic Evolution and Metallogeny of Pericratonic Terranes at the Ancient Pacific Margin of North America, Canadian and Alaskan Cordillera. Geological Association of Canada, Special Paper 45, pp. 75-105.

National Energy Board of Canada, 2016. The unconventional gas resources of Mississippian-Devonian Shales in the Liard Basin of British Columbia, the Northwest Territories, and Yukon. Energy Briefing Note, March, 2016. <https://www.cer-rec.gc.ca/en/data-analysis/energy-commodities/natural-gas/report/mississippian-devonian-shales/index.html> last accessed June 20, 2021.

Nelson, J.L., Colpron, M., Piercey, S.J., Dusel-Bacon, C., Murphy, D.C., and Roots, C.F. 2006. Paleozoic tectonic and metallogenic evolution of the pericratonic terranes in Yukon, northern British Columbia and eastern Alaska. In: Colpron, M. and Nelson, J.L., (Eds.), Paleozoic Evolution and Metallogeny of Pericratonic Terranes at the Ancient Pacific Margin of North America, Canadian and Alaskan Cordillera. Geological Association of Canada, Special Paper 45, pp. 323-360.

Nexen Energy ULC., 2014a. Well history report, Nexen Energy La Jolie, c-66-I/94-N-09. British Columbia Oil and Gas Commission, Well Report 28288.

Nexen Energy ULC., 2014b. Well history report, Nexen Energy Patry a-68-D/94-O-05. British Columbia Oil and Gas Commission, Well Report 28608.

Nexen Energy ULC., 2015. Well history report, Nexen Energy Beaver River, b-44-G/94-N-16; British Columbia Oil and Gas Commission, Well Report 29046.

Nexen Energy ULC., 2016. Well history report, Nexen Energy Dunedin, a-38-B/94-N-08. British Columbia Oil and Gas Commission, Well Report 29354.

Pan American Petroleum Corporation, 1960. Well history report, Pan American A-1 Beaver River b-63-K. British Columbia Oil and Gas Commission, Well Report 325.

Pan American Petroleum Corporation, 1967. Well history report, Pan Am Sheep, c-86-D. British Columbia Oil and Gas Commission, Well Report 2150.

Paradis, S., Bailey, S.L., Creaser, R.A., Piercey, S.J., and Schiarizza, P., 2006. Geochemistry and paleotectonic setting of the Eagle Bay assemblage and its polymetallic massive sulphide deposits, British Columbia, Canada. In: Colpron, M. and Nelson, J.L. (Eds)., Paleozoic Evolution and Metallogeny of Pericratonic Terranes at the Ancient Pacific Margin of North America, Canadian and Alaskan Cordillera. Geological Association of Canada, Special Paper 45, 383-414.

Peterhänsel, A., 2003. Depositional dynamics of a giant carbonate platform-the Famennian Palliser Formation of Western Canada. Unpublished Ph.D. Thesis, University of Saskatoon, 221 p.

Petrel Robertson Consulting Ltd. 2003. Exploration assessment of deep Devonian gas plays, NEBC. British Columbia Ministry of Energy and Mines, Petroleum Geology Open File 2003-3, 173p.

Peters, K. E., 1986. Guidelines for evaluating petroleum source rock using programmed pyrolysis. American Association of Petroleum Geologists, Bulletin, 70, 318-329.

Poco Petroleum Ltd., 2000. Well history report; Poco Chevron Patry, c-086-B/094-O-05. British Columbia Oil and Gas Commission, Well Report 10756.

Richards, B.C., 1989. Uppermost Devonian and Lower Carboniferous stratigraphy, sedimentation and diagenesis, southwestern District of Mackenzie and southeastern Yukon Territory (NTS 95B, C, F and G). Geological Survey of Canada, Bulletin 390, 135p.

Richards, B.C., and Higgins, A.C., 1988. Devonian-Carboniferous boundary beds of the Palliser and Exshaw formations at Jura Creek, Rocky Mountains, southwestern Alberta. In: McMillan, N.J., Embry, A.F., and Glass, D.J., (Eds.), Devonian of the World, V. II. Canadian Society of Petroleum Geologists, Memoir 14, pp. 399-412.

Richards, B. C., Bamber, E. W., Higgins, A. C., and Utting, J., 1993. Carboniferous. In: Stott, D.F. and Aitken, J. D. (Eds.) Sedimentary Cover of the Craton in Canada. Geological Survey of Canada, Geology of Canada Series 5, pp. 202-271.

Richards, B.C., Bamber, E.W., Henderson, C.M., Higgins, A.C., Johnston, D.I., Mamet, B.I., and Meijer Drees, N.C., 1994a. Uppermost Devonian (Famennian) and Lower Carboniferous (Tournaisian) at Jura Creek and Mount Rundle, southwestern Alberta. Geological Survey of Canada, Open File 2866, 81 p.

Richards, B.C., Barclay, J.E., Bryan, D., Hartling, A., Henderson, C.M. and Hinds, R.C., 1994b. Carboniferous strata of the Western Canada Sedimentary Basin. In: Mossop, G.D. and Shetsen, I., (compilers) Geological Atlas of the Western Canada Sedimentary Basin. Canadian Society of Petroleum Geologists and Alberta Research Council, pp. 221-250. <https://static.ags.aer.ca/files/document/Atlas/chapter_14.pdf> last accessed June 20, 2021.

Richards, B.C., Bamber, E.W., and Utting, J., 1997. Upper Devonian to Permian, Chapter 8. In: D.K. Norris (Ed.) Geology and Mineral and Hydrocarbon Potential of Northern Yukon Territory and Northwestern District of Mackenzie. Geological Survey of Canada, Bulletin 422, pp. 201-252.

Richards, B.C., Ross, G.M., and Utting, J., 2002. U- Pb geochronology, lithostratigraphy and biostratigraphy of tuff in the Upper Famennian to Tournaisian Exshaw Formation: Evidence for a mid-Paleozoic magmatic arc on the northwestern margin of North America. In: Hills, L.V., Henderson, C.M., and E.W. Bamber, E.W. (Eds.), Carboniferous and Permian of the World, Canadian Society of Petroleum Geologists, Memoir 19, pp.158-207.

Root, K. G., 2001. Devonian Antler fold and thrust belt and foreland basin development in the southern Canadian Cordillera: Implications for the Western Canada Sedimentary Basin. Bulletin of Canadian Petroleum Geology, 49, 7-36.

Ross, C.A. and Ross, J.R.P., 1985. Late Paleozoic depositional sequences are synchronous and worldwide. Geology, 13, 194 -197.

Ross, C.A. and Ross, J.R.P. 1988. Late Paleozoic transgressive-regressive deposition. In: Wilgus, C.K., Hastings, B.S., Posamentier, H., Van Wagoner, J., Ross, C.A. and Kendall, C.G.St.C., (Eds.), Society of Economic Paleontologists and Mineralogists Special Publication 42, pp. 227-247.

Ross, D.J.K. and Bustin, R.M. 2008. Characterizing the shale gas resource potential of Devonian-Mississippian strata in the Western Canada Sedimentary Basin: Application of an integrated formation evaluation. American Association of Petroleum Geology, Bulletin, 92, 87-125.

Ross, G.M., 1991. Tectonic setting of the Windermere Supergroup revisited. Geology, 19, 1125-1128.

Saltzman, M.R. 2005. Phosphorus, nitrogen, and the redox evolution of the Paleozoic oceans. Geology, 33, 573-576.

Saltzman, M.R., and Thomas, E. 2012. Carbon isotope stratigraphy. In: Gradstein F.M., Ogg, J.G., Schmitz, M., and Ogg, G. (Eds.), The Geologic Time Scale, Vol. 2. Elsevier, Amsterdam, pp. 207-232.

Saltzman, M.R., Young, S.A., Kump, L.R., Gill, B.C., Lyons, T.W., and Runnegar, B. 2011. Pulse of atmospheric oxygen during the late Cambrian. Proceedings of the National Academy of Sciences, 108, 3876-3881.

Sano, J.L., Ratcliffe, K.T. and Spain, D.R., 2013. Chemostratigraphy of the Haynesville Shale. In: Hammes, U., and J. Gale, J., (Eds.), Geology of the Haynesville Gas Shale in East Texas and West Louisiana, U.S.A. American Association of Petroleum Geologists Memoir 105, pp. 137-154.

Savoy, L.E., Harris, A.G., and Mountjoy, E.W., 1999. Extension of lithofacies and conodont biofacies models of Late Devonian to Early Carboniferous carbonate ramp and black shale systems, southern Canadian Rocky Mountains. Canadian Journal of Earth Sciences, 36, 1281-1298.

Savoy, L.E., Stevenson, R.K., and Mountjoy, E.W., 2000. Provenance of Upper Devonian – Lower Carboniferous miogeoclinal strata, southeastern Canadian Cordillera: link between tectonics and sedimentation. Journal of Sedimentary Research, 70, 181-193.

Scoates, J. S. and Friedman, R. M., 2008. Precise age of the platinuferous Merensky Reef, Bushveld Complex, South Africa, by the U-Pb ID-TIMS chemical abrasion ID-TIMS technique. Economic Geology, 103, 465-471.

Schmitz, M. D. and Schoene, B., 2007. Derivation of isotope ratios, errors, and error correlations for U-Pb geochronology using ^{205}Pb-^{235}U-(^{233}U)-spiked isotope dilution thermal ionization mass spectrometric data. Geochemistry, Geophysics, Geosystems 8, Q08006, doi:10.1029/2006GC001492.

Slatt, R.M. and O'Brien, N.R., 2011. Pore types in the Barnett and Woodford gas shales: contribution to understanding gas storage and migration pathways in fine grained rocks. American Association of Petroleum Geologists Bulletin. 95, 2017-2030.

Smith, M.T. and Gehrels, G.E., 1992. Structural geology of the Lardeau Group near Trout Lake, British Columbia: implications for the structural evolution of the Kootenay Arc. Canadian Journal of Earth Sciences, 29, 1305-1319.

Smith, M. T., Dickinson, W. R., and Gehrels, G. E., 1993. Contractional nature of Devonian–Mississippian Antler tectonism along the North American continental margin. Geology, 21, 21-24.

Speed, R.C. and Sleep, N.H., 1982. Antler orogeny and foreland basin: A model. Bulletin of the Geological Society of America, 93, 815-828.

Stacey, J.S., and Kramers, J.D., 1975. Approximation of terrestrial lead isotopic evolution by a two-stage model. Earth and Planetary Science Letters, 26, 207-221.

Stevenson, R.K., Whittaker, S., and Mountjoy, E.W., 2000. Geochemical and Nd isotopic evidence for sedimentary-source changes in the Devonian miogeocline of the southern Canadian Cordillera. Geological Society of America Bulletin, 112, 531-539.

Stott, D. F., McMechan, M. E., Taylor, G. C., and Muller, J. E. 1983. Geology of Pine Pass (93-O) map area, British Columbia. Geological Survey of Canada, Open File 925, 1:125,000 scale.

Stott, D. F., Goruk, G. L., and Pelletier, B. R., 1963. Geology, Trutch, British Columbia. Geological Survey of Canada Preliminary Map 12-1963, 1:253,440 scale.

Stott, D., F. and Taylor, G. C., 1968. Geology, Fort Nelson, west of seventh meridian, British Columbia. Geological Survey of Canada, Preliminary Map 3-1968, 1:253,440 scale.

Struik, L.C., 1988. Structural geology of the Cariboo Gold Mining District, east- central British Columbia. Geological Survey of Canada, Memoir 421, 100 p.

Taylor, G.C., and Stott, D.F., 1973. Tuchodi Lakes Map-area, British Columbia. Geological Survey of Canada Memoir 373, 37 p.

Taylor, G.C., and Stott, D.F., 1999. Geology, Toad River, British Columbia. Geological Survey of Canada, Map 1955A, 1:250,000 scale.

Tian, H., Pan, L., Zhang, T.W., Xiao, X.M., Meng, Z.P., and Huang, B.J., 2015. Pore characterization of organic-rich Lower Cambrian shales in Qiannan Depression of Guizhou Province, southwestern China. Marine and Petroleum Geology 62, 28-43.

Thirlwall, M. F., 2000. Inter-laboratory and other errors in Pb isotope analyses investigated using a ^{207}Pb-^{204}Pb double spike, Chemical Geology, 163, 299-322.

Thompson, R.I., 1989. Stratigraphy, tectonic evolution and structural analysis of the Halfway River map area (94B), northern Rocky Mountains, British Columbia. Geological Survey of Canada Memoir 425, 119p.

Tissot, B. P., and Welte, D. H. ,1978. Petroleum formation and occurrence. Springer-Verlag, Berlin, 538 p.

Wang, X., Sanei, H., Dai, S., Ardakani, O.H., Isinguzo, N., Kondla, D., and Tang, Y., 2016. A novel method to estimate mineral compositions of mudrocks: A case study for the Canadian unconventional petroleum systems. Marine and Petroleum Geology, 73, 322-332.

Warren, P.S. 1937. Age of the Exshaw shale in the Canadian Rockies. American Journal of Science, 33, 454-457.

Wedepohl, K.H., 1971. Environmental influences on the chemical composition of shales and clays. In: Ahrens, L.H., Press, F., Runcorn, S.K., Urey, H.C. (Eds.), Physics and Chemistry of the Earth. Pergamon, Oxford, pp. 305-333.

Wedepohl, K.H., 1991. The composition of the upper Earth's crust and the natural cycles of selected metals. In: Merian, E. (Ed.), Metals and their Compounds in the Environment. VCH-Verlagsgesellschaft, Weinheim, pp. 3-17.

Wheeler, J.O. and McFeely, P., 1991. Tectonic assemblage map of the Canadian Cordillera and adjacent parts of the United States of America, Geological Survey of Canada, Map 1712A, 1:2,000,000 scale.

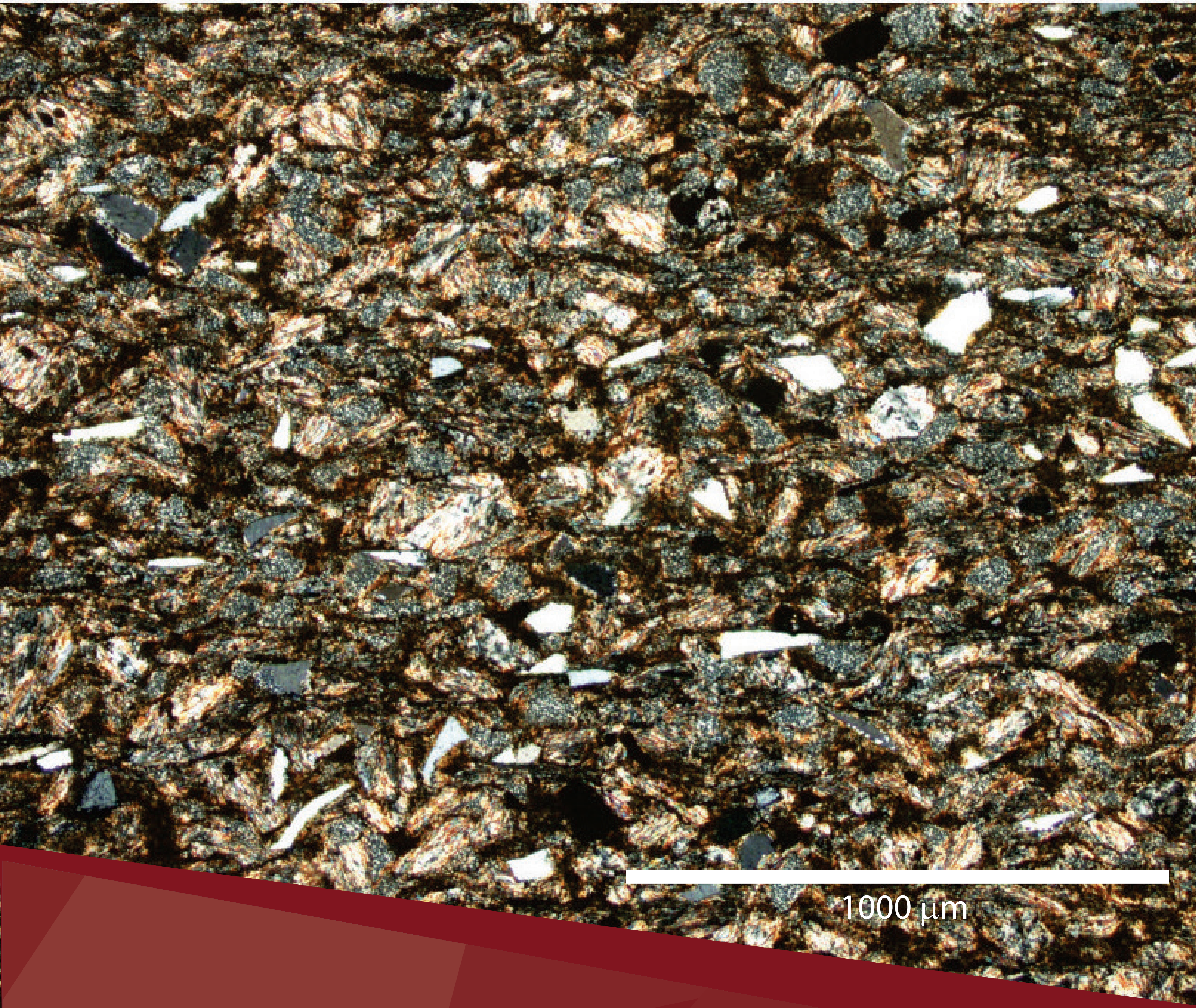

BRITISH COLUMBIA

Ministry of
Energy, Mines and
Low Carbon Innovation